

# New Zealand where did it come from?

## Provenance of the Rakaia Terrane.

Thesis submitted in accordance with the requirements of the University of Adelaide for an Honours Degree in Geology/Geophysics/Environmental Geoscience

James Christopher Russell Acott

November 2013



## NEW ZEALAND WHERE DID IT COME FROM? PROVENANCE OF THE RAKAIA TERRANE

### PROVENANCE OF THE RAKAIA TERRANE

#### ABSTRACT

The Rakaia Terrane comprises the majority of the basement of New Zealand, yet, to date, there are competing hypotheses as to its provenance along the Gondwana margin. These range from being adjacent to areas of Antarctica to originating against northern Queensland. To help solve these competing hypotheses, I combined the analysis of detrital zircon U-Pb geochronology with Hf isotope studies and trace element concentrations to constrain the provenance. Detrital muscovites were also dated using the  $^{40}\text{Ar}$ - $^{39}\text{Ar}$  total fusion technique. Detrital zircons yielded age populations at 1100-980 Ma, 580-450 Ma, ca. 320 Ma and ca. 230 Ma.  $\epsilon\text{Hf}_{(t)}$  values of these zircons largely range from -6 to +6 and the trace element concentrations suggest that the zircons are primarily sourced from granitoids. The  $^{40}\text{Ar}$ - $^{39}\text{Ar}$  ages yield two ages with the first at ca. 340 Ma and the second at ca. 250-220 Ma. The U-Pb ages and  $\epsilon\text{Hf}_{(t)}$  values for the Ordovician and older zircons are most similar to those from the Lachlan Fold Belt while the younger zircons show a close similarity to those from the New England Fold Belt. From multidimensional scaling maps there is a strong association between zircons from the Rakaia Terrane, north eastern Queensland and the Lachlan Fold Belt. The detrital muscovite data, however, is consistent with an exclusive New England source. Combining the data from different isotopic systems and different minerals, I interpret the provenance of the Rakaia Terrane as being derived from the New England, in the Triassic. The presence of Cambrian and Precambrian zircons, but only Phanerozoic muscovites, is interpreted as demonstrating that zircons were recycled in the New England region from older rocks now exposed in the Lachlan Orogen. These data constrain the provenance of the Rakaia Terrane and allows for more detailed reconstructions of the proto-Pacific margin of Gondwana.

#### KEYWORDS

New Zealand, Rakaia, Provenance, Detrital zircons, U-Pb, Geochronology, Hf-isotopes, Trace element,  $^{40}\text{Ar}$ - $^{39}\text{Ar}$

**TABLE OF CONTENTS**

New Zealand where did it come from? Provenance of the Rakaia Terrane.....	1
Provenance of the Rakaia Terrane .....	1
Abstract .....	1
Keywords.....	1
List of Figures and Tables .....	4
List of Supplementary Figures and Tables.....	5
Introduction .....	7
Geological Setting of the Rakaia Terrane .....	9
Geological History of the Potential Source Regions to the Rakaia Terrane .....	10
New England Fold Belt .....	10
Ross Orogeny.....	10
Brook Street Terrane.....	11
Methods .....	12
U-Pb zircon geochronology .....	12
Zircon Hf isotope analysis.....	14
<sup>40</sup> Ar- <sup>39</sup> Ar Dating .....	14
Trace element analysis.....	15
Observations and Results .....	16
Trace Element Compositions .....	16
U-Pb Geochronology .....	17
NZ1301 .....	17
NZ1302 .....	18
NZ1304 .....	19
NZ1321 .....	19
NZ1322 .....	20
NZ1323 .....	20
NZ1324 .....	20
NZ1325 .....	21
Total Rakaia Terrane .....	21
Hf Isotopes.....	23
<sup>40</sup> Ar- <sup>39</sup> Ar Ages.....	24
Discussion .....	25
Plausible Source Rock Types.....	25

Maximum Deposition Age .....	26
Source Constraints from U-Pb Data .....	26
Pre-Silurian Zircons .....	26
Pre-Jurassic Zircons .....	28
Source Constraints from Hf Data .....	31
Source Constraints from $^{40}\text{Ar}$ - $^{39}\text{Ar}$ Data .....	32
Conclusions .....	33
Acknowledgments .....	33
References .....	33
Appendix .....	43
Methods .....	43
Zircon Separation .....	43
U-Pb geochronology.....	44
Zircon Hf Isotopes .....	45
$^{40}\text{Ar}$ - $^{39}\text{Ar}$ Dating .....	46
Trace Element Analysis.....	46
Supplementary Tables.....	47

## LIST OF FIGURES AND TABLES

Figure 1: Location map of New Zealand, edited from Wandres et al. (2005) and Adams et al. (2007), displaying the sample locations from the North and South Islands. The table in the top right displays the different terranes throughout New Zealand and its corresponding symbol on the map. The sample locations are represented by blue dots with the sample name listed adjacent to it.....	8
Figure 2: Examples of cathodoluminescence images of zircons, Images a, b and c are from sample NZ1301, d is from NZ1322 and e, f are from NZ1323. Spots used for geochronology on each zircon are labelled with the corresponding $^{238}\text{U}/^{206}\text{Pb}$ age. The circles with T and Hf represent spots for the trace element concentrations and Hf isotope analysis respectively. ....	13
Figure 3: Trace element concentrations of Rakaia Terrane zircons compared with data from Belousova et al. (2002), the zircons were analysed were from sample NZ1301, NZ1304, NZ1323 and NZ1324. From each sample 30 zircons were analysed, resulting in 120 per graph, the data points have been superimposed on source fields, created by Belousova et al. (2002), allowing the determination of the source rock. In these graphs Ce* is the average of the chondrite-normalised La and Pr concentrations while Eu* is the average of the chondrite-normalised of Sm and Gd concentrations. Within the Granitoid field, 1 represents aplites and leucogranites, 2 granites; 3 granodiorites and tonalites. ....	18
Figure 4: Concordant detrital zircon ages, the red lines represent probability density plots with a 5% concordancy threshold and $2\sigma$ uncertainty. The blue shaded area is the corresponding kernel density estimator (Vermeesch 2012) with the histogram in grey. The sample name is given at the top with the number of concordant ages used in the graph compared with the total number analysed is given underneath. ....	22
Figure 5: All 523 concordant detrital zircon ages, the probability density plot, with $2\sigma$ uncertainty, is shown in red with the kernel density estimator (Vermeesch 2012) in blue and histogram in grey. The black dashed lines represent the major populations, the dashed rectangles represent the Ordovician to Neoproterozoic and the Neoproterozoic to Mesoproterozoic populations. The number of concordant ages graphed out of the total number of analyses is given under the graph title. ....	23
Figure 6: $\epsilon\text{Hf}_{(t)}$ values plotted against the corresponding $^{238}\text{U}/^{206}\text{Pb}$ zircon age, n is the total number of analyses. The analyses were taken from samples NZ1301, NZ1322, NZ1323 and NZ1325. The red rectangles represent the $\epsilon\text{Hf}$ range taken from Phillips et al. (2011), the blue rectangle represents the equivalent $\epsilon\text{Hf}$ range from Borg et al. (1990) and Goodge et al. (2012) the green rectangles the $\epsilon\text{Hf}$ range from detrital zircons published by Glen et al. (2011). The solid red line is the depleted mantle while the solid black line is the CHUR. ....	24
Figure 7: Age plots generated from $^{40}\text{Ar}-^{39}\text{Ar}$ total fusion ages taken from detrital muscovites. The red rectangles represent individual Ar ages with their associated error. The green lines represent the Ar ages of ca. 340 Ma and ca. 250-220 Ma. The sample the muscovites were taken from is given in the top left hand corner. The number of muscovites analysed, n, is given in the top right hand corner. The dashed black lines represent the maximum depositional age taken from the detrital zircon $^{238}\text{U}/^{206}\text{Pb}$ ages. ....	25

- Figure 8: The multidimensional scaling (MDS) map for the pre-Silurian zircons from the Rakaia Terrane in red (North, South), Squire et al. (2006) in dark blue (ST18, ST21, ST23, ST36, ST39, ST43, ST46, ST47, ST48, ST76, ST77), Glen et al. (2011) in green (mit, MIT, WILGA, WAH1, CARGO1-2, Branch, OR3), Sircombe (1999) in purple (HH, NSI, CH, SB, TS, SH, AB, ABR, BB, M, SH, H, R W150, L, HSB, HSC, TF, TC), Tucker et al. (2013) in orange (ERU, BBD4, ISIS, ERO1, Longmac1) and Veevers and Saeed (2011) in light blue (273, 274). If two distributions are connected by a solid line, from the Kolmogorov-Smirnov (KS) test, their distributions are the least dissimilar or most similar, if connected by a dotted line it is the second most similar distribution..... 39
- Figure 9: The QQ plot for the pre-Silurian zircons from the Rakaia Terrane in red (North, South), Squire et al. (2006) in dark blue (ST18, ST21, ST23, ST36, ST39, ST43, ST46, ST47, ST48, ST76, ST77), Glen et al. (2011) in green (mit, MIT, WILGA, WAH1, CARGO1-2, Branch, OR3), Sircombe (1999) in purple (HH, NSI, CH, SB, TS, SH, AB, ABR, BB, M, SH, H, R W150, L, HSB, HSC, TF, TC), Tucker et al. in orange (2013) (ERU, BBD4, ISIS, ERO1, Longmac1) and Veevers and Saeed (2011) in light blue (273, 274). If two distributions are connected by a solid line, from the Kolmogorov-Smirnov (KS) test, their distributions are the least dissimilar or most similar, if connected by a dotted line it is the second most similar distribution. .... 40
- Figure 10: The multidimensional scaling (MDS) map for the pre-Jurassic zircons from the Rakaia Terrane in red (01, 02, 04, 21, 22, 23, 24, 25), Squire et al. (2006) in dark blue (ST18, ST21, ST23, ST36, ST39, ST43, ST46, ST47, ST48, ST76, ST77), Glen et al. (2011) in green (mit, MIT, WILGA, WAH1, CARGO1-2, Branch, OR3), Sircombe (1999) in purple (HH, NSI, CH, SB, TS, SH, AB, ABR, BB, M, SH, H, R W150, L, HSB, HSC, TF, TC), Tucker et al. (2013) in orange (ERU, BBD4, ISIS, ERO1, Longmac1) and Veevers and Saeed (2011) in light blue (273, 274). If two distributions are connected by a solid line, from the Kolmogorov-Smirnov (KS) test, their distributions are the least dissimilar or most similar, if connected by a dotted line it is the second most similar distribution. .... 41
- Figure 11: The QQ plot for the pre-Jurassic zircons from the the Rakaia Terrane in red (01, 02, 04, 21, 22, 23, 24, 25), Squire et al. (2006) in dark blue (ST18, ST21, ST23, ST36, ST39, ST43, ST46, ST47, ST48, ST76, ST77), Glen et al. (2011) in green (mit, MIT, WILGA, WAH1, CARGO1-2, Branch, OR3), Sircombe (1999) in purple (HH, NSI, CH, SB, TS, SH, AB, ABR, BB, M, SH, H, R W150, L, HSB, HSC, TF, TC), Tucker et al. in orange (2013) (ERU, BBD4, ISIS, ERO1, Longmac1) and Veevers and Saeed (2011) in light blue (273, 274). If two distributions are connected by a solid line, from the Kolmogorov-Smirnov (KS) test, their distributions are the least dissimilar or most similar, if connected by a dotted line it is the second most similar distribution.... 42

## LIST OF SUPPLEMENTARY FIGURES AND TABLES

- Supplementary Table 1: The sample name and corresponding GPS coordinates for the outcrop the sample was taken from. .... 47
- Supplementary Table 2: Raw U-Pb data from sample NZ1301 ..... 48
- Supplementary Table 3: Raw U-Pb data from sample NZ1302 ..... 49
- Supplementary Table 4: Raw U-Pb data from sample NZ1304 ..... 50
- Supplementary Table 5: Raw U-Pb data from sample NZ1321 ..... 51

Supplementary Table 6: Raw U-Pb data from sample NZ1322 .....	52
Supplementary Table 7: Raw U-Pb data from sample NZ1323 .....	53
Supplementary Table 8: Raw U-Pb data from sample NZ1324 .....	54
Supplementary Table 9: Raw U-Pb data from sample NZ1325 .....	55
Supplementary Table 10: Raw Hf data from sample NZ1301 with corrected $\epsilon$ Hf values .....	56
Supplementary Table 11: Raw Hf data from sample NZ1322 with corrected $\epsilon$ Hf values .....	56
Supplementary Table 12: Raw Hf data from sample NZ1323 with corrected $\epsilon$ Hf values .....	57
Supplementary Table 13: Raw Hf data from sample NZ1325 with corrected $\epsilon$ Hf values .....	57
Supplementary Table 14: Raw $^{40}\text{Ar}$ - $^{39}\text{Ar}$ data from sample NZ1301 with the calculated total fusion age.....	58
Supplementary Table 15: Raw $^{40}\text{Ar}$ - $^{39}\text{Ar}$ data from sample NZ1303 with the calculated total fusion age.....	58
Supplementary Table 16: Raw $^{40}\text{Ar}$ - $^{39}\text{Ar}$ data from sample NZ1323 with the calculated total fusion age.....	58
Supplementary Table 17: Raw $^{40}\text{Ar}$ - $^{39}\text{Ar}$ data from sample NZ1324 with the calculated total fusion age.....	58
Supplementary Table 18: Raw $^{40}\text{Ar}$ - $^{39}\text{Ar}$ data from sample NZ1325 with the calculated total fusion age.....	58
Supplementary Table 19: Raw microprobe data from sample NZ1301 .....	59
Supplementary Table 20: Raw microprobe data from sample NZ1304 .....	60
Supplementary Table 21: Raw microprobe data from sample NZ1323 .....	61
Supplementary Table 22: Raw microprobe data from sample NZ1324 .....	62
Supplementary Table 23: Raw trace element data from sample NZ1301, concentrations given in ppm. ....	63
Supplementary Table 24: Raw trace element data from sample NZ1304, concentrations given in ppm. ....	63
Supplementary Table 25: Raw trace element data from sample NZ1323, concentrations given in ppm. ....	64
Supplementary Table 26: Raw trace element data from sample NZ1324, concentrations given in ppm. ....	64

## INTRODUCTION

The Rakaia Terrane is the largest basement terrane in New Zealand and, at present, a number of hypotheses exist as to where along the extensive eastern margin of Gondwana the Rakaia Terrane originated. Suggestions range from adjacent to East Antarctica (Wandres et al. 2004) to being shed off Queensland (Adams et al. 2007, Pickard et al. 2000). To test these hypotheses, I have undertaken the most extensive provenance analysis of the Rakaia Terrane sedimentary rocks, combining U-Pb, Hf and rare earth element analysis of detrital zircons with  $^{40}\text{Ar}$ - $^{39}\text{Ar}$  total fusion geochronology of detrital muscovites.

New Zealand's basement is made of a series of terranes that are thought to originate somewhere along the Palaeozoic Gondwana margin, extending from New Guinea to South America. The basement geology of the North and South Island of New Zealand is divided into three zones, the Western Province, The Median Tectonic Zone and the Eastern Province (Figure 1). The Torlesse Supergroup within the Eastern Province is composed of the Permian to Late Triassic Rakaia Terrane and the Pahau Terrane (Wandres et al. 2005).

Wandres et al. (2004) studied U-Pb ages of cobble to boulder sized igneous clasts from the Rakaia Terrane. They concluded that the Rakaia Terrane was likely sourced from Antarctica as zircon age distributions from the Rakaia Terrane matched known crystallisation ages of plutons and volcanics in the Amundsen Province. This contrasts with studies by Pickard et al. (2000) and Adams et al. (2007), however, who concluded the Rakaia Terrane was likely sourced from the New England Orogen and eastern

Australia respectively due to the overlapping zircon ages. Evident through the contrasting studies by Wandres et al. (2004), Pickard et al. (2000) and Adams et al. (2007) is that U-Pb zircon ages on their own are inconclusive and potentially provide misleading information (Adams et al. 2007, Howard et al. 2009, Pickard et al. 2000, Wandres et al. 2004).

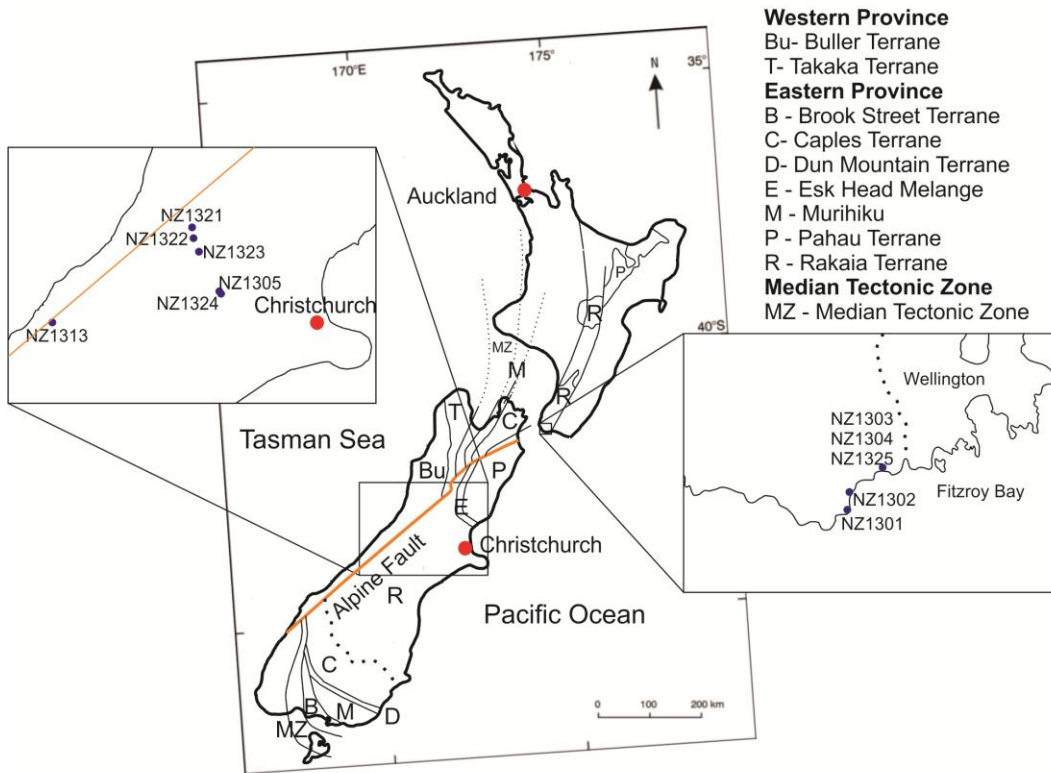


**Figure 1:** Location map of New Zealand, edited from Wandres et al. (2005) and Adams et al. (2007), displaying the sample locations from the North and South Islands. The table in the top right displays the different terranes throughout New Zealand and its corresponding symbol on the map. The sample locations are represented by blue dots with the sample name listed adjacent to it.

In this study I test whether the provenance of the Rakaia Terrane plausibly lies within Australia, Antarctica or New Zealand. To determine this, U-Pb and  $\epsilon\text{Hf}_{(t)}$  isotopic values were collected from detrital zircons within the Rakaia Terrane using a laser ablation inductively coupled plasma mass spectrometer (LA-ICP-MS) multicollector. Rare earth element (REE) values were also analysed. These data were compared with

$^{40}\text{Ar}$ - $^{39}\text{Ar}$  detrital muscovite single grain total fusion ages. The data is then compared with similar results from the three source regions to determine the Rakaia Terrane's provenance.

## GEOLOGICAL SETTING OF THE RAKAIA TERRANE

The micro-continent of New Zealand is largely underlain by rocks of the Torlesse Supergroup (Wandres et al. 2004). In the North and South Island the basement geology has been divided into three zones: the Western Province, The Median Tectonic Zone and the Eastern Province. The Torlesse Supergroup forms part of the Eastern Province and is divided into two terranes, the Rakaia Terrane and the Pahau Terrane (Figure 1). The Rakaia Terrane is Permian to Late Triassic in age and the Pahau Terrane is Late Jurassic to Early Cretaceous in age (Wandres et al. 2005). The two terranes are separated by the Esk Head Mélange (Mortimer 2004, Wandres et al. 2005, Wandres et al. 2004). The model favoured for the deposition of the Torlesse is a submarine fan model that has undergone an accretionary wedge model of deformation (Wandres et al. 2005). This submarine fan formed along Gondwana's proto-Pacific margin. It developed after the Neoproterozoic-Ordovician Ross Orogeny and the Late Devonian to Early Triassic New England Fold Belt (Wandres et al. 2004, Rosenbaum et al. 2012, Rosenbaum and Rubatto 2012). Lithologically, the Rakaia Terrane is largely dominated by turbiditic quartzofeldspathic fine - medium grained sandstones and mudstones. The lithology is largely monotonous, however, it does also contain minor amounts of Carboniferous-Permian basalts that have been interpreted as the oceanic crust the turbidites were deposited on (Mortimer 2004). It also contains minor amounts of volcanics, chert and some conglomerate layers.

## GEOLOGICAL HISTORY OF THE POTENTIAL SOURCE REGIONS TO THE RAKAIA TERRANE

### New England Fold Belt

The New England Fold Belt forms part of the Tasmanides orogenic collage in eastern Australia (Rosenbaum et al. 2012). This fold belt also forms the easternmost segment of a larger accretionary orogen, the Terra Australis Orogen (Cawood et al. 2011a). This orogeny recorded the Neoproterozoic to Early Mesozoic convergent plate margin of Gondwana (Cawood et al. 2011b). The New England Fold Belt, part of the Terra Australis Orogen, formed along this proto-Pacific margin of Gondwana and is composed of Late Devonian to Early Triassic subduction related sequences (Rosenbaum et al. 2012, Rosenbaum and Rubatto 2012). These sequences include a Devonian-Carboniferous volcanic arc, fore-arc basin and accretionary wedge sequences. There is also an abundance of Permian-Triassic magmatic rocks. The New England Fold Belt is split into the Tamworth Belt and the Tablelands Complex, which have undergone differing levels of metamorphism varying from prehnite-pumpellyite to lower greenschist to amphibolite facies. The boundary between these two areas is marked by the Peel-Manning Fault System, which is defined by blueschists, eclogites and serpentinites of Ordovician age (Rosenbaum et al. 2012). Within the Tablelands complex metamorphism has been dated at ca. 470 Ma, ca. 330 Ma and ca. 260 Ma (Fukui et al. 2012).

### Ross Orogeny

The Ross Orogeny formed part of an orogenic belt that also formed the Delamerian Orogen in Australia and the Tyennan Orogen in Tasmania (Federico et al. 2009, Godard and Palmeri 2013). This orogenic belt is a direct result of the convergent tectonics along

Gondwana's proto-Pacific margin, during the final stages of Gondwana formation in the Neoproterozoic to Early Palaeozoic (Collins and Pisarevsky 2005). Lithologically it is characterised by the Granite Harbour Intrusive series that encompasses granitoid magmatism active during the entire orogenic event. This magmatic belt is dominantly calc-alkaline in composition, however, there is some alkaline, adakitic and A-type magmatism present (Goodge et al. 2012). The different areas of the Ross Orogen underwent differing levels of metamorphism. Northern Victoria Land largely underwent metamorphism within the granulite-amphibolite facies with peak metamorphism occurring at ca. 495-480 Ma. Southern Victoria Land reached peak metamorphism within the greenschist facies. The Central Transantarctic Mountains underwent metamorphism within the amphibolite-granulite facies with biotite cooling ages of 490-480 Ma (Goodge 2007). These metamorphic ages are similar to Vincenzo et al. (2007) which gave ages of biotite and muscovites of  $486.3 \pm 3.5$  Ma and  $489.9 \pm 3.5$  Ma respectively.

### **Brook Street Terrane**

Like the Rakaia Terrane, the Brook Street Terrane comprises part of the Eastern Province in the South Island of New Zealand (Wandres et al. 2004). It is Permian in age and is believed to be an island arc system (Mortimer 2004, Spandler et al. 2005). Lithologically, the terrane is composed largely of volcanogenic sequences. These include basaltic to andesitic volcaniclastics, plagioclase- and clinopyroxene-phyric basalts and some sedimentary rocks. The terrane has undergone metamorphism dominantly in the prehnite-pumpellyite facies, there are some areas, however, that have undergone greenschist facies metamorphism (Spandler et al. 2005). Dating of hornblendes from the Longwood Range gave  $^{40}\text{Ar}$ - $^{39}\text{Ar}$  of 215-245 Ma (Mortimer et al.

1999). The limited studies done on the Brook Street Terrane have largely focused on the Takitimu Mountains and Longwood Ranges. The Takitimu Mountains consist mainly of mafic volcanics which are dominantly tholeiitic. The Longwood Ranges consist of plutonic rocks that have tonalite-trondjemite-granodiorite affinities (Nebel et al. 2007).

## METHODS

Eleven samples were taken from the Rakaia Terrane of the North and South Island of New Zealand, five from the North Island and six from the South Island. Sandstones were targeted and the location of each sample recorded (Supplementary Table 1). A more detailed methodology is given in the Appendix.

### U-Pb zircon geochronology

Techniques used for zircon U-Pb geochronology follow those of Payne et al. (2006) and Wade et al. (2008). The samples were jaw crushed, disc milled and sieved. Zircons from the 400-79  $\mu\text{m}$  fraction were concentrated via panning, magnetic and heavy liquid separation. The zircons were then hand-picked and mounted into epoxy resin mounts. Back-scattered electron and cathodoluminescence (Figure 2) imaging of the mounted zircons was done on a Phillips XL40 Scanning Electron Microscope (SEM) with a Gatan CL detector. The U-Pb analyses were carried out on a New Wave UP-213 laser attached to an Agilent 7500cx ICP-MS at Adelaide Microscopy, University of Adelaide. A spot size of 30  $\mu\text{m}$  with a laser frequency of 5 Hz and output laser percentage of 55% was chosen with ablation times of around 80 seconds. Fractionation was corrected for using primary zircon standard GJ-1 (Thermal ionization mass spectrometry (TIMS) normalization data  $^{207}\text{Pb}/^{206}\text{Pb} = 608.3$  Ma,  $^{238}\text{U}/^{206}\text{Pb} = 600.7$  Ma and  $^{235}\text{U}/^{207}\text{Pb} = 602.2$  Ma; Jackson et al. 2004).

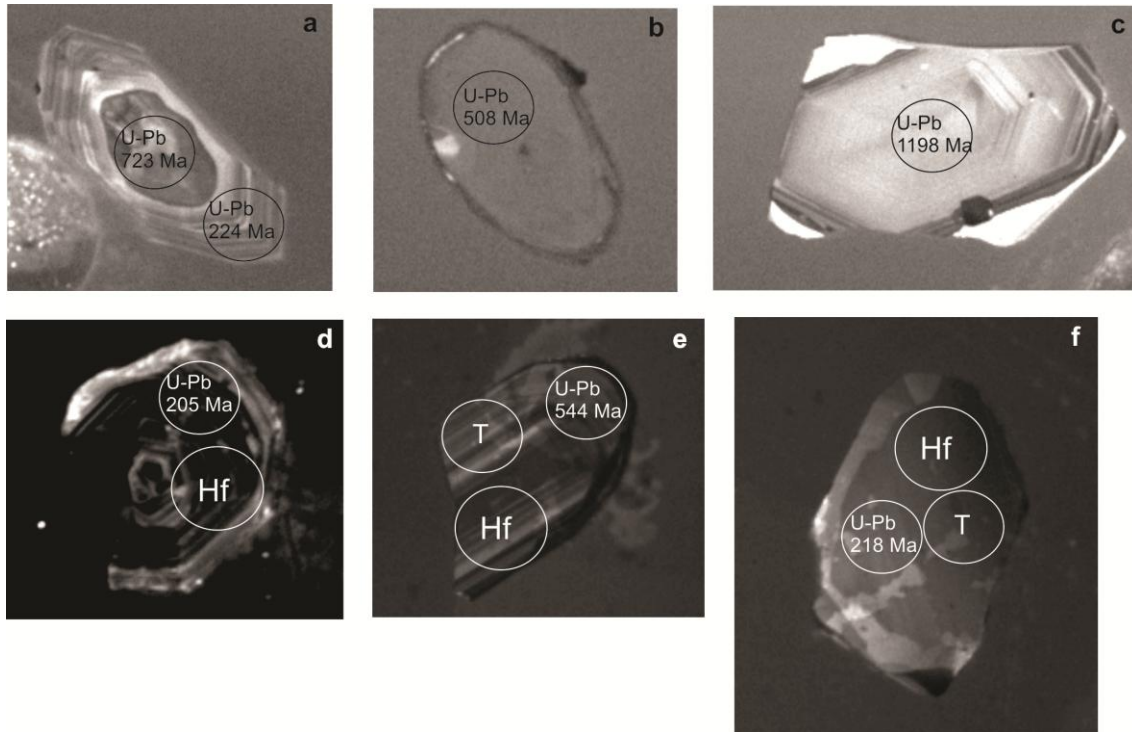


**Figure 2:** Examples of cathodoluminescence images of zircons. Images a, b and c are from sample NZ1301, d is from NZ1322 and e, f are from NZ1323. Spots used for geochronology on each zircon are labelled with the corresponding  $^{238}\text{U}/^{206}\text{Pb}$  age. The circles with T and Hf represent spots for the trace element concentrations and Hf isotope analysis respectively.

Accuracy of the methodology was verified by repeat analysis of the Plešovice zircon ( $^{238}\text{U}/^{206}\text{Pb} = 337.13 \pm 0.37$  Ma). The weighted average ages obtained during this study for Plešovice were  $354 \pm 19$  Ma for  $^{207}\text{Pb}/^{206}\text{Pb}$ ,  $334 \pm 4$  Ma for  $^{238}\text{U}/^{206}\text{Pb}$ , and  $335 \pm 3$  Ma for  $^{235}\text{U}/^{207}\text{Pb}$ , 95% confidence; n=20 (Sláma et al. 2008). Data were rejected based on the presence of common lead based on a combination of intensity of the raw  $^{204}\text{Pb}$  counts, and following this, weighted average  $^{207}\text{Pb}/^{206}\text{Pb}$  age calculations at  $2\sigma$  confidence are reported. Due to the unresolvable isobaric interference of Hg on  $^{204}\text{Pb}$ , no common Pb correction was undertaken. The data were further refined by rejecting data  $>5\%$  discordant. All zircon data are given in Supplementary Tables 2-9.

### Zircon Hf isotope analysis

Methods for zircon Hf isotopes analyses follow that of Griffin et al. (2006b) and Payne et al. (2013). The analyses were undertaken on a LA-MC-ICPMS with an attached New Wave UP-193 Excimer laser and Thermo-Scientific Neptune multicollector at the University of Adelaide Waite Campus. This Excimer laser delivered a beam of 198nm UV light with beam diameter of 35  $\mu\text{m}$  with a repetition rate of 5 Hz. For the analyses the masses 172, 175, 176, 177, 178, 179 and 180 were all measured concurrently. Prior to any analyses, the data were normalised such that  $^{179}\text{Hf}/^{177}\text{Hf} = 0.7325$ . Interference of  $^{176}\text{Lu}$  on  $^{176}\text{Hf}$  was corrected for by calculating  $^{176}\text{Lu}/^{176}\text{Hf}$  with the isotope  $^{175}\text{Lu}$  and  $^{176}\text{Lu}/^{175}\text{Lu}$  equals 0.02669 following Patchett (1983). The interference of  $^{176}\text{Yb}$  on  $^{176}\text{Hf}$  was corrected by measuring the isotope  $^{172}\text{Yb}$  and coupling this with  $^{176}\text{Yb}/^{172}\text{Yb}$  values to calculate  $^{176}\text{Yb}/^{177}\text{Hf}$ . The  $^{176}\text{Yb}/^{172}\text{Yb}$  ratio was calculated by adding Yb to the JMC475 Hf standard to find the value of  $^{176}\text{Yb}/^{172}\text{Yb}$  that gives the value required to yield a known value of  $^{176}\text{Hf}/^{177}\text{Hf}$  (Griffin et al. 2004). Both prior to, and during, the analyses the standard Mudtank zircons were analysed to ensure accuracy, average corrected value  $^{176}\text{Hf}/^{177}\text{Hf} = 0.282515 \pm 0.000021$  with  $2\sigma$  confidence and  $n=11$  (Griffin et al. 2006a, Howard et al. 2009). The  $^{176}\text{Hf}/^{177}\text{Hf}$  ratios were calculated from the measured  $^{176}\text{Lu}/^{176}\text{Hf}$  values giving an uncertainty of  $<\pm 0.05\text{Hf}$ . The decay constant of  $1.856 \times 10^{-11} \text{ y}^{-1}$  for  $^{176}\text{Lu}$  as calculated in Scherer et al. (2001) was selected for the calculation of  $\epsilon\text{Hf}$  values. All the Hf data are given in Supplementary Table 10-13.

### $^{40}\text{Ar}-^{39}\text{Ar}$ Dating

From the samples selected for  $^{40}\text{Ar}-^{39}\text{Ar}$  dating, unaltered, optically transparent,  $>400$   $\mu\text{m}$ -muscovites were separated. These minerals were separated using a Frantz magnetic separator, and then carefully hand-picked under an Olympus SZ51 microscope and sent

to the Western Australian Argon Isotope Facility (WAAIF), at Curtin University. There the muscovites were leached in diluted HF for one minute and then thoroughly rinsed with distilled water in an ultrasonic cleaner. Samples were loaded into 10 large wells of one 1.9 cm diameter and 0.3 cm depth aluminium disc. These wells were bracketed by small wells that included Fish Canyon sanidine (FCs) used as a neutron fluence monitor for which an age of  $28.305 \pm 0.036$  Ma ( $1\sigma$ ) was adopted (Renne et al. 2010) based on the calibration by Jourdan and Renne (2007). The mean J-values computed from standard grains within the small pits range from  $0.0026752 \pm 0.0000040$  (0.15%) to  $0.0026644 \pm 0.000054$  (0.20%) determined as the average and standard deviation of J-values of the small wells for each irradiation disc. Mass discrimination was monitored using an automated air pipette and provided a mean value of  $1.00646 \pm 0.00238$  per dalton (atomic mass unit) relative to an air ratio of  $298.56 \pm 0.31$  (Lee et al. 2006). The correction factors for interfering isotopes were  $(^{39}\text{Ar}-^{37}\text{Ar})_{\text{Ca}} = 7.30 \times 10^{-4}$  ( $\pm 11\%$ ),  $(^{36}\text{Ar}-^{37}\text{Ar})_{\text{Ca}} = 2.82 \times 10^{-4}$  ( $\pm 1\%$ ) and  $(^{40}\text{Ar}-^{39}\text{Ar})_{\text{K}} = 6.76 \times 10^{-4}$  ( $\pm 32\%$ ). The samples were fusion heated using a 110 W Spectron Laser System with a Nd-YAG laser for 60 seconds. Ar isotopes (Supplementary Table 14-18) were measured in a static mode using a MAP 215-20 mass spectrometer with a Balzers SEV 217 electron multiplier. Data acquisition was done with the Argus program and then processed using ArArCALC software and ages calculated using decay constants from Renne et al. (2010).

### Trace element analysis

Trace element analysis was undertaken on zircons previously dated by U-Pb following the method outlined by Belousova et al. (2002). This was undertaken on a Cameca SX51 electron microprobe located at Adelaide Microscopy, The University of Adelaide.

Spot analyses were conducted using a beam current of 20 nA and an accelerating voltage of 15 kV, with a defocused beam of 5 micron. Concentrations calculated on the microprobe (Supplementary Table 19-22) were in percent oxide (Ox%). Calibration was done on natural and synthetic mineral standards supplied by Astimex, Taylor, and P&H. The trace element compositions (Supplementary Table 23-26) were then collected via LA-ICP-MS, at Adelaide Microscopy, following the methods of Raimondo et al. (2011).  $^{178}\text{Hf}$  was used as the internal standard for the zircons, this was pre-determined from the microprobe results. Zircons were analysed using an Agilent 7500cc quadrupole ICP-MS with an attached New Wave UP-213 Nd-YAG laser. A spot size of 30  $\mu\text{m}$  was chosen with a repetition rate of 5 Hz with the energy set to produce a fluence of ca. 7  $\text{Jcm}^{-2}$ . The machine was tuned to peak sensitivity to minimize the production of interfering oxide species so that  $^{232}\text{Th}^{16}\text{O}/^{232}\text{Th}$  was routinely  $< 0.5\%$ . Data were collected using a time-resolved data acquisition in fast peak jumping mode and then processed using the GLITTER software (Achterbergh et al. 2001). The results were calibrated against the NIST 610 standard glass with the coefficients of Pearce et al. (1997) Groups of 15 analyses were bracketed by repeat analyses of the NIST 610 standard which corrected for any instrument drift. A linear drift correction based on the analysis sequence and on the bracketing of NIST-610 was applied to the count rate of each sample.

## OBSERVATIONS AND RESULTS

### Trace Element Compositions

The trace element compositions from samples NZ1301, -04, -23 and -24 (Figure 3) define likely source rocks for the zircons (Belousova et al. 2002). The data are almost

entirely confined within the granitoid field of Belousova et al. (2002) with some scattered data points falling within the carbonatite and lamproite field. Within the granitoid field, the data are essentially confined within the granodiorite and tonalite field with a few data points suggesting a granite source.

### **U-Pb Geochronology**

#### NZ1301

From the 120 zircons analysed, 94 ages fell within the concordancy range ( $\leq 5\%$  discordance). The largest significant population, with 31 zircons, forming approximately 33% of the total ages, ranges in age from ca. 240-200 Ma. The other populations range in age from ca. 350-300 Ma, ca. 520-415 Ma and ca. 1060-910 Ma which comprise around 9, 13 and 7% and contain 8, 12 and 7 zircons respectively. The youngest <5% discordant  $^{238}\text{U}/^{206}\text{Pb}$  age,  $202.4 \pm 2.37$  Ma, is taken as the maximum deposition age, which is Rhaetian in age.

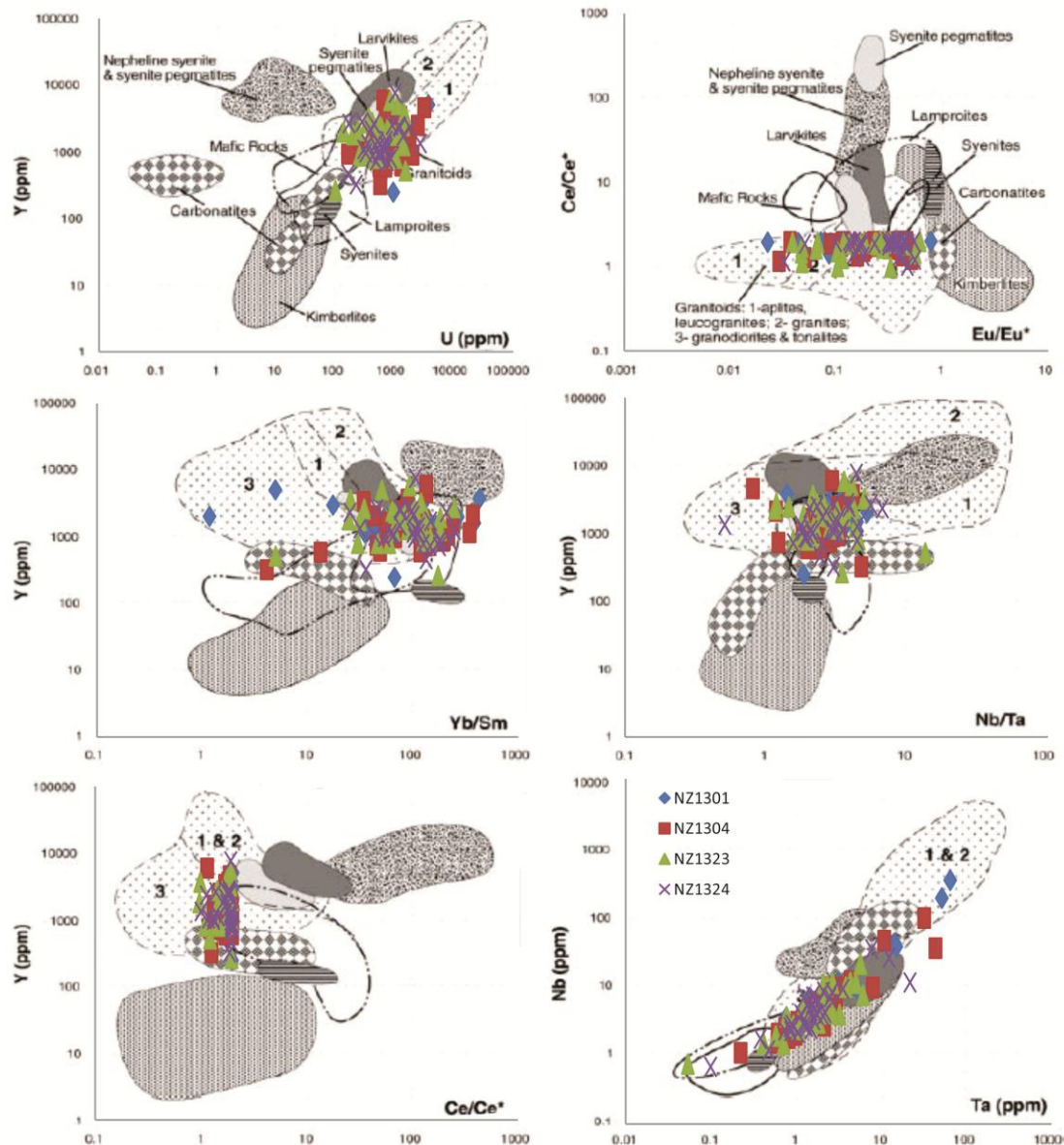


**Figure 3:** Trace element concentrations of Rakaia Terrane zircons compared with data from Belousova et al. (2002), the zircons were analysed were from sample NZ1301, NZ1304, NZ1323 and NZ1324. From each sample 30 zircons were analysed, resulting in 120 per graph, the data points have been superimposed on source fields, created by Belousova et al. (2002), allowing the determination of the source rock. In these graphs Ce\* is the average of the chondrite-normalised La and Pr concentrations while Eu\* is the average of the chondrite-normalised Sm and Gd concentrations. Within the Granitoid field, 1 represents aplites and leucogranites, 2 granites; 3 granodiorites and tonalites.

### NZ1302

From the 120 zircons analysed, 77 ages fell within the concordancy range ( $\leq 5\%$  discordance). The largest significant population with 28 zircons, ranges in age from ca.

260-200 Ma and comprise 36% of the total ages. The remaining populations range in age from ca. 360-300 Ma, ca. 600-500 Ma and ca. 1040-950 Ma. These populations comprise 10, 20 and 8% with 8, 16 and 6 zircons respectively. The youngest <5% discordant  $^{238}\text{U}/^{206}\text{Pb}$  age of  $205.6 \pm 2.67$  Ma, which is Rhaetian in age, is taken as the maximum depositional age.

#### NZ1304

From the 120 zircons analysed, 67 ages fell within the concordancy range ( $\leq 5\%$  discordance). The largest significant population, with 34 zircons, comprises 50% of the total ages ranges in age from 250-200 Ma. The remaining populations, ca. 490-450 Ma, ca. 580-520 Ma and ca. 1100-900 Ma, comprise 9, 7 and 10% with 6, 5 and 7 zircons respectively. The youngest <5% discordant  $^{238}\text{U}/^{206}\text{Pb}$  age of  $205.6 \pm 2.68$  Ma, which is Rhaetian in age, is taken as the maximum depositional age.

#### NZ1321

From the 71 zircons analysed, 21 ages fell within the concordancy threshold ( $\leq 5\%$  discordance). The largest significant population, with 5 zircons, comprises 23% of the total ages and ranges in age from ca. 260-210 Ma. The remaining populations comprise 13, 13 and 18% of the total ages and range in age from ca. 510-460 Ma, ca. 620-540 Ma and ca. 1040-900 Ma and contain 3, 3 and 4 zircons. The youngest <5% discordant  $^{238}\text{U}/^{206}\text{Pb}$  age of  $222.4 \pm 3.11$  Ma, which is Norian in age, is taken as the maximum depositional age.

### NZ1322

From the 120 zircons analysed, 55 fell within the concordancy threshold. The most significant population, containing 28 zircons, ranges in age from ca. 270-200 Ma and comprises 51% of the total ages. The remaining populations range in age from ca. 550-430 Ma and ca. 1100-900 Ma, comprise 20 and 11% and contain 11 and 6 zircons respectively. The youngest <5% discordant  $^{238}\text{U}/^{206}\text{Pb}$  age of  $202.2 \pm 2.21$  Ma, which is Rhaetian in age, is taken as the maximum depositional age.

### NZ1323

From the 120 zircons analysed, 79 fell within the concordancy threshold. The most significant population, with 38 zircons, ranges in age from 270-200 Ma and comprises 48% of the total ages. The remaining populations range in age from ca. 350-310 Ma, 590- 480 Ma and ca. 1050-950 Ma which comprise 6, 22 and 6% with 5, 17 and 5 zircons respectively. The youngest <5% discordant  $^{238}\text{U}/^{206}\text{Pb}$  age of  $205.5 \pm 2.7$  Ma, which is Rhaetian in age, is taken as the maximum depositional age.

### NZ1324

From the 120 zircons analysed, 58 fell within the concordancy threshold. The most significant population, with 31 zircons, ranges in age from ca. 270-220 Ma and comprises 53% of the total ages. The remaining populations, ca. 350-300 Ma and 560-490 Ma, comprise 7 and 22% respectively of the total ages and contain 4 and 13 zircons. The youngest <5% discordant  $^{238}\text{U}/^{206}\text{Pb}$  age of  $219.5 \pm 2.49$ , which is Norian in age, is taken as the maximum depositional age.

**NZ1325**

From the 120 zircons analysed, 71 fell within the concordancy threshold. The most significant population, with 24 zircons, ranges in age from ca. 270-210 Ma and comprises 33% of the total ages. The remaining populations, ca. 500-450 Ma, ca. 610-540 Ma and 1120-930 Ma comprises 9, 15 and 15% respectively of the total ages, these populations contain 7, 11 and 11 zircons respectively. The youngest <5% discordant  $^{238}\text{U}/^{206}\text{Pb}$  age of  $213.7 \pm 2.79$ , which is Norian in age, is taken as the maximum depositional age.

**TOTAL RAKAIA TERRANE**

The detrital age results for all eight samples are shown in Figure 4. When these ages are compiled there are four populations (Figure 5), one in the Triassic (ca. 230 Ma), one in the mid-Carboniferous (ca. 320 Ma), a Neoproterozoic to Ordovician population (ca. 580-450 Ma) and a Mesoproterozoic to Neoproterozoic population (ca. 1100-980 Ma). These populations do not contain all the detrital ages, with ages also recorded from 930 – 580 Ma. When the rims and cores of the same zircon were dated, both yielded similar ages, otherwise the rims were dominantly Carboniferous to Triassic in age (Figure 2).

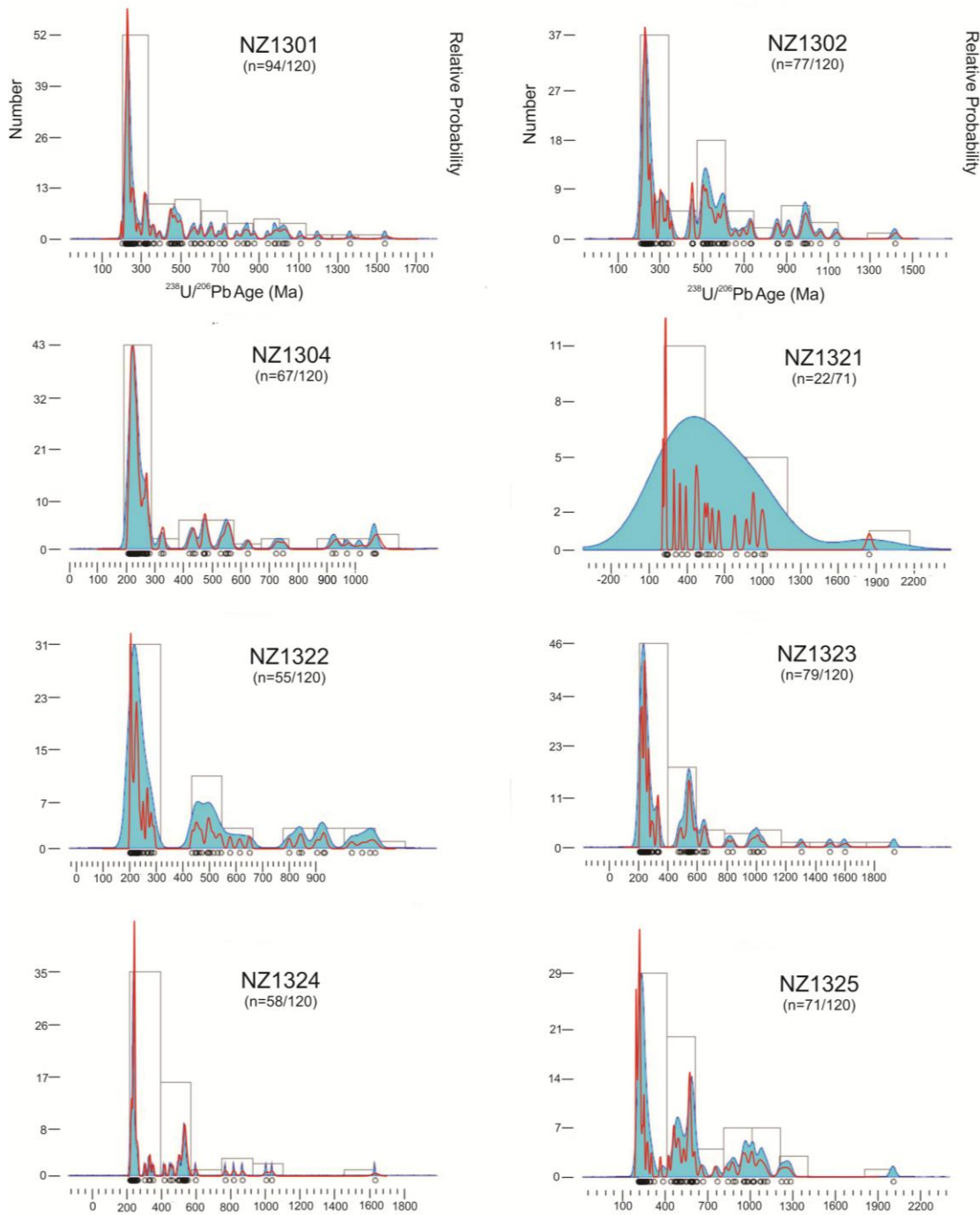


**Figure 4: Concordant detrital zircon ages, the red lines represent probability density plots with a 5% concordancy threshold and  $2\sigma$  uncertainty. The blue shaded area is the corresponding kernel density estimator (Vermeesch 2012) with the histogram in grey. The sample name is given at the top with the number of concordant ages used in the graph compared with the total number analysed is given underneath.**

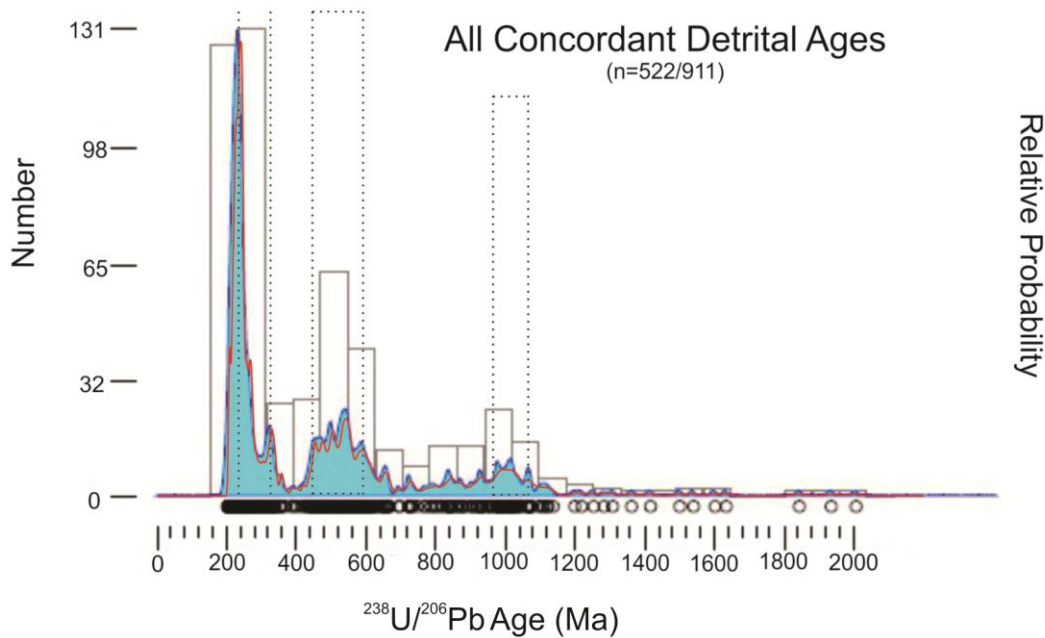


**Figure 5:** All 523 concordant detrital zircon ages, the probability density plot, with  $2\sigma$  uncertainty, is shown in red with the kernel density estimator (Vermeesch 2012) in blue and histogram in grey. The black dashed lines represent the major populations, the dashed rectangles represent the Ordovician to Neoproterozoic and the Neoproterozoic to Mesoproterozoic populations. The number of concordant ages graphed out of the total number of analyses is given under the graph title.

## Hf Isotopes

The corrected  $\epsilon\text{Hf}_{(t)}$  values from the Rakaia Terrane are given in Figure 6, isotope ratios were taken from samples NZ1301, -22, -23 and -25.

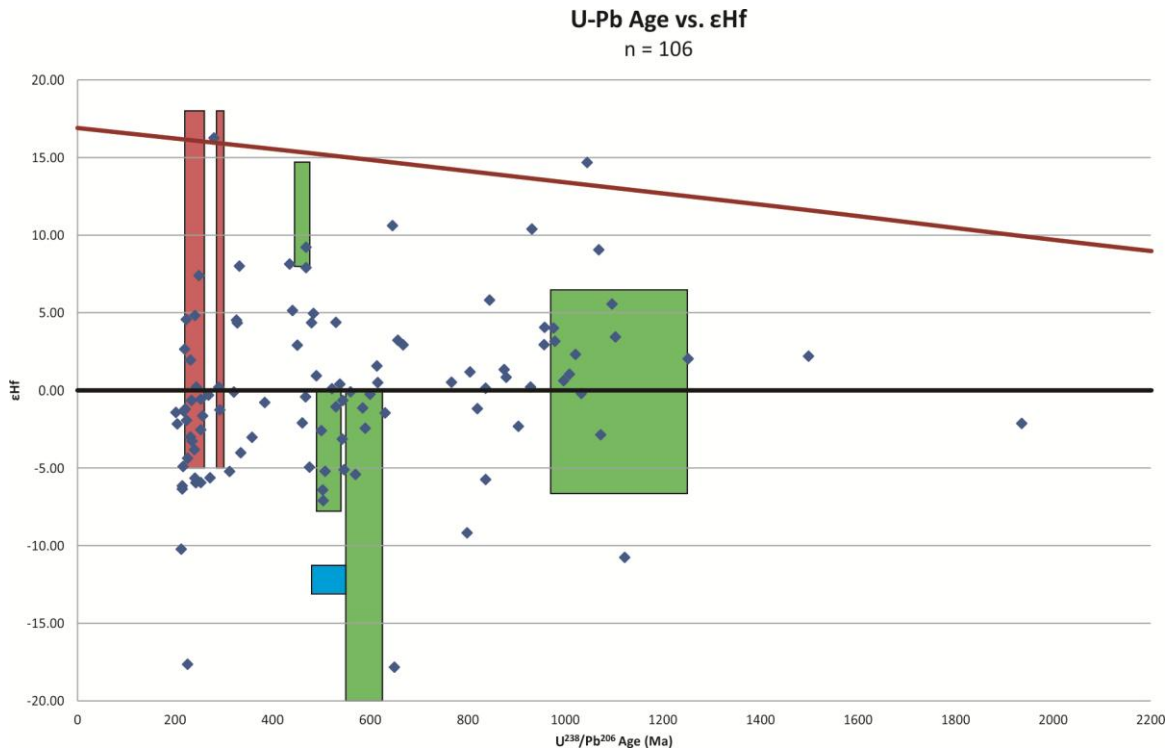


**Figure 6:**  $\epsilon\text{Hf}_{(t)}$  values plotted against the corresponding  $^{238}\text{U}/^{206}\text{Pb}$  zircon age, n is the total number of analyses. The analyses were taken from samples NZ1301, NZ1322, NZ1323 and NZ1325. The red rectangles represent the  $\epsilon\text{Hf}$  range taken from Phillips et al. (2011), the blue rectangle represents the equivalent  $\epsilon\text{Hf}$  range from Borg et al. (1990) and Goodge et al. (2012) the green rectangles the  $\epsilon\text{Hf}$  range from detrital zircons published by Glen et al. (2011). The solid red line is the depleted mantle while the solid black line is the CHUR.

#### $^{40}\text{Ar}-^{39}\text{Ar}$ Ages

From each sample the fusion ages were calculated from individual detrital muscovites.

Sample NZ1301 has detrital muscovites that range in  $^{40}\text{Ar}-^{39}\text{Ar}$  age from ca. 240-210

Ma. Sample NZ1303 contains muscovites that largely range from ca. 250-230 Ma with

one muscovite with a ca. 340 Ma age. The  $^{40}\text{Ar}-^{39}\text{Ar}$  ages from sample NZ1323 range

from ca. 240-210 Ma. In sample NZ1324 the ages range from ca. 250-240 Ma and in

NZ1325 the ages vary from ca. 270-240 Ma. From the Ar data, age plots were

generated (Figure 7) which give two ages, the first in the Carboniferous (ca. 340 Ma)

and the second in the Triassic (ca. 250-220 Ma). These plots give the age when the

provenance was cooled below  $\sim 350^\circ$  as this is the approximate closure temperature of

Ar in muscovite (Adams 2003).

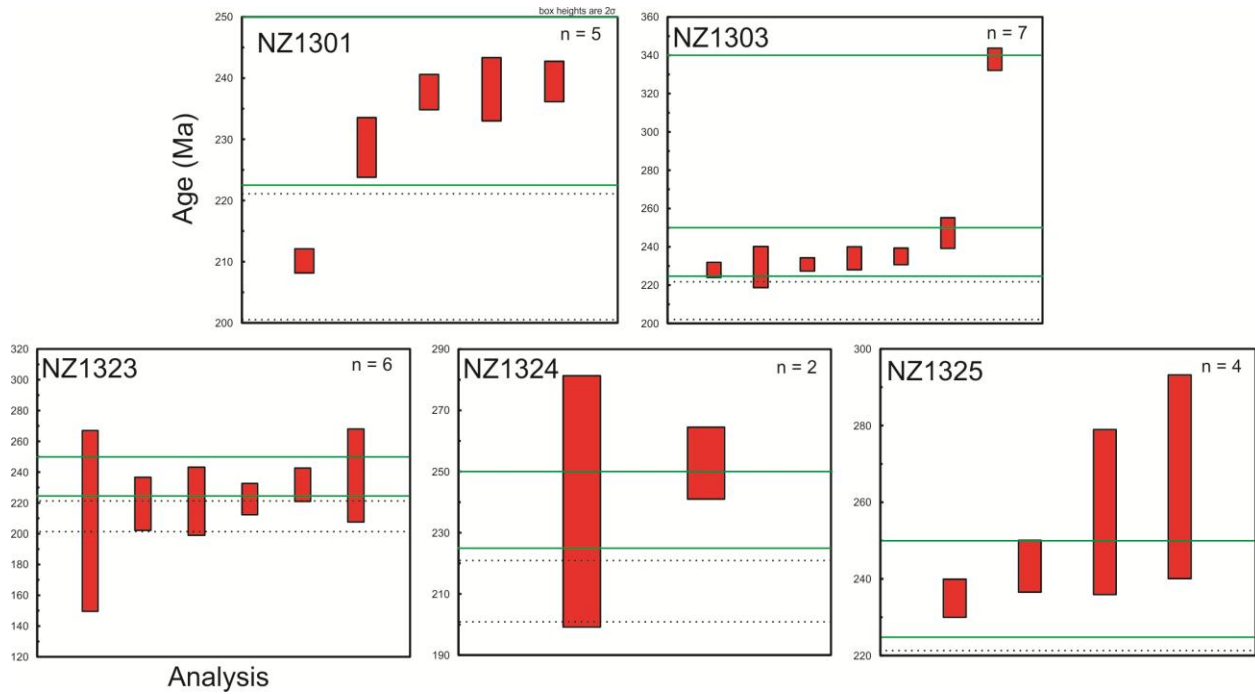


**Figure 7:** Age plots generated from  $^{40}\text{Ar}$ - $^{39}\text{Ar}$  total fusion ages taken from detrital muscovites. The red rectangles represent individual Ar ages with their associated error. The green lines represent the Ar ages of ca. 340 Ma and ca. 250-220 Ma. The sample the muscovites were taken from is given in the top left hand corner. The number of muscovites analysed, n, is given in the top right hand corner. The dashed black lines represent the maximum depositional age taken from the detrital zircon  $^{238}\text{U}/^{206}\text{Pb}$  ages.

## DISCUSSION

### Plausible Source Rock Types

Since the provenance of these zircons is poorly understood, gaining an understanding of their likely source region will allow a more plausible determination of their provenance.

From the 120 zircons analysed for trace elements, the majority of these lay within the granodiorite and tonalite field with scattered data points within the granite, carbonatite and lamproite field. From this the zircons were likely formed within a plutonic intermediate to felsic rock with possible minor inputs from sub-volcanic ultramafics and carbonatites. When these results are divided into their respective populations, the Carboniferous – Triassic population are entirely derived from plutonic intermediate-felsic rocks, the pre-Silurian populations however appear to have minor inputs from the

sub-volcanic ultra-mafic rocks and carbonatites. This suggests a possible change in source region or a changing sediment transport system.

### **Maximum Deposition Age**

The maximum deposition age varies slightly depending on the sample. From each sample the youngest ages within the concordant threshold were taken as the maximum deposition age. These concordant ages range from ca. 222 – 202 Ma, giving an Upper Triassic maximum depositional age.

### **Source Constraints from U-Pb Data**

Zircon age distributions are considered with respect to the three potential source regions, the New England Fold Belt, the Brook Street Terrane and the Ross Orogen, that are described in the introduction.

#### **PRE-SILURIAN ZIRCONS**

When considering pre-Silurian zircons solely, two major populations are apparent. The Neoproterozoic to Ordovician population, ca. 580-450 Ma, in the Rakaia Terrane, roughly correlates with a 600-500 Ma population, the “Pacific-Gondwana igneous component”, which has been identified throughout Gondwana (Cawood et al. 2007, Fergusson et al. 2013, Meinhold et al. 2013). The Ross Orogen, specifically Terre Adelie Land, has granitic rocks of similar age, 580-575 Ma and 515-500 Ma (Goodge and Fanning 2010). There are also the granitoids of the Granite Harbour Intrusive series that range in age from 550 – 480 Ma (Goodge et al. 2012). The New England area cannot be a plausible original source region of these zircons as there is no magmatic activity of similar age. However, the Upper Cretaceous Winton Formation of north

eastern Queensland has similar aged detrital zircons that may be sourced from the same region as the Rakaia Terrane (Tucker et al. 2013). Moving further south to the Lachlan Fold Belt, specifically the Macquarie Arc, magmatic activity has been recorded throughout the Cambrian and Ordovician (Crawford et al. 2007, Glen et al. 2011).

Within the Lachlan Fold Belt there were three phases of largely calc-alkaline magmatism, the first ca. 480 Ma, the second from ca. 468-455 Ma and the third from ca. 449-443 Ma. Detrital zircons have also been recorded, varying in age from ca. 1250-970 Ma, 625-550 Ma and 540-490 Ma (Glen et al. 2011). Sircombe (1999) and Squire et al. (2006) both collected U-Pb zircon ages throughout Victoria which overlap with the Rakaia population. Sircombe (1999) collected zircons from modern beach sands while the zircons from Squire et al. (2006) were extracted from metasedimentary rocks. However, if these zircons were to be shed from these regions into the Rakaia Terrane, then the population distributions should be similar. Methods outlined by Vermeesch (2013) allow different zircon populations to be compared statistically with multidimensional scaling (MDS) maps and QQ plots (Figures 8 & 9). A QQ plot compares two distributions by dividing them up into ten quartiles. These quartiles are then plotted against each other and if they are similar the data will lie on the diagonal 1:1 line. An MDS map is a visual representation of the dissimilarity between the two distributions, based on the Kolmogorov-Smirnov (KS) test. If two populations on a MDS map are connected by a solid line then their distributions are the most similar or least dissimilar, if connected by a dotted line then that is the second most similar distribution. This provides a visual representation as to the similarities of distributions. From Figure 8 the pre-Silurian Rakaia zircons are predominantly associated with populations from Sircombe (1999). There is also associations with data from Tucker et

al. (2013) and Squire et al. (2006). These pre-Silurian zircons are therefore plausibly sourced from the Lachlan Fold Belt and share similar features as the Winton Formation detritus of north-eastern Queensland. No magmatism occurred within the Brook Street Terrane prior to the Triassic so it is only a possible source of the Triassic population.

The other pre-Silurian population within the Rakaia Terrane is Meso- to Neoproterozoic in age, ca. 1100-980 Ma. This population also overlaps with a 1300-1000 Ma population also identified throughout Gondwana (Cawood et al. 2007, Fergusson et al. 2013, Meinhold et al. 2013). Zircon ages within this range from Sircombe (1999), Tucker et al. (2013) and Squire et al. (2006) again make the Lachlan Fold Belt and north eastern Queensland plausible source regions.

Not all of the pre-Silurian zircons are within these major populations, there are still a number of middle Neoproterozoic zircons (ca. 980-540 Ma) not accounted for. Detrital studies of Antarctica produced ages within this range (Veevers and Saeed 2008, Veevers and Saeed 2011). As these detrital populations are associated with the Rakaia Terrane in Figure 8, Antarctica is a plausible source region. The Leviathan Formation along with the St Arnaud and Grampians Group, in the Lachlan Fold Belt, also contain Neoproterozoic zircons of this age (Squire et al. 2006). The Winton Formation in north eastern Queensland also has detrital zircons within this range, again supporting the Lachlan Fold Belt and north eastern Queensland as plausible source regions.

## PRE-JURASSIC ZIRCONS

Including the pre-Jurassic zircons there are two major populations, the first of which is in the Carboniferous, ca. 320 Ma. Throughout the northern New England area,

magmatism has been recorded from ca. 360-305 Ma, peaking around 325-315 Ma (Williams and Pulford 2008, Bryan et al. 2004). The magmatism within the northern New England area is restricted to the Connors and Auburn Arches. Within the Northern Connors Arch the oldest suite, the granitoid Urannah Suite, has been dated at  $305 \pm 5$  Ma (Murray 2003). Within the Auburn Arch, the oldest suite has been dated at 330-320 Ma (Murray 2003). The granites within this region have been classified as granodiorites (Murray 2003). Carboniferous magmatism has also been recorded in the Southern New England area, peaking at ca. 347-327 Ma and continuing until 303 Ma. This occurred within the Carroll-Nandewar region within the Tamworth Belt and is rhyolitic to dacitic in composition (Roberts et al. 2004, Williams and Pulford 2008). Within Antarctica, known Carboniferous magmatism is largely confined to the Robertson Bay Terrane within northern Victoria Land. This suite is dominantly composed of granitoids, the Admiralty Intrusives, with minor felsic volcanics, the Gallipoli Volcanics. The reported ages of this suite are ca. 350 Ma (Talarico and Kleinschmidt 2008). The age of ca. 350 Ma from Antarctica corresponds to a gap in the detrital ages from the Rakaia Terrane, suggesting that it is unlikely to be the source of these zircons. In the northern New England area magmatism peaks at 325-315 Ma, which corresponds with the Carboniferous peak (ca. 320 Ma) in the Rakaia detrital ages. Because of this, it is likely the New England area is the source region due to its close proximity to Gondwana's proto-Pacific margin, the overlapping zircon ages and the similarity between zircon trace element calculated source composition and exposed granitoids in New England.

The Triassic population from the Rakaia Terrane occurs at ca. 230 Ma. Within the New England Fold Belt Permian and Triassic magmatism has been well documented

(Holcombe et al. 1997, Cawood et al. 2011a, Rosenbaum et al. 2012). This magmatism produced voluminous I-type granitoids from 260-220 Ma, I and S type granitoids from 300-285 Ma and granodiorites from 280-260 Ma (Rosenbaum et al. 2012). Antarctica also has magmatic events occurring from ca. 236-199 Ma and ca. 180-160 Ma, which involved granitoid emplacement followed by volcanic rocks (Storey et al. 1992). Magmatism within the Brook Street Terrane was older from ca. 290 – 260 Ma and was dominantly basaltic – andesitic in composition (Mortimer et al. 1999, Spandler et al. 2005). The Brook Street Terrane is therefore not a plausible source region. Magmatism within Antarctica is largely too young and is today found away from the facing margin of New Zealand. This supports the New England area being the most plausible source of the zircons.

This means that the pre-Silurian zircons are plausibly sourced from the Lachlan Fold Belt and share similar features as the Winton Formation detritus of north-eastern Queensland, while the pre-Jurassic zircons are sourced from the New England area. Using the QQ plots and MDS maps from Vermeesch (2013) and plotting the pre-Jurassic zircons from the Sircombe (1999), Squire et al. (2006), Tucker et al. (2013), Veevers and Saeed (2008) and the Rakaia Terrane on an MDS map (Figure 10) there is a close association with the Rakaia Terrane and the Winton Formation data from Tucker et al. (2013). From the MDS of the pre-Silurian zircons (Figure 8) there is a spread of plausible source regions. When these pre-Silurian zircons, however, are included with the pre-Jurassic zircons (Figure 10) there is a strong association with the Rakaia and eastern Australia. These pre-Silurian zircons were therefore plausible recycled into the New England area. This recycling would also explain the Triassic rims on older cores,

as when the zircons were shed into the New England area, the associated magmatism would result in growth zonation around these older cores. The similarity with the detritus from the Winton Formation is also interpreted by the fact that the Winton Formation was sourced from the New England/central Queensland region (Tucker et al. 2013).

### Source Constraints from Hf Data

$\epsilon$ Hf and  $\epsilon$ Nd studies from the possible source regions are used here to compare with the data produced in this study. Phillips et al. (2011) described the  $\epsilon$ Hf from the New England Fold Belt which range from -5 to +18. Borg et al. (1990) calculated  $\epsilon$ Nd values from the Ross Orogen which ranged from -10.46 to -11.81. The equation  $\epsilon$ Hf = 1.36 $\epsilon$ Nd + 2.95 from Vervoort et al. (1999) means that Hf data and whole rock Nd data can be compared. Using this equation the equivalent  $\epsilon$ Hf from the Ross Orogen is approximately -11.28 to -13.11. The  $\epsilon$ Hf values calculated by Nebel et al. (2007) for the Brook Street Terrane ranged from +12.0 to +13.4 and +10.4 to +11.4. Similar studies were also done in the Lachlan Fold Belt, the ca. 490-540 detrital population has  $\epsilon$ Hf values that range from -7.78 to 0 and the 550-625 Ma  $\epsilon$ Hf values from -26.6 to 0 (Glen et al. 2011) Ordovician zircons with  $\epsilon$ Hf values up to +15 have also been recorded in the Fairbridge and Cargo Volcanics. The Late Mesoproterozoic detrital population has  $\epsilon$ Hf from -6.44 - +6.47 (Glen et al. 2011). From Figure 6 most of the data is confined within the  $\epsilon$ Hf field taken from Phillips et al. (2011), supporting the New England area being the source of these zircons. The Ross Orogen is discounted as a possible zircon source region because there are no overlapping data (Figure 6). Within the  $\epsilon$ Hf range from Glen et al. (2011) there is some overlap with the Rakaia data. There is still a

significant amount of data that aren't accounted for, suggesting the areas of the Lachlan sampled by Glen et al. (2011) are not the only source of pre-Silurian zircons.

### **Source Constraints from $^{40}\text{Ar}$ - $^{39}\text{Ar}$ Data**

From the age plots in Figure 7 there are two ages at ca. 340 Ma and ca. 250-220 Ma. These ages overlap with the two youngest detrital peaks in the detrital ages from the Rakaia Terrane (Figure 5). Fukui et al. (2012) determined three stages of metamorphism within the New England Fold Belt which occurred at ca. 470 Ma, ca. 330 Ma and ca. 260 Ma.  $^{40}\text{Ar}$ - $^{39}\text{Ar}$  studies undertaken in the Ross Orogen by Vincenzo et al. (2007) analysed both biotites and muscovites, which gave closure ages of  $486.3 \pm 3.5$  Ma and  $486.9 \pm 3.5$  Ma respectively. Mortimer et al. (1999) also undertook  $^{40}\text{Ar}$ - $^{39}\text{Ar}$  studies from hornblendes taken from the Brook Street Terrane which ranged in age from 251-245 Ma. Metamorphism within the Lachlan Fold Belt occurred largely within the Ordovician with  $^{40}\text{Ar}$ - $^{39}\text{Ar}$  of ca. 453 Ma, ca. 440 Ma, ca. 426 Ma and 410-390 Ma (Foster et al. 1998). From this these muscovites are most plausibly sourced from the New England area and the Brooke Street Terrane due to the overlapping Ar ages. As muscovite is not as resistant to erosion and transport as zircon they are less likely to be recycled. If they are recycled however and metamorphosed then the Ar ages would be reset. The Ar data, therefore, supports an interpretation of the turbidites being sourced from the New England area with the pre-Silurian zircons being recycled into the New England area. They cannot be sourced from the Brook Street Terrane as metamorphism within this terrane would have reset the ca. 340 Ma muscovite populations.

## CONCLUSIONS

The data collected from the Rakaia zircons constrain its plausible source region along the east coast of Australia and eliminates Antarctica and the Brook Street Terrane as possible source regions. The Rakaia Terrane had four significant detrital populations in the Triassic, Carboniferous, Ordovician and Proterozoic. The  $\epsilon\text{Hf}_{(t)}$  values ranged from -6 to +6 with rare element analysis indicating a granitoid source region. From this the zircons are interpreted to have been sourced from north eastern Queensland and south - south eastern Victoria. The  $^{40}\text{Ar}/^{39}\text{Ar}$  ages gave two ages in the Carboniferous and the Triassic, suggesting the New England area as the exclusive source. The pre-Silurian zircons were therefore recycled into the New England Area before being eroded and further transported into the Rakaia Terrane along with zircons from contemporaneous magmatism from the New England Fold Belt.

## ACKNOWLEDGMENTS

I thank Alan Collins for discussions and guidance. I also thank Adelaide Microscopy, especially Ben Wade and Aoife McFadden, for use and training on the SEM XL-40, New-Wave LA ICP-MS and the Cameca SX51 Electron Microprobe. I would also like to thank Justin Payne for use of the Thermo-Scientific Neptune Multicollector at the Waite Campus, University of Adelaide and Fred Jourdan for analysing the Ar-Ar data. Finally I would like to thank Katie Howard for ongoing training throughout the year and William Hagger for assistance in the field.

## REFERENCES

- ACHTERBERGH V., et al. 2001 Data reduction software for LA-ICP-MS, *Laser Ablation-ICPMS in the Earth Sciences*, vol. 29, pp. 239-243.
- ADAMS C. J. 2003 K-Ar geochronology of Torlesse supergroup metasedimentary rocks in Canterbury, New Zealand, *Journal of the Royal Society of New Zealand*, vol. 33, pp. 165-187.
- ADAMS C. J., CAMPBELL H. J. & GRIFFIN W. L. 2007 Provenance comparisons of the Permian to Jurassic tectonostratigraphic terranes in New Zealand: perspectives from detrital zircon age patterns, *Geologic Magazine*, vol. 144, pp. 701-729.

- BELOUSOVA E. A., *et al.* 2002 Igneous zircon: Trace element composition as an indicator of source rock type, *Contrib Mineral Petrol* vol. 143, pp. 602-622.
- BORG S. G., DEPAOLO D. J. & M S. B. 1990 Isotopic Structure and Tectonics of the Central Transantarctic Mountains, *Journal of Geophysical Research* vol. 95, pp. 6647-6667.
- BRYAN S. E., *et al.* 2004 U-Pb geochronology of Late Devonian to Early Carboniferous extension-related silicic volcanism in the northern New England fold Belt, *Australian Journal of Earth Sciences*, vol. 51, pp. 645-664.
- CAWOOD P. A., JOHNSON R. W. & NEMCHIN A. A. 2007 Early Palaeozoic orogenesis along the Indian margin of Gondwana: Tectonic response to Gondwana assembly *Earth and Planetary Sciences Letters*, vol. 255, pp. 70-84.
- CAWOOD P. A., *et al.* 2011a Orogenesis without collision: stabilizing the Terra Australis accretionary orogen, eastern Australia, *Geological Society of America Bulletin*, vol. 123, pp. 2240-2255.
- CAWOOD P. A., PISAREVSKY S. A. & LEITCH E. C. 2011b Unraveling the New England orocline, east Gondwana accretionary margin *Tectonics*, vol. 30.
- COLLINS A. S. & PISAREVSKY S. A. 2005 Amalgamating eastern Gondwana: The evolution of the Circum-Indian Orogens, *Earth-Science Reviews*, no. 71, pp. 229-270.
- CRAWFORD A. J., *et al.* 2007 Middle and Late Ordovician magmatic evolution of the Macquarie Arc, Lachlan Orogen, New South Wales, *Australian Journal of Earth Sciences*, vol. 54, pp. 181-214.
- FEDERICO L., *et al.* 2009 The Cambrian Ross Orogeny in northern Victoria Land (Antarctica) and New Zealand: A synthesis, *Gondwana Research*, vol. 15, pp. 188-196.
- FERGUSSON C. L., *et al.* 2013 Evolution of a Cambrian active continental margin: The Delamerian-Lachlan connection in southeastern Australia from a zircon perspective, *Gondwana Research*.
- FOSTER D. A., *et al.* 1998 Chronology and tectonic framework of turbidite-hosted gold deposits in the Western Lachlan Fold Belt, Victoria: 40Ar-39Ar results *Ore Geology Reviews* vol. 13, pp. 229-250.
- FUKUI S., *et al.* 2012 Tectono-metamorphic evolution of high-P/T and low-P/T metamorphic rocks in the Tia Complex, southern New England Fold Belt, eastern Australia: Insights from K-Ar chronology *Journal of Asian Earth Sciences*, vol. 59, pp. 62-69.
- GLEN R. A., *et al.* 2011 U-Pb and Hf isotope data from zircons in the Macquarie Arc, Lachlan Orogen: Implications for arc evolution and Ordovician palaeogeography along part of the east Gondwana margin *Gondwana Research* vol. 19, pp. 670-685.
- GODARD G. & PALMERI R. 2013 High-pressure metamorphism in Antarctica from the Proterozoic to the Cenozoic: A review and geodynamic implications, *Gondwana Research*, vol. 23, pp. 844-854.
- GOODGE J. W. 2007 Metamorphism in the Ross orogen and its bearing on Gondwana margin tectonics, *Geological Society of America Special Paper*, vol. 419, pp. 185-203.
- GOODGE J. W. & FANNING C. M. 2010 Composition and age of the East Antarctic Shield in eastern Wilkes Land determined by proxy from Oligocene-Pleistocene

- glaciomarine sediment and Beacon Supergroup sandstones, Antarctica, *GSA Bulletin*, vol. 122, pp. 1135-1159.
- GOODGE J. W., et al. 2012 Temporal, isotropic and spatial relations of Early Palaeozoic Gondwana-margin arm magmatism, central transantarctic mountains, Antarctica *Journal of Petrology*, vol. 53, pp. 2027-2065.
- GRiffin W. L., et al. 2004 Archean crustal evolution in the northern Yilgarn Craton: U-Pb and Hf-isotope evidence from detrital zircons *Precambrian Research*, vol. 131, pp. 231-282.
- GRiffin W. L., et al. 2006a Comment: Hf-isotope geterogeneity in zircon 91500, *Chemical Geology*, vol. 233, pp. 358-262.
- GRiffin W. L. B., E A , WALTERS S. G. & O'REILLY S. Y. 2006b Archaean and Proterozoic crustal evolution in the Eastern Succession of the Mt Isa district, Australia: U-Pb and Hf-isotope studies of detrital zircons, *Australian Journal of Earth Sciences*, vol. 53, pp. 125-149.
- HOLCOMBE R. J. S., C J , et al. 1997 Tectonic Evolution of the Northern New England Fold Belt: The Permian-Triassic Hunter Bowen event pp. 1-21.
- HOWARD K. E., et al. 2009 Detrital zircon ages: Improving interpretation via Nd and Hf isotropic data *Chemical Geology* vol. 262, pp. 277-292.
- JACKSON S. E., et al. 2004 The application of laser ablation-inductively coupled plasma-mass spectrometry to in situ U-Pb zircon geochronoly, *Chemical Geology*, vol. 211, pp. 47-69.
- JOURDAN F. & RENNE P. R. 2007 Age calibration of the Fish Canyon Sanidine 40Ar/39Ar dating standard using primary K-Ar standards *Geochimica et Cosmochimica Acta*, vol. 71, pp. 387-402.
- KOPPERS A. A. P. 2002 ArArCALC - software for 40Ar/39Ar age calculations *Computers & Geosciences* vol. 28, pp. 605-619.
- LEE J. Y., et al. 2006 A redetermination of the isotropic abundances of atmospheric Ar *Geochimica et Cosmochimica Acta*, vol. 70, pp. 4507-4512.
- MEINHOLD G., MORTON A. C. & AVIGAD D. 2013 New insights into peri-Gondwana paleogeograpgy and the Gondwana super-fan system from detrital zircon U-Pb ages *Gondwana Research* vol. 23, pp. 661-665.
- MORTIMER N. 2004 New Zealand's Geological Foundations *Gondwana Research*, vol. 7, pp. 261-272.
- MORTIMER N., et al. 1999 Geology and thermochronometry of the east edge of the Median Batholith (Median Tectonic Zone): a new perspective on Permian to Cretaceous crustal growth of New Zealand *The Island Arc*, vol. 8, pp. 404-425.
- MURRAY C. 2003 Granites of the Northern New England Orogen, *The Ishihara Symposium: Granites and Associated Metallogenesis*, pp. 101-107.
- NEBEL O., et al. 2007 Hf-Nd-Pb isotope evidence from Permian arc rocks for the long-term presence of the Indian-Pacific mantle boundary in the SW Pacific *Earth and Planetary Sciences Letters*, vol. 254, pp. 377-392.
- PATCHETT J. 1983 REE and Hf in Orgueil - new isotope-dilution data for evalutation of the planetary Hf isotopic growth curve and the Lu-176 Cosmic clock, *Meteoritics*, vol. 18, no. 4, pp. 372-373.

- PAYNE J. L., BAROVICH K. M. & HAND M. 2006 Provenance of metasedimentary rocks in the northern Gawler Craton, Australia: Implications for Palaeoproterozoic reconstructions, *Precambrian Research*, vol. 148, pp. 275-291.
- PAYNE J. L., *et al.* 2013 Reassessment of relative oxide formation rates and molecular interferences on *in situ* lutetium-hafnium analysis with laser ablation MC-ICP-MS *Journal of Analytical Atomic Spectrometry*, pp. 1068-1079.
- PEARCE N. J. G., *et al.* 1997 A compilation of New and Published Major and Trace Element Data for NIST SRM 610 and NIST SRM 612 Glass Reference Materials, *The Journal of Geostandards and Geoanalysis* vol. 21, pp. 115-144.
- PHILLIPS G., LANDENBERGER B. & BELOUSOVA E. A. 2011 Building the New England Batholith, eastern Australia - Linking granite petrogenesis with geodynamic setting using Hf isotopes in zircon *Lithos* vol. 122, pp. 1-12
- PICKARD A. L., ADAMS C. J. & BARLEY M. E. 2000 Australian provenance for Upper Permian to Cretaceous rocks forming accretionary complexes on the New Zealand sector of the Gondwanaland margin *Australian Journal of Earth Sciences*, vol. 47, pp. 987-1007.
- RAIMONDO T., *et al.* 2011 Assessing the geochemical and tectonic impacts of fluid-rock interaction in the mid-crustal shear zones: a case study from the intracontinental Alice Springs Orogeny, central Australia *Journal of Metamorphic Geology*, vol. 29, pp. 821-850.
- RENNE P. R., *et al.* 2010 Joint determination of the 40K decay constants and  $^{40}\text{Ar}^*/40\text{K}$  for the Fish Canyon sanidine standard, and improved accuracy for the  $40\text{Ar}/39\text{Ar}$  geochronology *Geochimica et Cosmochimica Acta*, vol. 74, pp. 5349-5367.
- ROBERTS J., OFFLER R. & FANNING C. M. 2004 Upper Carboniferous to Lower Permian volcanic successions of the Carroll-Nandewar region, northern Tamworth Belt, southern New England Orogen, Australia, *Australian Journal of Earth Sciences*, vol. 51, pp. 205-232.
- ROSENBAUM G., PENGFEI L. & RUBATTO D. 2012 The contorted New England Orogen (eastern Australia): New evidence from U-Pb geochronology of early Permian granitoids, *Tectonics*, vol. 31.
- ROSENBAUM G. & RUBATTO D. 2012 Triassic asymmetric subduction rollback in the southern New England Orogen (eastern Australia): the end of the Hunter-Bowen Orogeny, *Australian Journal of Earth Sciences* vol. 59, pp. 965-981.
- SCHERER E., MUNKER C. & MEZGER K. 2001 Calibration of the lutetium-hafnium clock, *Science*, vol. 293, pp. 683-687.
- SIRCOMBE K. N. 1999 Tracing provenance through the isotope ages of littoral and sedimentary detrital zircon, eastern Australia, *Sedimentary Geology*, no. 124, pp. 47-67.
- SLÁMA J., *et al.* 2008 Plešovcie zircon - A new natural reference material for U-Pb and Hf isotopic microanalysis, *Chemical Geology*, vol. 249, pp. 1-35.
- SPANDLER C., *et al.* 2005 Igneous rocks of the Brook Street Terrane, New Zealand: implications for Permian tectonics of eastern Gondwana and magma genesis in modern intra-oceanic volcanic arcs, *New Zealand Journal of Geology and Geophysics*, vol. 48, pp. 167-183.

- SQUIRE R. J., *et al.* 2006 Did the Transgondwanan Supermountain trigger the explosive radiation of animals on Earth?, *Earth and Planetary Sciences Letters*, vol. 250, pp. 116-133.
- STOREY B. C., *et al.* 1992 Role of subduction-plate boundary forces during the initial stages of Gondwana break-up: evidence from the proto-Pacific margin of Antarctica, *Geological Society, London, Special Publications*, vol. 68, pp. 149-163.
- TALARICO F. & KLEINSCHMIDT G. 2008 The Antarctic Continent in Gondwanaland: A Tectonic Review and Potential Research Targets for Future Investigations. In FLORINDO F. & SIEGERT M. eds. *Developments in Earth and Environmental Sciences*. pp. 259-310.
- TUCKER R. T., *et al.* 2013 Detrital zircon age constraints for the Winton Formation, Queensland: Contextualizing Australia's Late Cretaceous dinosaur faunas, *Gondwana research*, vol. 24, no. 767-779.
- VEEVERS J. J. & SAEED A. 2008 Gamburtsev Subglacial Mountains provenance of Permian-Triassic sandstones in the Prince Charles Mountains and offshore Prydz Bay: Integrated U-Pb and TDM ages and host-rock affinity from detrital zircons, *Gondwana Research*, vol. 14, pp. 316-342.
- VEEVERS J. J. & SAEED A. 2011 Age and composition of Antarctic bedrock reflected by detrital zircons, erratics, and recycled microfossils in Prydz Bay-Wilkes Land-Ross Sea-Marie Byrd Land sector (70°–240°E) *Gondwana Research*, vol. 20, pp. 710-738.
- VERMEESCH P. 2012 On the visualisation of detrital age distributions, *Chemical Geology*, no. 312-313, pp. 190-194.
- VERMEESCH P. 2013 Multi-sample comparison of detrital age distributions, *Chemical Geology*, vol. 341, pp. 140-146.
- VERVOORT J. D., *et al.* 1999 Relationships between Lu-Hf and Sm-Nd isotopic systems in the global sedimentary system, *Earth and Planetary Science Letters*, vol. 168, pp. 79-99.
- VINCENZO G. D., TALARICO F. & KLEINSCHMIDT G. 2007 An 40Ar-39Ar Investigation of the Mertz Glacier area (George V Land, Antarctica): Implications for the Ross Orogen-East Antarctic Craton relationship and Gondwana reconstructions, *Precambrian Research*, vol. 152, no. 152, pp. 93-118.
- WADE B. P., *et al.* 2008 Origin of metasedimentry and igneous rocks from the Entia Dome, eastern Arunta region, central Australia: a U-Pb LA-ICPMA, SHRIMP and Sm - Nd isotope study *Australian Journal of Earth Sciences*, vol. 55, pp. 703-719.
- WANDRES A. M., BRADSHAW J. D. & IRELAND T. 2005 The Paleozoic-Mesozoic recycling of the Rakaia Terrane, South Island, New Zealand: sandstone clast and sandstone petrology, geochemistry, and geochronology *New Zealand Journal of Geology and Geophysics*, vol. 48, pp. 229-245.
- WANDRES A. M., *et al.* 2004 Provenance of the sedimentary Rakaia sub-terrane, Torlesse Terrane, South Island, New Zealand: the use of igneous clast composition to define the source, *Sedimentary Geology* vol. 168, pp. 193-226.

WILLIAMS I. S. & PULFORD A. K. 2008 The contribution of geochronology to understanding the Paleozoic geological history of Australia, *Australian Journal of Earth Sciences*, vol. 55, pp. 821-848.

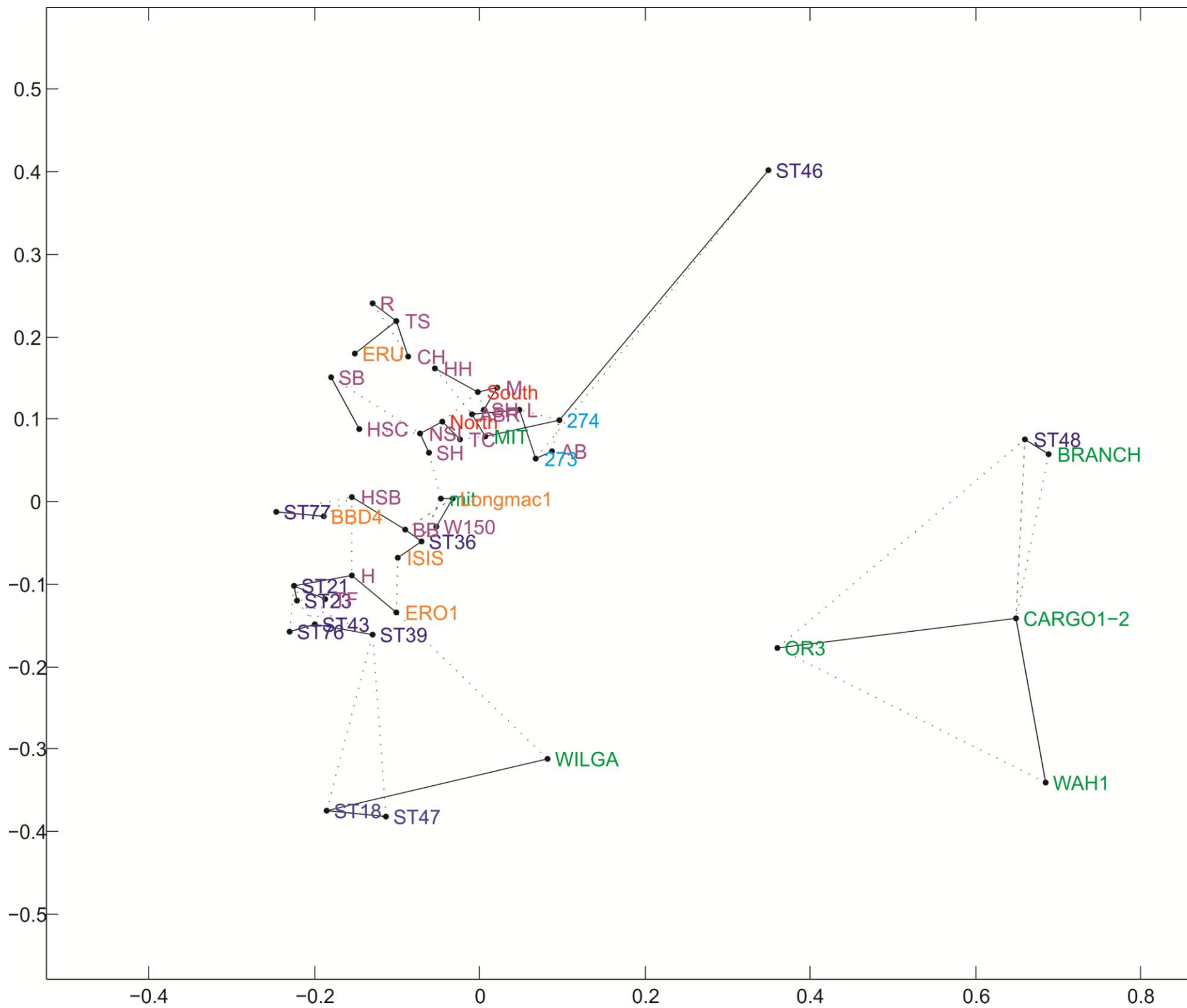


**Figure 8:** The multidimensional scaling (MDS) map for the pre-Silurian zircons from the Rakaia Terrane in red (North, South), Squire et al. (2006) in dark blue (ST18, ST21, ST23, ST36, ST39, ST43, ST46, ST47, ST48, ST76, ST77), Glen et al. (2011) in green (mit, MIT, WILGA, WAH1, CARGO1-2, Branch, OR3), Sircombe (1999) in purple (HH, NSI, CH, SB, TS, SH, AB, ABR, BB, M, SH, H, R W150, L, HSB, HSC, TF, TC), Tucker et al. (2013) in orange (ERU, BBD4, ISIS, ERO1, Longmac1) and Vevers and Saeed (2011) in light blue (273, 274). If two distributions are connected by a solid line, from the Kolmogorov-Smirnov (KS) test, their distributions are the least dissimilar or most similar, if connected by a dotted line it is the second most similar distribution.

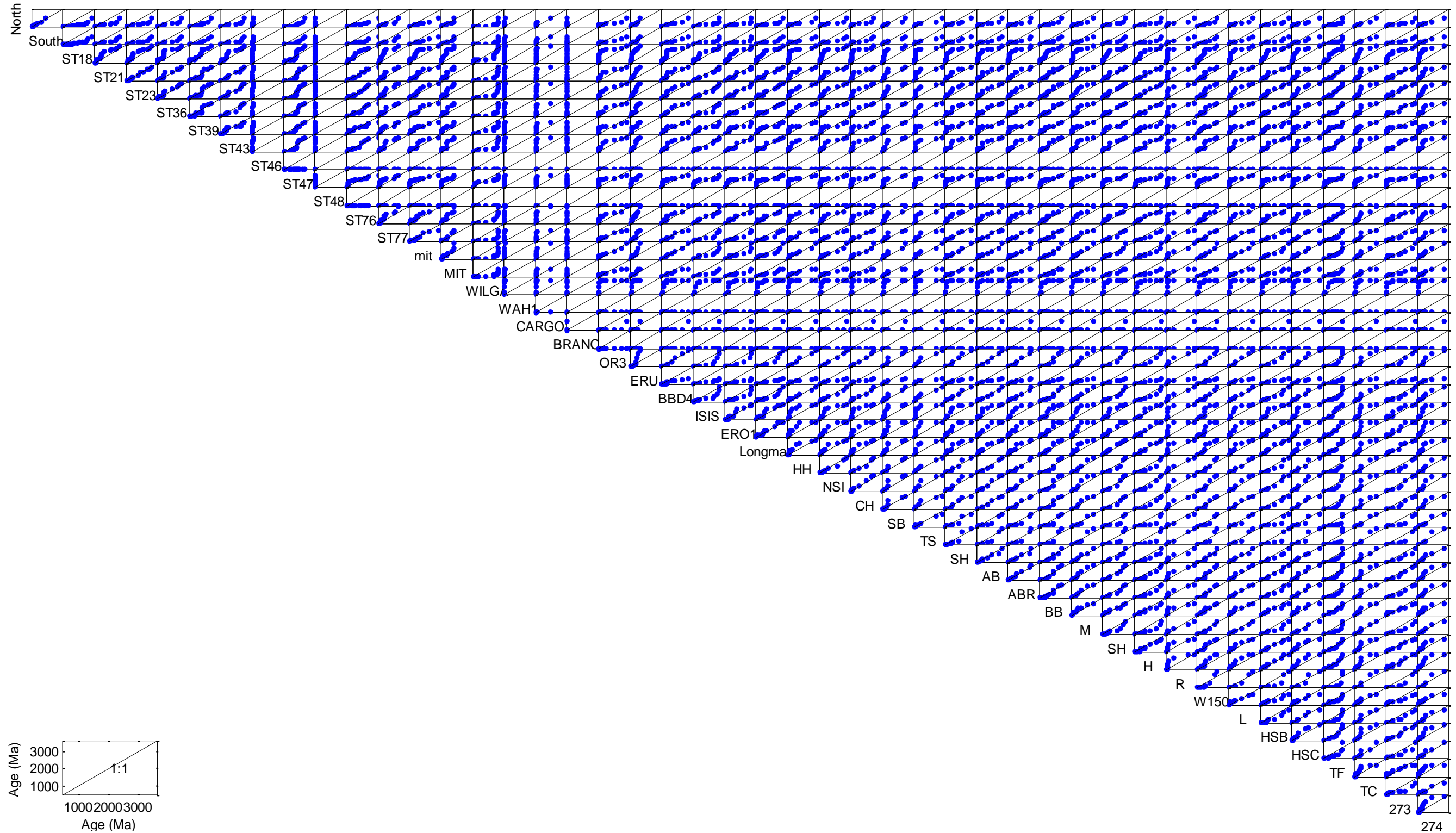
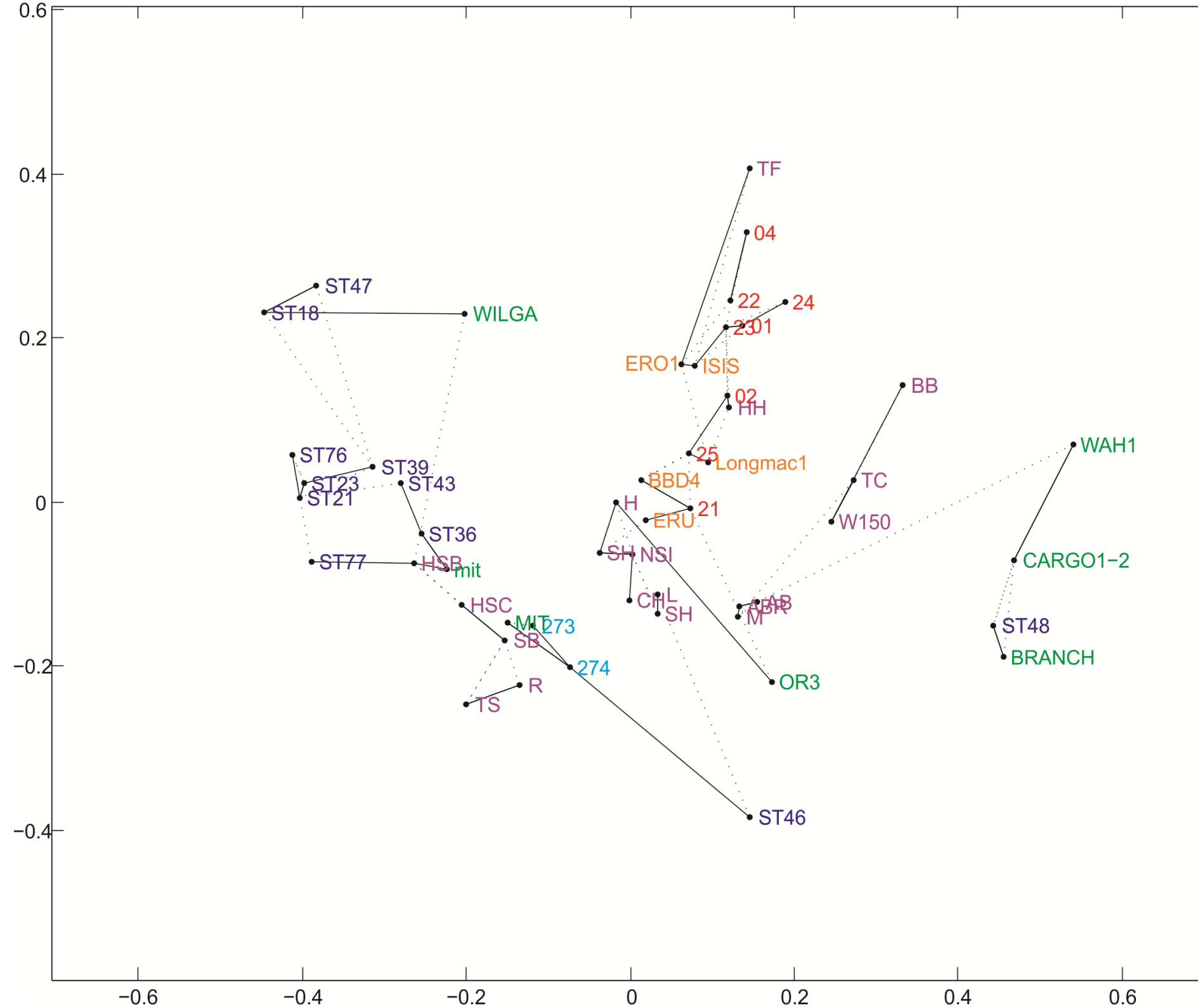


Figure 9: The QQ plot for the pre-Silurian zircons from the Rakaia Terrane in red (North, South), Squire et al. (2006) in dark blue (ST18, ST21, ST23, ST36, ST39, ST43, ST46, ST47, ST48, ST76, ST77), Glen et al. (2011) in green (mit, MIT, WILGA, WAH1, CARGO1-2, Branch, OR3), Sircombe (1999) in purple (HH, NSI, CH, SB, TS, SH, AB, ABR, BB, M, SH, H, R W150, L, HSB, HSC, TF, TC), Tucker et al. in orange (2013) (ERU, BBD4, ISIS, ERO1, Longmac1) and Vevers and Saeed (2011) in light blue (273, 274). If two distributions are connected by a solid line, from the Kolmogorov-Smirnov (KS) test, their distributions are the least dissimilar or most similar, if connected by a dotted line it is the second most similar distribution.



**Figure 10:** The multidimensional scaling (MDS) map for the pre-Jurassic zircons from the Rakaia Terrane in red (01, 02, 04, 21, 22, 23, 24, 25), Squire et al. (2006) in dark blue (ST18, ST21, ST23, ST36, ST39, ST43, ST46, ST47, ST76, ST77), Glen et al. (2011) in green (mit, MIT, WILGA, WAH1, CARGO1-2, Branch, OR3), Sircombe (1999) in purple (HH, NSI, CH, SB, TS, SH, AB, ABR, BB, M, SH, H, R W150, L, HSB, HSC, TF, TC), Tucker et al. (2013) in orange (ERU, BBD4, ISIS, ERO1, Longmac1) and Veevers and Saeed (2011) in light blue (273, 274). If two distributions are connected by a solid line, from the Kolmogorov-Smirnov (KS) test, their distributions are the least dissimilar or most similar, if connected by a dotted line it is the second most similar distribution.

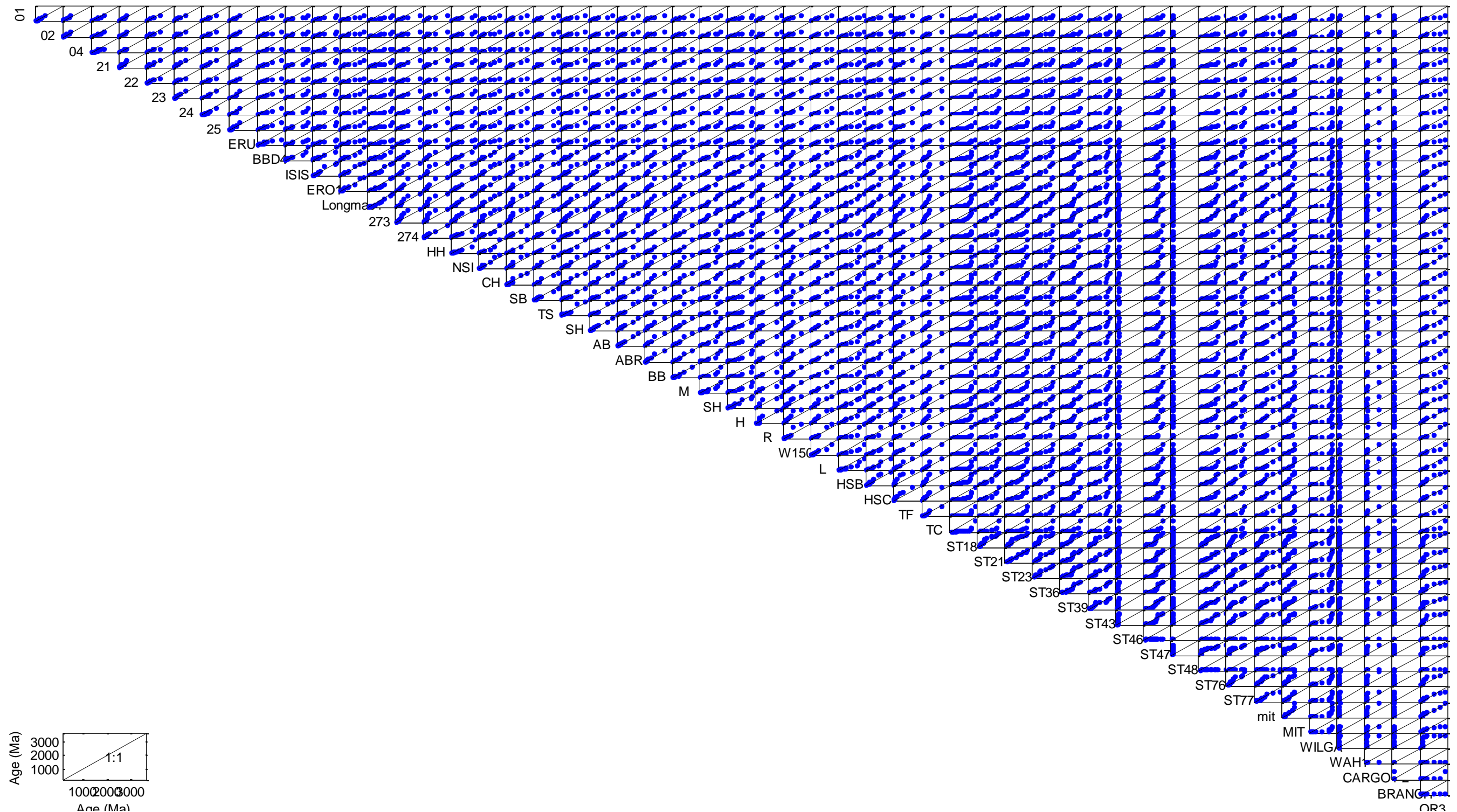


Figure 11: The QQ plot for the pre-Jurassic zircons from the the Rakaia Terrane in red (01, 02, 04, 21, 22, 23, 24, 25), Squire et al. (2006) in dark blue (ST18, ST21, ST23, ST36, ST39, ST43, ST46, ST47, ST48, ST76, ST77), Glen et al. (2011) in green (mit, MIT, WILGA, WAH1, CARGO1-2, Branch, OR3), Sircombe (1999) in purple (HH, NSI, CH, SB, TS, SH, AB, ABR, BB, M, SH, H, R, W150, L, HSB, HSC, TF, TC), Tucker et al. in orange (2013) (ERU, BBD4, ISIS, ERO1, Longmac1) and Veevers and Saeed (2011) in light blue (273, 274). If two distributions are connected by a solid line, from the Kolmogorov-Smirnov (KS) test, their distributions are the least dissimilar or most similar, if connected by a dotted line it is the second most similar distribution.

## APPENDIX

### Methods

#### ZIRCON SEPARATION

Using a diamond saw the samples were then cut to the appropriate size for the jaw crusher. Prior to use the stage and blade were thoroughly cleaned using a hose attached to a nearby sink to ensure no contamination. The sample was placed on the stage and pushed through to ensure that it did not come into contact with the arbor or the shaft. The saw and water was then turned on, ensuring it just covered the blade and the sample and the sample was slowly pushed through. Small rectangles, approximately 6 cm x 2 cm x 1 cm, were also cut from six of the samples to be turned into thin sections. These were done using bricks for safety purposes. Before being crushed in the jaw crusher the pieces of samples were dried on a hotplate and placed in a clearly labelled sample bag. Cleaning the jaw crusher involved removing the collection tray and opening up the crusher. Compressed air was then used to remove any loose particles before the jaws were brushed clean with a wire brush. Before reassembly the jaws and collection tray were wiped clean with ethanol and dried with compressed air. A representative proportion, usual half, the of the sample was then crushed and sieved using an Endecotts EFL2000 Sieve Shaker and a Flexistack. The sieve contained two pieces of sieve mesh, a piece of 400 µm and a piece of 79 µm mesh. This divided the sample into three fractions, a >400 µm fraction, a <79 µm fraction, and a 400-79 µm fraction which contained the zircons. After the sample had been sieved for approximately a minute the >400 µm fraction was milled using a disc mill. Before use the disc mill was cleaned by opening the latch at the front of the mill. The inside of the mill was then brushed before use of compressed air to remove any finer particles. The inside of the mill, including the discs was wiped clean with ethanol before the disc mill was reassembled. Finally the collection tray beneath the discs was removed and wiped clean before being reinserted into the disc mill. The coarse fraction was then milled down to 20 mm before being sieved again. The distance between the discs was then set to 5 mm and the newly sieved coarse fraction was then milled down to 5 mm before being sieved again. This procedure of milling and sieving was then repeated with the milling stages going from 5 mm → 3 mm → 1 mm → 0.5 mm. After the final sieving the three fractions and the sieve mesh were then bagged and cleanly labelled with the fraction size and sample number. The zircon fraction was then panned to remove any light material. The panning process involved wetting the zircon fraction in a small pan and shaking it to concentrate the zircons in the bottom of the pan. This small pan was then dipped into a larger pan filled with water to remove the lighter material on the surface. This process was repeated until all the light material had been removed. The remaining heavy material was then collected in a piece of filter paper and dried on a hot plate. The light material was also collected in pieces of filter paper and dried in an oven before being bagged. Once dried any magnetic material was removed by passing a magnet over the samples, as zircon is not magnetic anything collected in this stage was discarded. The inclined chute on the Isodynamic Magnetic Separator Model L-1 Franz was unscrewed and cleaned with compressed air as was the rest of the Franz before the chute was screwed

back into place. The Franz was first set to 1.5 amperes and the coaxial vibrator to the maximum 10 before the heavy material was Franzed in stages. Once the entire sample had passed through the Franz, it was set to >1.7 amps, 1.8 amps in this case, and the non-magnetic material was passed through the separator again. Once this run on the Franz was complete the magnetic material was bagged and the zircons within the non-magnetic material were further concentrated with heavy liquids. The heavy liquids were set up, in a “Safe-Tee” series 200 Fume Cupboard, so the 50 mL burette would drain into a funnel containing a piece of filter paper which would capture the zircons while the heavy liquids were filtered through and recapture the heavy liquid, methylene iodide, was poured into a funnel placed on top of the burette ensuring the tap was firmly closed. The non-magnetic material from the Franz was then also poured in and thoroughly stirred. The heavy material was allowed to settle to the bottom before being drained by opening the tap briefly. This procedure of stirring and draining was repeated five times before the filter paper containing the concentrate removed from the system and was washed with acetone ten times into a waste disposal bottle. The remaining material was drained into a separate piece of filter paper and the heavy liquids allowed to drain into the bottle. Once fully filtered the bottle of heavy liquids was replaced with a 250 mL conical flask and the system cleaned with acetone. The heavy material was then dried on a hot plate and viewed with a microscope to determine the presence of zircon. If the concentrate contained zircon it was transferred to a vial for mounting. If it contained no zircons the procedure of panning, franzing and heavy liquids separation was repeated. The lighter material was also dried on the hot plate and bagged. The entire set up for the heavy liquids was then washed cleaned ten times with acetone into the waste disposal bottle. Once separated the zircons were mounted on a clean glass slide. A single piece of double sided adhesive tape was laid carefully onto the slide ensuring no air bubbles formed. A single piece of adhesive tape was then laid, adhesive side up, onto of the double sided tape, again ensuring no air bubbles. The rubber mould was placed on the single sided tape and the inside of the mould engraved into the tape, forming the boundary of the mount. The zircons were then poured into a clean petri dish and using a pick and a pair of Olympus SZ51 microscopes transferred from the dish to the mount. Once approximately 300 zircons had been mounted the inside of the rubber mount was lubricated and was realigned with the engraved outline. An epoxy mix of one part epoxy hardener 20-8132-008 and five parts epoxy resin 20-8130-032 was combined and thoroughly mixed. This epoxy mix was carefully poured down the side of the rubber mount until around 1 cm of mix was within the mould. A small piece of paper with the sample number was then submerged just below the surface of the resin and allowed to dry for at least 24 hours. Once dried the rubber mount was twisted off the epoxy block and the tape removed. The surfaces of the mounts were then manually ground down until the cores of the zircons were exposed. The surfaces were then polished for 10 minutes using a Struers DP-U4 cloth lap and diamond paste before being carbon coated.

## U-Pb GEOCHRONOLOGY

U-Pb zircon geochronology was undertaken via Laser Ablation Inductively Coupled Plasma Mass Spectrometry (LA-ICP-MS). Back-scattered electrons and cathodoluminescence imaging of the zircon grains was done on a Phillips XL40 Scanning Electron Microscope to map the zircons and determine any internal structures

(Figure 3) within the individual grains mounted in the epoxy mount. U-Pb analyses were carried out on a New Wave UP-213 laser attached to an Agilent 7500cx inductively coupled plasma mass spectrometry (ICP-MS) at Adelaide Microscopy, the University of Adelaide. Ablation was conducted in a helium atmosphere after which argon gas was added immediately after to the cell to aid transport of material. A spot size of 30  $\mu\text{m}$  was chosen in order to target textural domains within the grains, while maximizing signal intensity at the mass spectrometer. A laser frequency of 5 Hz and output laser percentage of 55% resulted in an average fluence of 7 J/cm<sup>2</sup> at the ablation site and an ablation time of 80 seconds. Measured isotopes were <sup>204</sup>Pb, <sup>206</sup>Pb, <sup>207</sup>Pb, <sup>238</sup>U, <sup>208</sup>Pb and <sup>232</sup>Th with dwell times of 10, 15, 30, 15, 10 and 10 ms respectively. Mass <sup>204</sup>Pb was measured as a monitor of common lead content, and due to the unresolvable isobaric interference of <sup>204</sup>Hg on <sup>204</sup>Pb common lead corrections were not conducted. Age calculations and corrections were done in the GLITTER software through the use of the primary zircon standard GJ-1, TIMS normalization data <sup>207</sup>Pb/<sup>206</sup>Pb = 608.3 Ma, <sup>206</sup>Pb/<sup>238</sup>U = 600.7 Ma and <sup>207</sup>Pb/<sup>235</sup>U = 602.2 Ma (Jackson et al. 2004). An overestimated uncertainty of 1% was assigned to the TIMS derived normalization age for GJ-1. Instrument drift was also corrected for in GLITTER via standard bracketing every 10-15 unknowns and application of a linear correction. Accuracy of the methodology was verified by repeat analysis of Plesovice zircon (<sup>206</sup>Pb/<sup>238</sup>U = 337.13  $\pm$  0.37). The weighted average ages for Plesovice were  $354 \pm 19$  for <sup>207</sup>Pb/<sup>206</sup>Pb,  $334 \pm 4$  Ma for <sup>206</sup>Pb/<sup>238</sup>U, and  $335 \pm 3$  Ma for <sup>207</sup>Pb/<sup>235</sup>U (95% confidence; n=20). Due to the unresolvable <sup>204</sup>Hg on <sup>204</sup>Pb interference, isotope ratios are presented uncorrected for common lead, with concordia plots generated using Isoplot/Ex 3.71. Data was rejected based on the presence of common lead based on a combination of intensity of the raw <sup>204</sup>Pb counts, and following this, weighted average <sup>207</sup>Pb/<sup>206</sup>Pb age calculations at  $2\sigma$  confidence are reported.

## ZIRCON HF ISOTOPES

Hf analyses were undertaken on zircons, previously dated for U-Pb ages, mounted within epoxy moulds using the methods described in Griffin *et al.* (2006b). This was undertaken on a LA-MC-ICPMS with an attached New Wave UP-193 Excimer laser and Thermo-Scientific Neptune Multicollector at the University of Adelaide Waite Campus. This Excimer laser delivered a beam of 198nm UV light. For the analyses a beam diameter of 35  $\mu\text{m}$  with a repetition rate of 5 Hz was chosen. For the analyses the 172, 175, 176, 177, 178, 179 and 180 were all measured concurrently. Prior to any analyses the data was normalised such that <sup>179</sup>Hf/<sup>177</sup>Hf is equal to 0.7325. Interference of <sup>176</sup>Lu on <sup>176</sup>Hf was corrected for by calculating <sup>176</sup>Lu/<sup>176</sup>Hf with the isotope <sup>175</sup>Lu and <sup>176</sup>Lu/<sup>175</sup>Lu equals 0.02669 following Patchett (1983). The interference of <sup>176</sup>Yb on <sup>176</sup>Hf was corrected in a similar fashion. It was corrected by measuring the isotope <sup>172</sup>Yb and coupling this with <sup>176</sup>Yb/<sup>172</sup>Yb values to calculate <sup>176</sup>Yb/<sup>177</sup>Hf. The <sup>176</sup>Yb/<sup>172</sup>Yb were calculated by adding Yb to the JMC475 Hf standard to find the value of <sup>176</sup>Yb/<sup>172</sup>Yb that gives the value required to yield a known value of <sup>176</sup>Hf/<sup>177</sup>Hf (Griffin *et al.* 2004). Both prior to the analysis and during the analyses the standard Mudtank zircons to ensure accuracy (Average corrected value <sup>176</sup>Hf/<sup>177</sup>Hf =  $0.282515 \pm 0.000021$  with  $2\sigma$  confidence and n=11 ((Griffin *et al.* 2006a, Howard *et al.* 2009)). The <sup>176</sup>Hf/<sup>177</sup>Hf ratios were calculated from the measured <sup>176</sup>Lu/<sup>176</sup>Hf values giving an

uncertainty of  $<\pm 0.05\text{Hf}$ . The decay constant of  $1.856 \times 10^{-11} \text{ y}^{-1}$  for  $^{176}\text{Lu}$  as calculated in Scherer *et al.* (2001) was selected for the calculation of  $\epsilon\text{Hf}$  values.

#### $^{40}\text{Ar}$ - $^{39}\text{Ar}$ DATING

From the samples selected for  $40\text{Ar}/39\text{Ar}$  dating unaltered, optically transparent,  $>400 \mu\text{m}$ -muscovites were separated. These minerals were separated using a Frantz magnetic separator, and then carefully hand-picked under an Olympus SZ51 microscope. The selected muscovites were leached in diluted HF for one minute and then thoroughly rinsed with distilled water in an ultrasonic cleaner. Samples were loaded into 10 large wells of 1.9 cm diameter and 0.3 cm depth aluminium disc. These wells were bracketed by small wells that included Fish Canyon sanidine (FCs) used as a neutron fluence monitor for which an age of  $28.305 \pm 0.036 \text{ Ma}$  ( $1\sigma$ ) was adopted (Renne *et al.* 2010) based on the calibration by Jordan and Renne (2007). The discs were Cd-shielded (to minimize undesirable nuclear interference reactions) and irradiated in the Hamilton McMaster University nuclear reactor (Canada) in position 5C. The mean J-values computed from standard grains within the small pits range from  $0.0026752 \pm 0.0000040$  (0.15%) to  $0.0026644 \pm 0.0000054$  (0.20%) determined as the average and standard deviation of J-values of the small wells for each irradiation disc. Mass discrimination was monitored using an automated air pipette and provided a mean value of  $1.00646 \pm 0.00238$  per dalton (atomic mass unit) relative to an air ratio of  $298.56 \pm 0.31$  (Lee *et al.* 2006). The correction factors for interfering isotopes were  $(^{39}\text{Ar}-^{37}\text{Ar})_{\text{Ca}} = 7.30 \times 10^{-4}$  ( $\pm 11\%$ ),  $(^{36}\text{Ar}-^{37}\text{Ar})_{\text{Ca}} = 2.82 \times 10^{-4}$  ( $\pm 1\%$ ) and  $(^{40}\text{Ar}-^{39}\text{Ar})_{\text{K}} = 6.76 \times 10^{-4}$  ( $\pm 32\%$ ). The  $^{40}\text{Ar}$ - $^{39}\text{Ar}$  analyses were performed at the Western Australian Argon Isotope Facility at Curtin University, operated by a consortium consisting of Curtin University and the University of Western Australia. The samples were fusion heated using a 110 W Spectron Laser Systems, with a continuous Nd-YAG (IR; 1064 nm) laser. The gas was purified in a stainless steel extraction line using three SAES AP10 getters and a liquid nitrogen condensation trap. Ar isotopes were measured in static mode using a MAP 215-50 mass spectrometer (resolution of  $\sim 500$ ; sensitivity of  $4 \times 10^{-14} \text{ mol/V}$ ) with a Balzers SEV 217. The data acquisition was performed with the Argus program written by M.O. McWilliams and ran under a LabView environment. The raw data were processed using the ArArCALC software (Koppers 2002) and the ages have been calculated using the decay constants recommended by Renne *et al.* (2010). Integrated ages ( $2\sigma$ ) are calculated using the total gas released for each Ar isotope.

#### TRACE ELEMENT ANALYSIS

Trace Element Analysis were undertaken on 120 zircons from 4 different samples, previously dated for U-Pb ages, mounted within epoxy moulds following the method outlined by Belousova *et al.* (2002). This was undertaken Cameca SX51 electron microprobe located at Adelaide Microscopy, The University of Adelaide. Spot analyses were conducted using a beam current of 20 nA and an accelerating voltage of 15 kV, with a defocused beam of 5 micron. Concentrations calculated on the microprobe included the percent oxide (wt%) of Oxygen (O), Hafnium (Hf), Silica (Si) and Zirconium (Zr). Calibration was done on natural and synthetic mineral standards supplied by Astimex, Taylor, and P&H. The trace element compositions were

preformed via laser ablation inductively coupled mass-spectrometry, at Adelaide Microscopy, following the methods of Raimondo *et al.* (2011). Zircons were analysed using an Agilent 7500cc quadrupole ICP-MS with an attached New Wave UP-213 Nd-YAG laser. The elements analysed for were Titanium (Ti), Yttrium (Y), Niobium (Nb), Hafnium (Hf), Tantalum (Ta), Lanthanum (La), Cerium (Ce), Praseodymium (Pr), Samarium (Sm), Europium (Eu), Gadolinium (Gd), Ytterbium (Yb), Lutetium (Lu), Thorium (Th) and Uranium (U). A spot size of 30 µm was chosen with a repetition rate of 5 Hz with the energy set to produce a fluence of  $\sim 7 \text{ Jcm}^{-2}$ . Ablation was conducted in a helium atmosphere to which argon gas was also added. The machine was tuned to peak sensitivity to minimize the production of interfering oxide species so that  $^{232}\text{Th}^{16}\text{O}/^{232}\text{Th}$  was routinely  $< 0.5\%$ . Data was collected using a time-resolved data acquisition in fast peak jumping mode and then processed using the GLITTER software (Achterbergh *et al.* 2001). The acquisition time for each analyses was 60 seconds with 30 seconds of background and 30 seconds of zircon ablation. The results were calibrated against the NIST 610 standard glass with the coefficients of Pearce *et al.* (1997) Groups of 15 analyses were bracketed by repeat analyses of the NIST 610 standard which corrected for any instrument drift. A linear drift correction based on the analysis sequence and on the bracketing of NIST-610 was applied to the count rate of each sample.  $^{178}\text{Hf}$  was used as the internal standard for the zircons, this was pre-determined from the microprobe results.

## Supplementary Tables

Sample Number	Coordinates
NZ1301	41°21'29.34"S 174°43'31.09"E
NZ1302	41°21'13.65"S 174°43'42.74"E
NZ1303	41°20'47.19"S 174°44'46.36"E
NZ1304	41°20'47.19"S 174°44'46.36"E
NZ1305	43°18'01.27"S 171°44'52.29"E
NZ1313	43°23'17.7"S 170°12'32.5"E
NZ1321	42°51'45.24"S 171°33'28.1"E
NZ1322	42°55'56.85"S 171°33'33.79"E
NZ1323	43°01'15.90"S 171°35'49.83"E
NZ1324	43°18'05.0"S 171°45'07.98"E
NZ1325	41°20'47.19"S 174°44'46.36"E

**Supplementary Table 1:** The sample name and corresponding GPS coordinates for the outcrop the sample was taken from.

Grain	Pb204 (ppm)	Pb206 (ppm)	Pb207 (ppm)	Pb208 (ppm)	Th232 (ppm)	U238 (ppm)	Pb207/Pb206	Pb206/U238	Pb207/U235	Pb208/Th232	Pb207/Pb206 ± 2σ	Pb206/U238 ± 2σ	Pb207/U235 ± 2σ	Pb208/Th232 ± 2σ	Rho	Concordancy								
Z1	39	15728	832	3938	299192	450086	0.05145	0.00072	0.04004	0.00047	0.28402	0.00419	0.01041	0.0002	261.2	31.9	253.1	2.94	253.8	3.32	209.3	4	0.936522	99.72419228
Z2	18	4240	226	1450	130773	140936	0.05196	0.00125	0.03447	0.00044	0.24689	0.00593	0.00879	0.0002	283.5	54.03	218.5	2.74	224	4.83	176.8	3.94	0.936522	97.54464286
Z3	22	44185	2636	9964	386732	618391	0.05812	0.00068	0.08204	0.00096	0.65732	0.00835	0.02047	0.0004	533.8	25.74	508.3	5.71	513	5.12	409.5	7.91	0.936522	99.08382066
Z4	31	17499	905	3918	386442	633714	0.05033	0.00069	0.0319	0.00038	0.22131	0.00324	0.00803	0.00017	210.1	31.62	202.4	2.37	203	2.69	161.6	3.32	0.936522	99.7044335
Z5	32	139605	8625	8430	272690	1627608	0.0602	0.00065	0.09869	0.00115	0.81905	0.0099	0.02471	0.00051	610.9	23.28	606.7	6.73	607.5	5.53	493.4	9.96	0.936522	99.86831276
Z6	15	71362	4894	10022	197476	670728	0.06705	0.00096	0.11881	0.0014	1.09827	0.01616	0.04132	0.00145	839.3	29.47	723.7	8.04	752.5	7.82	818.4	28.16	0.936522	96.17275748
Z7	28	17872	1040	2466	115715	293118	0.05681	0.00088	0.07228	0.0009	0.56603	0.00922	0.01716	0.00049	483.4	34.28	449.9	5.42	455.5	5.98	343.8	9.8	0.936522	98.77058178
Z8	24	24523	1278	5181	405925	715867	0.05123	0.00068	0.0386	0.00045	0.27263	0.00382	0.01051	0.00026	251.3	30.37	244.2	2.78	244.8	3.05	211.3	5.14	0.936522	99.75490196
Z9	29	14818	782	2523	205008	475156	0.05166	0.00083	0.0366	0.00045	0.26063	0.00436	0.0101	0.00029	270.3	36.37	231.7	2.81	235.2	3.51	203.2	5.83	0.936522	98.51190476
Z10	10	11493	662	956	45279	201835	0.05521	0.00141	0.07068	0.00103	0.53783	0.01373	0.1688	0.0009	420.7	55.59	440.3	6.19	437	9.07	338.2	17.89	0.936522	100.7551487
Z11	2	9177	476	2151	193475	302271	0.05103	0.00085	0.03541	0.00041	0.24274	0.00414	0.00937	0.00025	242.3	37.87	218.7	2.58	220.7	3.38	188.5	5.08	0.936522	99.09379248
Z12	28	12765	784	3783	331311	433330	0.06058	0.00093	0.03379	0.00041	0.2821	0.00447	0.00693	0.00028	624.2	32.65	214.2	2.54	252.3	3.54	193.7	5.6	0.936522	84.89892985
Z13	22	43400	3686	7783	130486	247065	0.08301	0.00092	0.20414	0.00241	2.33593	0.02887	0.04855	0.00086	1269.4	21.31	1197.5	12.88	1223.3	8.79	958.2	16.58	0.864389	97.89095071
Z14	26	9139	558	2127	153725	270855	0.0599	0.00092	0.03901	0.00047	0.32216	0.00514	0.1154	0.00024	600	32.82	246.7	2.93	283.6	3.95	231.9	4.74	0.864389	86.9887165
Z15	34	17829	940	8589	737708	585495	0.05147	0.00074	0.0359	0.00044	0.25469	0.00388	0.00958	0.0002	261.7	32.51	227.3	2.73	230.4	3.14	192.7	4.05	0.864389	98.65451389
Z16	18	10676	560	1290	114769	353568	0.05112	0.00089	0.03608	0.00046	0.25424	0.00458	0.0091	0.00024	246.1	39.44	228.5	2.85	230	3.71	183.2	4.82	0.864389	99.34782609
Z17	43	9784	524	2803	263365	344522	0.05175	0.00111	0.0351	0.00048	0.25037	0.00549	0.00838	0.00025	274.2	48.53	222.4	2.98	226.9	4.46	168.8	4.96	0.864389	98.01674747
Z18	40	13457	706	2742	240138	430906	0.05112	0.00079	0.03716	0.00046	0.26188	0.00426	0.0094	0.00023	246.2	35.07	235.2	2.87	236.2	3.43	189.2	4.57	0.864389	99.57662997
Z19	26	5080	301	1140	99371	168217	0.05712	0.00172	0.03767	0.00057	0.29662	0.00882	0.009	0.00035	495.5	65.44	238.4	3.56	263.8	6.91	181	6.97	0.864389	90.37149356
Z20	32	2341	210	367	5915	20211	0.08771	0.00211	0.13573	0.00188	1.64134	0.03913	0.0522	0.00191	1376.1	45.4	820.5	10.68	986.2	15.04	1028.5	36.68	0.864389	83.19813425
Z21	26	100913	5590	22680	1526951	2450903	0.05339	0.00066	0.05044	0.00063	0.37128	0.00518	0.01173	0.00032	345.3	27.66	317.2	3.88	320.6	3.83	235.6	6.43	0.864389	98.93948846
Z22	28	7590	452	1550	129067	250665	0.05752	0.00111	0.03712	0.00049	0.29434	0.00584	0.00927	0.00027	511.2	42.07	234.9	3.06	262	4.58	186.6	5.42	0.864389	89.65648855
Z23	22	34385	2631	3140	65977	249264	0.07355	0.00103	0.17121	0.00222	1.73599	0.0267	0.03703	0.00119	1029.1	27.79	1018.8	12.21	1022	9.91	735	23.29	0.864389	99.68688485
Z24	17	7755	424	1586	117262	211389	0.05255	0.00111	0.04517	0.00061	0.32726	0.00698	0.01062	0.00035	309.4	46.68	284.8	3.77	287.5	5.34	213.6	7.04	0.864389	99.06086957
Z25	11	18818	1001	4853	441601	627552	0.05147	0.00078	0.03647	0.00046	0.25877	0.00421	0.00897	0.00028	262	34.55	230.9	2.88	233.7	3.4	180.5	5.52	0.864389	98.80188276
Z26	49	13085	796	2510	228994	471740	0.05085	0.00167	0.03483	0.00054	0.27886	0.00793	0.0077	0.00033	531.3	62.47	220.7	3.34	249.8	6.29	155	6.53	0.758365	88.35068054
Z27	17	6572	378	1599	121718	210040	0.055																	

Grain	Pb204 (ppm)	Pb206 (ppm)	Pb207 (ppm)	Pb208 (ppm)	Th232 (ppm)	U238 (ppm)	Pb207/Pb206	Pb206/U238	Pb207/U235	Pb208/Th232	Pb207/Pb206 Age (Ma)	Pb206/U238 $\pm 2\sigma$	Pb207/U235 $\pm 2\sigma$	Pb208/Th232 $\pm 2\sigma$	Rho	Concordancy								
Z1	1	27635	1725	6128	225277	357127	0.06056	0.00078	0.09912	0.0013	0.82783	0.01232	0.02472	0.00091	623.5	27.7	609.2	7.62	612.4	6.84	493.7	18.03	0.881277	99.47746571
Z2	0	6270	330	1327	128848	220069	0.05112	0.00096	0.03633	0.00049	0.2561	0.00509	0.00932	0.00037	246.3	42.84	230	3.05	231.5	4.12	187.4	7.33	0.678613	99.35205183
Z3	0	23078	1355	3284	158379	396850	0.0571	0.00083	0.07282	0.00095	0.57348	0.00919	0.01917	0.00088	494.8	32.15	453.1	5.69	460.3	5.93	383.7	17.47	0.814096	98.43580274
Z4	10	13757	930	2029	70730	153567	0.06569	0.00096	0.11398	0.00151	1.0325	0.01672	0.02629	0.00112	796.4	30.44	695.8	8.73	720.2	8.35	524.5	22.13	0.818092	96.61205221
Z5	14	4681	307	1086	87112	162163	0.06386	0.00138	0.03603	0.0005	0.31734	0.00699	0.0144	0.00057	737.1	44.94	228.2	3.1	279.9	5.38	229.9	11.38	0.630019	81.52911754
Z6	0	87913	5235	373	12701	1174789	0.05801	0.00077	0.0937	0.0012	0.74961	0.01118	0.02702	0.00152	529.8	29.15	577.4	7.1	568	6.49	539	29.98	0.858688	101.6549296
Z7	0	25819	1980	5570	119870	200842	0.0746	0.00102	0.16391	0.00216	1.68606	0.02598	0.04264	0.00199	1057.5	27.57	978.5	11.94	1003.3	9.82	843.9	38.58	0.855229	97.52815708
Z8	7	19086	1151	2871	118327	291752	0.05868	0.00087	0.08406	0.00112	0.68018	0.01115	0.02235	0.00109	555.3	31.88	520.3	6.67	526.9	6.74	446.7	21.51	0.812789	98.7473904
Z9	17	17823	1014	1979	127759	470415	0.05555	0.00085	0.04809	0.00064	0.36834	0.00618	0.01437	0.00075	434.1	33.34	302.8	3.91	318.4	4.59	288.4	15.04	0.793205	95.10050251
Z10	18	10244	534	2520	248056	385911	0.05084	0.00088	0.03378	0.00045	0.23676	0.00438	0.00939	0.0005	233.4	39.46	214.2	2.83	215.8	3.6	188.8	9.96	0.720091	99.25857275
Z11	0	4205	231	1212	109048	143927	0.05385	0.00143	0.0364	0.00052	0.27029	0.01021	0.00607	0.00152	364.8	58.56	230.5	3.25	249.4	5.75	205.3	13.41	0.53629	94.89501853
Z12	0	15751	851	1224	80469	421079	0.05274	0.00085	0.04782	0.00064	0.34767	0.00607	0.01406	0.0008	317.5	36	301.1	3.93	303	4.57	282.1	16	0.766565	99.37293729
Z13	4	7640	468	639	28736	132275	0.05993	0.00117	0.07313	0.001	0.60394	0.01229	0.02703	0.00136	600.2	41.66	455	6.03	479.7	7.78	414.7	26.88	0.671953	94.85094851
Z14	0	1787	141	333	7609	15799	0.07733	0.00241	0.14353	0.00228	1.5301	0.04721	0.04099	0.00294	1129.6	60.73	864.6	12.87	942.5	18.95	811.9	57.12	0.514847	91.73474801
Z15	1	2057	123	352	25258	57704	0.05878	0.00207	0.04654	0.00074	0.37706	0.01321	0.01328	0.00096	559.1	74.88	293.3	4.57	324.9	9.74	266.7	19.16	0.453851	90.27393044
Z16	10	3413	181	1091	109486	12678	0.05175	0.00134	0.0353	0.0005	0.25184	0.00663	0.00864	0.00035	274.5	58.27	223.6	3.12	228.1	5.37	173.9	7.09	0.53803	98.02718106
Z17	0	28036	1498	3648	396224	1110741	0.05122	0.00071	0.03241	0.00043	0.23286	0.00361	0.00798	0.00031	290.8	30.83	205.6	2.67	212.6	2.97	160.6	6.21	0.85581	96.7074318
Z18	2	27939	1823	1990	60105	306342	0.06337	0.00092	0.11977	0.00163	1.04639	0.01718	0.02914	0.00127	720.7	30.61	729.3	9.39	727.1	8.53	580.6	24.97	0.828915	100.3025719
Z19	11	4518	273	764	65185	149871	0.059	0.0014	0.03815	0.00054	0.31026	0.00747	0.0102	0.00052	566.9	50.84	241.3	3.38	274.4	5.79	205.1	10.31	0.587901	87.9731778
Z20	0	8687	469	1753	124457	221061	0.05282	0.001	0.04917	0.00067	0.35801	0.00767	0.01262	0.00069	320.9	46.47	309.5	4.14	310.7	5.73	253.4	13.71	0.636025	99.61377535
Z21	0	10688	654	2768	244700	377274	0.05972	0.00099	0.03705	0.00051	0.30501	0.00549	0.00994	0.00043	593.6	35.15	234.5	3.16	270.3	4.27	200	8.58	0.764757	86.7554569
Z22	6	9214	501	1302	118773	328282	0.05304	0.00091	0.03638	0.0005	0.266	0.00493	0.00964	0.00043	330.5	38.37	230.4	3.09	239.5	3.95	193.8	8.67	0.741553	96.20041754
Z23	0	4389	274	885	7864	161395	0.06088	0.00141	0.03491	0.0005	0.29296	0.00691	0.01008	0.00053	635.1	48.92	221.2	3.12	260.9	5.43	202.7	10.68	0.607226	84.78344193
Z24	10	9920	558	664	47046	226753	0.05498	0.00094	0.03659	0.00057	0.42894	0.00791	0.01253	0.00063	411.5	37.47	354.9	4.71	362.4	5.62	251.7	12.63	0.737821	97.93046358
Z25	0	12875	699	2943	241109	389635	0.05308	0.00095	0.04149	0.00056	0.3036	0.00574	0.01077	0.00061	332.1	40.02	262.1	3.44	269.2	4.47	216.5	12.27	0.713895	97.36255572
Z26	4	94114	5469	492	21054	1513751	0.05657	0.00075	0.08116	0.00067	0.63287	0.00972	0.0205	0.00105	474	29.25	503	6.47	497.9	6.04	410.2	20.86	0.866423	101.0243021
Z27	5	3570	2875	1968	43690	290758	0.07483	0.																

Grain	Pb204 (ppm)	Pb206 (ppm)	Pb207 (ppm)	Pb208 (ppm)	Th232 (ppm)	U238 (ppm)	Pb207/Pb206	Pb206/U238	Pb207/U235	Pb208/Th232	Pb207/Pb206 Age (Ma)	$\pm 2\sigma$	Pb206/U238 Age (Ma)	$\pm 2\sigma$	Pb207/U235 Age (Ma)	$\pm 2\sigma$	Pb208/Th232 Age (Ma)	$\pm 2\sigma$	Rho	Concordancy		
Z1	4	17763	966	1992	171713	598245	0.05241	0.00081	0.03635	0.00047	2.6267	0.00434	0.0094	0.00031	303.4	34.82	230.2	2.9	236.8	3.49	189.1	6.15 0.847593 97.21283784
Z2	21	11903	737	2501	151705	301610	0.05962	0.00088	0.04957	0.00065	0.4075	0.00657	0.01381	0.0004	589.8	31.64	311.9	3.98	347.1	4.74	277.3	8.01 0.847593 89.85883031
Z3	14	44992	2432	5363	510818	1405223	0.05212	0.00067	0.03926	0.00049	0.2822	0.00407	0.00857	0.00027	290.6	29.17	248.3	3.06	252.4	3.22	172.5	5.47 0.847593 98.37559429
Z4	6	9696	564	1745	137610	314713	0.05564	0.00099	0.04068	0.00057	0.31212	0.00595	0.01033	0.00034	437.7	38.55	257.1	3.53	275.8	4.61	207.8	6.9 0.847593 93.21972444
Z5	0	11787	653	1853	142845	340994	0.05321	0.0008	0.04448	0.00059	0.32641	0.00541	0.01079	0.00033	337.9	33.48	280.5	3.66	286.8	4.14	216.9	6.66 0.847593 97.80334728
Z6	13	9203	507	1986	194629	351114	0.05293	0.00097	0.03241	0.00043	0.23661	0.00451	0.00834	0.00031	325.5	40.84	205.6	2.68	215.6	3.71	167.8	6.15 0.847593 95.36178108
Z7	9	6519	420	1084	41931	98901	0.06173	0.00111	0.08549	0.00119	0.72771	0.01395	0.0214	0.00075	664.7	38.06	528.8	7.04	555.2	8.2	428	14.93 0.847593 95.24495677
Z8	0	8480	473	1822	161840	298643	0.05339	0.0009	0.03704	0.00051	0.27268	0.005	0.0093	0.00032	345.3	37.74	234.4	3.16	244.8	3.99	187.1	6.36 0.847593 95.75163399
Z9	70	51756	3771	10569	664299	1124199	0.06972	0.00111	0.0561	0.00073	0.53938	0.00913	0.01397	0.00075	920.1	32.29	351.9	4.44	438	6.02	280.4	14.98 0.847593 80.34246575
Z10	2	9506	568	810	1695	162942	0.05729	0.00091	0.07558	0.00103	0.59712	0.01044	0.01711	0.00066	502.2	34.67	469.7	6.15	475.4	6.64	342.8	13.02 0.847593 98.80100968
Z11	11	11976	787	3013	107228	154868	0.06279	0.00093	0.10148	0.00139	0.87879	0.01461	0.0232	0.00084	701.2	31.21	623.1	8.11	640.3	9.7	463.5	16.55 0.847593 97.31375918
Z12	12	4366	303	1140	91309	153803	0.06623	0.00134	0.03729	0.00053	0.34055	0.00721	0.01028	0.00041	813.7	41.66	236	3.32	297.6	5.46	206.8	8.15 0.847593 79.30107527
Z13	20	13342	732	772	48763	337348	0.021	0.0008	0.05238	0.00072	0.37785	0.00648	0.01303	0.00054	299.1	34.45	329.1	4.42	325.5	4.78	261.6	10.68 0.847593 101.1059908
Z14	7	10949	627	3407	336501	404082	0.05433	0.00094	0.03592	0.0005	0.26915	0.00505	0.00824	0.00035	384.8	38.14	227.5	3.14	242	4.04	166	7.07 0.847593 94.00826446
Z15	0	15012	916	3168	128494	223654	0.05807	0.00086	0.08896	0.00125	0.71946	0.01216	0.02011	0.00081	531.8	32.64	554.7	7.4	550.3	7.18	402.4	16.07 0.847593 100.79956339
Z16	4	5999	341	1058	9208	211343	0.05455	0.00118	0.03544	0.00049	0.26653	0.00589	0.0096	0.00035	393.9	47.58	224.5	3.04	239.9	4.72	193.1	6.95 0.817108 93.58065861
Z17	8	16298	914	2796	22651	497101	0.05362	0.00076	0.04030	0.00058	0.3181	0.0051	0.01039	0.0003	354.9	31.8	271.6	3.6	280.4	3.93	208.9	5.99 0.817108 96.86162625
Z18	19	5321	297	1243	127201	197839	0.05352	0.00109	0.03467	0.00048	0.25580	0.00542	0.00848	0.00027	351	45.34	219.7	3.01	231.4	4.38	170.7	5.4 0.817108 94.94382022
Z19	14	8589	462	2030	202784	315737	0.05159	0.0009	0.03487	0.00047	0.24808	0.00461	0.00835	0.00027	267.2	39.59	221	2.94	225	3.75	168.1	5.41 0.817108 98.22222222
Z20	0	6296	327	1852	192756	246161	0.04976	0.00091	0.03335	0.00046	0.22879	0.00447	0.0078	0.00023	183.9	42.17	211.5	2.87	209.2	3.69	156.9	4.69 0.817108 101.0994264
Z21	4	66755	4556	2361	72294	793158	0.06335	0.00097	0.11847	0.00174	1.034	0.01795	0.02211	0.00089	719.9	32.04	721.7	10.03	720.9	8.96	442	17.57 0.817108 100.1109724
Z22	8	8692	481	1589	160670	332461	0.05291	0.00086	0.03407	0.00046	0.24852	0.00438	0.0079	0.00025	325	36.25	216	2.89	225.4	3.56	159.1	5.02 0.817108 95.8296362
Z23	11	9938	556	1570	152436	384717	0.05305	0.00082	0.03368	0.00046	0.24633	0.00418	0.0079	0.00024	330.8	34.62	213.6	2.85	223.6	3.41	156.9	4.84 0.817108 95.52772809
Z24	8	11262	615	2744	282087	429670	0.05224	0.00085	0.03432	0.00047	0.24713	0.00438	0.0079	0.00028	295.9	36.66	217.5	2.93	224.2	3.56	160.5	5.6 0.817108 97.01159679
Z25	17	23745	1871	2318	44011	170641	0.07548	0.00098	0.17914	0.00237	1.86409	0.02764	0.04062	0.00146	1081.4	25.8	1062.3	12.96	1068.4	9.8	843.6	28.35 0.817108 99.42905279
Z26	7	4377	242	1008	95658	158068	0.05294	0.00112	0.03585	0.0005	0.26165	0.00575	0.00841	0.00031	326.4	47.34	227.1	3.13	236	4.63	169.3	6.18 0.817108 96.22881356
Z27	0	15963	876	2907	274846	572351	0.05257	0.00078	0.03605	0.00048	0.26126	0.00428	0.00859	0.00032	310	33.36	228.3	3.01	235.7	3.44		

# Provenance of the Rakaia Terrane

51

Grain	Pb204 (ppm)	Pb206 (ppm)	Pb207 (ppm)	Pb208 (ppm)	Th232 (ppm)	U238 (ppm)	Pb207/Pb206	Pb206/U238	Pb207/U235	Pb208/Th232	Pb207/Pb206 ± 2σ	Pb206/U238 ± 2σ	Pb207/U235 ± 2σ	Pb208/Th232 ± 2σ	Rho	Concordancy
										Age (Ma)						
Z1	0	4919	289	44	388	75589	0.05632	0.00122	0.08054	0.00109	0.62532	0.0139	0.09259	0.0173	464.1	47.8
Z2	9	42738	2595	2789	92678	703512	0.05742	0.00071	0.0786	0.00104	0.62331	0.00898	0.02269	0.0007	507.3	26.92
Z3	7	8262	514	1758	158329	30352	0.05886	0.001	0.03493	0.00048	0.28347	0.00517	0.00851	0.00028	562.1	36.7
Z4	14	18801	2004	2043	32909	135120	0.10141	0.00125	0.17656	0.0023	2.46882	0.03509	0.04903	0.00157	1650	22.76
Z5	12	4427	265	1150	88676	127935	0.05705	0.00126	0.04405	0.00061	0.34646	0.00785	0.03049	0.00038	492.8	47.8
Z6	0	16839	1304	3008	232142	391064	0.07385	0.00104	0.05475	0.00072	0.57572	0.0087	0.03048	0.00038	1037.5	28.1
Z7	12	38059	2334	1351	52876	543332	0.05763	0.00076	0.09297	0.00127	0.73876	0.01134	0.01894	0.0007	515.5	29.05
Z8	19	102030	16184	17871	169584	351632	0.15132	0.00184	0.37158	0.00487	0.3739	0.11115	0.00333	0.00033	221.3	2.96
Z9	0	54408	6302	19799	237194	24535	0.10972	0.00131	0.33075	0.0044	5.00368	0.0712	0.06561	0.00231	1794.8	21.6
Z10	6	4055	249	1690	156845	143087	0.05822	0.00133	0.03728	0.00054	0.29925	0.00706	0.00843	0.00033	537.5	49.76
Z11	0	11355	608	7044	672468	38168	0.05134	0.0019	0.03733	0.00064	0.62687	0.0099	0.03841	0.00076	255.9	85.27
Z12	5	10460	642	2416	111247	178765	0.05835	0.00094	0.07697	0.0106	0.61921	0.01995	0.07168	0.00073	542.8	34.74
Z13	0	11100	610	2292	212299	385148	0.05225	0.00083	0.0379	0.00052	0.27301	0.00481	0.00871	0.00036	296.2	35.91
Z14	0	9057	531	2631	235838	308925	0.05569	0.00093	0.03871	0.00054	0.29719	0.00543	0.00908	0.00039	439.6	36.29
Z15	17	6994	473	1485	16959	249158	0.0642	0.00111	0.30399	0.00263	0.01011	0.0044	0.748.3	36.12	236.7	3.28
Z16	12	19429	1125	4478	428795	737265	0.05542	0.00074	0.03577	0.00049	0.27014	0.0042	0.00807	0.00022	429	29.23
Z17	23	6308	382	1807	169572	23257	0.05752	0.00154	0.03742	0.0006	0.29667	0.0081	0.00766	0.00031	511.1	58.16
Z18	32	2935	432	1521	67752	84329	0.14168	0.00254	0.04653	0.00069	0.90835	0.01708	0.01764	0.00054	2247.8	30.64
Z19	9	6524	416	1229	108744	165599	0.06126	0.001	0.05274	0.00075	0.45417	0.00863	0.00887	0.00028	648.4	38.09
Z20	79	35932	3435	3386	27014	348036	0.09145	0.00109	0.13903	0.00191	1.75229	0.02546	0.095	0.00278	1455.9	22.52
Z21	0	5762	399	1630	131704	201559	0.06652	0.00116	0.03833	0.00054	3.05138	0.00665	0.00962	0.0003	822.9	36.05
Z22	15	29359	2811	1347	37594	337641	0.09176	0.0013	0.11328	0.00154	1.43212	0.02332	0.02813	0.00124	1462.3	27.71
Z23	15	10317	770	1627	35093	80327	0.07208	0.00117	0.1703	0.00239	1.69167	0.03009	0.03696	0.0014	98.8	32.91
Z24	0	4092	294	644	45166	144323	0.06907	0.00141	0.03821	0.00056	0.53669	0.00782	0.01112	0.00042	900.8	41.55
Z25	1	1202	100	388	2199	35688	0.0801	0.0049	0.04343	0.00102	0.47935	0.02651	0.04149	0.0107	1199.4	117.34
Z26	0	50709	3198	7773	264045	634587	0.06037	0.00075	0.10789	0.00148	0.89772	0.01349	0.02	0.0074	615.7	26.76
Z27	12	17550	1085	3462	298967	632713	0.05943	0.00087	0.03769	0.00053	0.30875	0.00517	0.00891	0.00033	583	31.38
Z28	0	9262	580	1636	16942	209211	0.06038	0.001	0.05963	0.00084	4.96196	0.00906	0.01496	0.00059	617.1	35.33
Z29	10	9864	647	1329	61086	261078	0.06315	0.0010	0.05097	0.00072	0.44363	0.00791	0.01659	0.00068	713.4	33.71
Z30	0	10740	663	784	30159	162631	0.05949	0.00098	0.08927	0.00126	0.73195	0.01313	0.02022	0.00086	584.9	34.59
Z31	14	54748	4093	2334	53802	470177	0.07183	0.00086	0.15514	0.0021	1.35886	0.02219	0.03444	0.00103	981.1	24.14
Z32	13	7243	433	1075	90338	245916	0.05732	0.00098	0.03939	0.00055	3.11115	0.00582	0.00922	0.00028	503.4	37.18
Z33	3	2326	172	833	65371	75040	0.07097	0.00207	0.04055	0.00063	0.39654	0.01155	0.01016	0.00038	956.4	58.49
Z34	17	9244	663	569	11954	131491	0.06896	0.0011	0.09067	0.00126	0.86184	0.01571	0.03766	0.00144	897.5	32.71
Z35	22	5918	353	1067	92123	204929	0.05695	0.00103	0.03854	0.00054	0.30251	0.00857	0.00866	0.00027	488.9	39.62
Z36	0	11034	673	2360	114137	236306	0.05848	0.00092	0.06441	0.00081	0.51919	0.00899	0.01625	0.00055	547.8	33.92
Z37	5	4515	381	1365	108532	177500	0.08023	0.00197	0.03492	0.00058	0.38614	0.00611	0.00897	0.00038	1202.6	47.63
Z38	5	32981	2442	4044	85091	279596	0.07083	0.00091	0.15583	0.00211	1.52126	0.02275	0.03732	0.00127	952.6	25.93
Z39	8	10012	7171	8129	209403	1024838	0.06806	0.00083	0.12961	0.00174	1.21593	0.01767	0.03010	0.00106	870.5	25.16
Z40	30	6274	429	1522	12409	22024	0.06517	0.00116	0.30799	0.00054	0.34124	0.00655	0.00936	0.00034	779.7	36.85
Z41	0	5758	319	10744	197307	205306	0.0103	0.00363	0.00555	0.00028	0.82824	0.00591	0.00856	0.00033	331.1	44.29
Z42	20	23315	1782	1609	31331	20641	0.07306	0.00112	0.14585	0.00198	1.46873	0.02459	0.03991	0.00183	1015.7	30.76
Z43	0	4368	272	869	81077	162535	0.05896	0.00166	0.03679	0.00059	0.299	0.085	0.00775	0.00039	565.4	60.22
Z44	30	20208	1470	3368	566860	106953	0.05010	0.0017	0.04389	0.00064	0.38492	0.00759	0.01024	0.00045	914.6	32.03
Z45	0	16388	940	1722	155125	443202	0.05449	0.00082	0.04911	0.00068	0.35882	0.00617	0.00831	0.00033	391.4	33.09
Z46	7	7068	426	2432	192491	214558	0.05792	0.00107	0.04256	0.00059	0.33965	0.00662	0.01052	0.00035	526.4	40.29
Z47	5	2622	174	1694	37650	406197	0.06417	0.00169	0.02818	0.00137	0.82015	0.02196	0.00668	0.00124	747.1	54.8
Z48	0	5405	364	1592	149405	204519	0.06484	0.00115	0.03459	0.00048	0.30904	0.00586	0.00868	0.00027	781.8	35.95
Z49	2	6450	388	1538	139116	235395	0.05772	0.00107	0.03628	0.00051	0.28857	0.00572	0.00889	0.0003	518.8	40.58
Z50	5	1186	75	394	33128	40501	0.06106	0.0028	0.0389	0.00067	0.3273	0.01483	0.00998	0.00043	641.3	95.64
Z51	0	17213	1011	789	66464	395337	0.05652	0.00081	0.05666	0.00076	0.44127	0.00711	0.01012	0.00039	472.1	31.77
Z52	8	6220	405	1035	42745	104887	0.06252	0.00139	0.07867	0.00116	0.67774	0.01553	0.02034	0.00093	691.9	46.72
Z53	5	26383	1998	623	12447	209064	0.07028	0.00098	0.16678	0.00227	1.67368	0.02591	0.04114	0.00169	1008.8	26.97
Z54	0	2791	188	1416	122056	91835	0.06521	0.00167	0.03969	0.00059	0.35673	0.00929	0.00909	0.00039	781.8	35.09
Z55	0	3670	228	973	134018	205994	0.013	0.00358	0.00592	0.00028	0.29728	0.00699	0.00907	0.00037	601.6	48.71
Z56	3	16209	930	4121	395632	604679	0.05498	0.00083	0.0356	0.00049	0.26975	0.00456	0.00838	0.00033	411.3	33.19
Z57	0	6194	352	3000	305474	233922	0.0547	0.00123	0.03551	0.00052	0.26777	0.00623	0.00821	0.00038		

Grain	Pb204 (ppm)	Pb206 (ppm)	Pb207 (ppm)	Pb208 (ppm)	Th232 (ppm)	U238 (ppm)	Pb207/Pb206	Pb206/U238	Pb207/U235	Pb208/Th232	Pb207/Pb206 Age (Ma)	$\pm 2\sigma$	Pb206/U238 Age (Ma)	$\pm 2\sigma$	Pb207/U235 Age (Ma)	$\pm 2\sigma$	Pb208/Th232 Age (Ma)	$\pm 2\sigma$	Rho	Concordancy				
Z1	1	7131	378	1148	97521	242255	0.05251	0.00117	0.03706	0.00069	0.01162	0.00052	307.6	49.69	234.6	3.21	241.1	4.88	233.4	10.46	0.83561	97.30402323		
Z2	0	36297	5834	2180	24696	149654	0.15724	0.00186	0.32055	0.00432	6.94663	0.09967	0.08325	0.00267	2426.2	19.91	1792.4	21.08	2104.6	12.73	1616.3	49.88	0.83561	85.16582724
Z3	8	20118	1517	1906	45373	170578	0.07377	0.00096	0.15556	0.0021	1.58161	0.02415	0.03971	0.00132	1035.3	26.14	932	11.74	963	9.5	787.2	25.72	0.83561	96.78089304
Z4	0	1773	122	522	17569	21973	0.06843	0.00304	0.09932	0.00183	0.93559	0.04036	0.02831	0.00174	881.7	89.31	610.4	10.76	670.6	21.17	564.2	34.29	0.83561	91.02296451
Z5	8	7890	426	2110	203857	289723	0.05285	0.00089	0.03574	0.00049	0.26033	0.00479	0.00984	0.00035	322.2	37.88	226.4	3.06	234.9	3.86	197.9	6.96	0.83561	96.38143891
Z6	4	6048	351	1536	134284	205245	0.05707	0.00109	0.03809	0.00053	0.29957	0.00603	0.01076	0.00042	493.5	41.63	241	3.28	266.1	4.71	216.3	8.4	0.83561	90.56745584
Z7	16	10641	614	3803	383805	414179	0.05659	0.00091	0.03334	0.00045	0.25994	0.00457	0.00937	0.00036	474.7	35.49	211.4	2.82	234.7	3.68	188.4	7.21	0.83561	90.07243289
Z8	18	12322	668	3367	335113	484758	0.05301	0.00083	0.03325	0.00045	0.24289	0.00418	0.00963	0.00038	329	34.89	210.8	2.82	220.8	3.42	193.7	7.56	0.83561	95.47101449
Z9	0	22878	1195	4542	441528	816789	0.05099	0.00073	0.03664	0.00049	0.25746	0.00418	0.0099	0.00041	240.2	32.78	231.9	3.07	232.6	3.37	199.2	8.14	0.83561	99.69905417
Z10	12	10561	631	2697	262823	409552	0.05837	0.00093	0.0336	0.00046	0.27035	0.00472	0.00983	0.00041	543.7	34.5	213	2.85	243	3.78	197.7	8.23	0.83561	87.65432099
Z11	11	8257	452	3170	308855	306185	0.05353	0.00097	0.03495	0.00048	0.25788	0.00496	0.0098	0.00044	351.2	40.35	221.5	3	233	4	197.1	8.77	0.83561	95.06437768
Z12	2	15791	1178	1783	37736	148482	0.07281	0.00106	0.13863	0.00188	1.39144	0.02271	0.04526	0.00203	1008.8	29.32	836.9	10.64	885.3	9.64	894.7	39.19	0.83561	94.53292669
Z13	6	9060	501	1959	187707	344668	0.05411	0.00114	0.03239	0.00044	0.24154	0.00517	0.01013	0.00061	375.5	46.7	205.5	2.75	219.7	4.23	203.8	12.22	0.83561	93.53664087
Z14	0	18919	1540	4099	74940	128300	0.07937	0.00117	0.19014	0.00256	0.20809	0.00339	0.05268	0.00257	1181.5	28.95	1122.1	13.86	1142.4	11.2	1037.6	49.3	0.83561	98.22303922
Z15	283	10822	4587	11427	95011	213161	0.41384	0.00583	0.06497	0.00088	3.70639	0.05743	0.11497	0.00567	3960.2	20.94	405.8	5.3	1572.7	12.39	2199.6	102.83	0.83561	25.80275959
Z16	5	13339	1098	2420	44167	92028	0.08065	0.0011	0.18655	0.00249	0.27042	0.03218	0.05155	0.0017	1212.9	26.71	1102.7	13.52	1140.3	10.63	1015.9	32.74	0.758406	96.70262212
Z17	11	12314	658	537	37599	348961	0.0524	0.00082	0.04445	0.00058	0.32115	0.00544	0.01322	0.00053	303	35.12	280.4	3.6	282.8	4.18	265.5	10.59	0.758406	99.15134371
Z18	13	4675	321	1409	130415	188689	0.06724	0.00129	0.03186	0.00044	0.29532	0.00595	0.01016	0.00037	845.1	39.44	202.2	2.76	262.7	4.66	204.4	7.31	0.758406	76.96992767
Z19	11	26456	1616	1827	63632	387991	0.05973	0.00081	0.08788	0.00116	0.72367	0.01115	0.02685	0.001	593.8	28.9	543	6.9	552.8	6.57	535.5	19.67	0.758406	98.22720695
Z20	10	18136	1051	504	21609	313285	0.0567	0.0008	0.07405	0.00098	0.57889	0.00914	0.02195	0.00092	479.2	31.12	460.5	5.87	463.7	5.88	438.8	18.16	0.758406	99.30989864
Z21	14	2309	129	504	44938	81201	0.055	0.00181	0.03549	0.00054	0.26912	0.00878	0.01035	0.0005	412.1	71.13	224.8	3.33	242	7.02	208.1	10	0.758406	92.8925196
Z22	10	6603	355	1277	123193	259207	0.05265	0.00097	0.03292	0.00045	0.23893	0.00467	0.0097	0.0039	313.5	41.21	208.8	2.82	217.5	3.83	195	7.73	0.758406	96.36298293
Z23	10	1290	88	258	24861	50991	0.0669	0.00238	0.03267	0.00052	0.30139	0.01066	0.00962	0.0047	834.6	72.53	207.3	3.24	267.5	8.32	193.5	9.49	0.758406	77.4953271
Z24	20	7056	388	2343	167182	182877	0.05443	0.00124	0.04631	0.00063	0.3475	0.00793	0.01319	0.00074	388.7	49.9	291.8	3.87	302.8	5.98	264.9	14.82	0.758406	96.3672391
Z25	11	4491	254	1215	104374	149037	0.05559	0.00127	0.03803	0.00053	0.29123	0.00678	0.01076	0.00051	435.8	49.64	240.4	3.3	259.5	5.34	216.4	10.18	0.758406	92.63969171
Z26	10	4494	239	1041	98375	161626	0.05219	0.00115	0.03537	0.00049	0.25457	0.00579	0.00986	0.00046	293.8	49.62	224.1	3.07	230.3	4.69	198.3	9.15	0.758406	97.30785931
Z27	17	6																						

Grain	Pb204 (ppm)	Pb206 (ppm)	Pb207 (ppm)	Pb208 (ppm)	Th232 (ppm)	U238 (ppm)	Pb207/Pb206	Pb206/U238	Pb207/U235	Pb208/Th232	Pb207/Pb206 ± 2σ	Age (Ma)	Pb206/U238 ± 2σ	Pb207/U235 ± 2σ	Pb208/Th232 ± 2σ	Rho	Concordancy							
Z1	6	9806	646	1915	130715	293101	0.06324	0.00153	0.04381	0.00066	0.38174	0.00933	0.01132	0.00054	716.4	50.47	276.4	4.07	328.3	6.85	227.5	10.75	0.828506	84.19128846
Z2	10	21260	1767	1653	26547	123773	0.07955	0.00102	0.22466	0.00302	2.46389	0.03671	0.0488	0.00149	1186	25.15	1306.4	15.9	1261.5	10.76	963.1	28.73	0.828506	103.5592549
Z3	5	26970	1507	3504	217570	663863	0.05347	0.00075	0.05352	0.00073	0.39461	0.00631	0.01278	0.00043	348.8	31.49	336.1	4.45	337.7	4.59	256.7	8.54	0.828506	99.52620669
Z4	0	5234	295	1337	117435	182223	0.05418	0.00108	0.03705	0.00052	0.27677	0.00578	0.00923	0.00032	378.4	44.38	234.5	3.21	248.1	4.59	185.7	6.36	0.828506	94.51833938
Z5	22	11512	609	2348	235928	442799	0.05085	0.00123	0.0352	0.00054	0.24681	0.00614	0.00783	0.0004	234.1	55.01	223	3.34	224	5	157.6	8.05	0.828506	99.55357143
Z6	9	15931	995	1007	32733	195727	0.05991	0.00084	0.10539	0.00141	0.8704	0.01369	0.02499	0.00089	600.2	30.01	645.9	8.22	635.8	7.43	498.9	17.5	0.828506	101.5885499
Z7	0	6702	377	1037	90772	230740	0.05387	0.00098	0.03807	0.00053	0.2827	0.00547	0.00912	0.00033	365.4	40.49	240.8	3.28	252.8	4.33	183.6	6.65	0.828506	95.25316456
Z8	9	6521	443	1161	75172	200597	0.06492	0.00123	0.04322	0.00062	0.38686	0.00774	0.01247	0.00051	771.8	39.35	272.8	3.83	332.1	5.67	250.5	10.09	0.828506	82.14393255
Z9	0	33441	2510	4246	88747	263915	0.07225	0.00096	0.16402	0.00218	1.63371	0.02483	0.03970	0.00154	993.1	26.89	979.1	12.1	983.3	9.57	788.6	29.85	0.828506	99.57286688
Z10	1	5814	303	980	82226	183190	0.05007	0.00097	0.04106	0.00057	0.28343	0.00578	0.00976	0.00039	198.2	44.5	259.4	3.51	253.4	4.58	196.3	7.85	0.828506	102.3677979
Z11	10	2823	162	510	23268	47088	0.0553	0.00145	0.07751	0.00113	0.5909	0.01575	0.01813	0.00081	424.3	57.06	481.3	6.74	474.1	10.05	363.1	16.03	0.828506	102.1001273
Z12	8	30513	1878	371	10012	421373	0.05879	0.00087	0.09563	0.00131	0.77503	0.01277	0.03097	0.00159	559.4	31.84	588.8	7.72	582.6	7.31	616.5	31.17	0.828506	101.064195
Z13	14	2420	153	562	25830	0.06134	0.00175	0.0726	0.00109	0.61375	0.01755	0.01894	0.00097	651	60.1	451.8	6.58	485.9	11.05	379.4	19.18	0.828506	92.98209508	
Z14	10	1361	130	260	6734	20624	0.09207	0.00272	0.08442	0.00135	1.0712	0.03113	0.0347	0.00187	1468.7	55.1	522.4	8.02	739.3	15.26	665.4	36.64	0.828506	70.66143649
Z15	9	3706	281	1105	80506	123269	0.07339	0.00158	0.03816	0.00054	0.38596	0.00846	0.01215	0.00062	1024.7	42.96	241.4	3.35	331.4	6.2	244.1	12.44	0.828506	72.84248642
Z16	0	7987	415	1440	151727	320472	0.05053	0.00126	0.03406	0.00052	0.23727	0.00609	0.00775	0.00035	219.5	56.66	215.9	3.25	216.2	5	156.1	7.06	0.71617	99.86123959
Z17	9	6247	407	2584	261599	245653	0.06373	0.00119	0.033	0.00046	0.28983	0.00574	0.00826	0.00029	732.6	39.19	209.3	2.88	258.4	4.52	166.3	5.74	0.71617	80.99845201
Z18	0	11197	668	1694	67735	164544	0.05853	0.00087	0.08717	0.00116	0.70094	0.0116	0.02071	0.0007	542.8	32.42	538.8	6.88	539.4	6.92	414.4	13.84	0.71617	99.88876529
Z19	0	7512	402	1571	40565	251727	0.05246	0.0009	0.03826	0.00052	0.27661	0.00512	0.00924	0.00032	305.6	38.74	242	3.21	248	4.07	185.9	6.49	0.71617	97.58064516
Z20	3	12115	637	3103	268401	401046	0.05164	0.00081	0.03859	0.00051	0.27464	0.00469	0.00964	0.00035	269.6	35.42	244.1	3.19	246.4	3.74	193.9	7	0.71617	99.06655844
Z21	6	5471	286	1011	91523	179719	0.05127	0.00103	0.03943	0.00055	0.27862	0.00509	0.00903	0.00035	253.1	45.7	249.3	3.4	249.6	4.68	181.7	6.98	0.71617	99.87980769
Z22	12	2892	215	615	12595	22401	0.07345	0.00197	0.15997	0.00241	1.61869	0.04337	0.01427	0.00211	1026.3	53.44	956.6	13.37	977.5	16.82	817.5	40.97	0.71617	97.86189258
Z23	2	2696	148	490	39202	86526	0.05401	0.00147	0.04	0.00058	0.29769	0.00822	0.0103	0.00046	371.1	60.12	252.8	3.6	264.6	6.44	207.7	9.24	0.71617	95.5404384
Z24	6	12340	727	1597	104379	334048	0.05787	0.00091	0.04794	0.00065	0.38223	0.00664	0.01218	0.00049	524.5	34.48	301.8	4	328.7	4.87	244.7	9.86	0.71617	91.8124582
Z25	0	20780	1110	4385	421923	576445	0.05253	0.00078	0.03554	0.00048	0.25723	0.00428	0.0084	0.00035	308.5	33.55	225.1	2.97	232.4	3.46	169.1	7.02	0.71617	96.85886403
Z26	0	7099	363	1528	141979	247976	0.05054	0.00097	0.03692	0.00051	0.25672	0.00521	0.00876	0.00039	215.8	43.8	233.7	3.16	232	4.21	176.3	7.88	0.71617	100.7327586
Z27	0	13093	681	3011	281449	462732	0.05114	0.00084	0.03678	0.0005	0.25917	0												

Grain	Pb204 (ppm)	Pb206 (ppm)	Pb207 (ppm)	Pb208 (ppm)	Th232 (ppm)	U238 (ppm)	Pb207/Pb206	Pb206/U238	Pb207/U235	Pb208/Th232	Pb207/Pb206 Age (Ma)	$\pm 2\sigma$	Pb206/U238 Age (Ma)	$\pm 2\sigma$	Pb207/U235 Age (Ma)	$\pm 2\sigma$	Pb208/Th232 Age (Ma)	$\pm 2\sigma$	Rho	Concordancy				
Z1	15	8387	494	3580	267341	242857	0.05706	0.0015	0.04055	0.00057	0.31892	0.00825	0.01009	0.00034	493.1	57.42	256.2	3.54	281.1	6.35	202.9	6.75	0.883007	91.14194237
Z2	5	7639	422	2145	175543	241002	0.0536	0.00127	0.03662	0.00049	0.27061	0.00638	0.00934	0.00029	354.1	52.89	231.9	3.04	243.2	5.1	187.9	5.81	0.883007	95.35361842
Z3	15	9915	564	2571	210436	317905	0.0555	0.001	0.03531	0.00043	0.27018	0.00494	0.00965	0.00026	432.1	39.37	223.7	2.7	242.8	3.95	194.2	5.2	0.883007	92.13344316
Z4	18	7466	418	2029	160388	234973	0.05514	0.00097	0.03507	0.00042	0.26661	0.00474	0.01029	0.00026	417.8	38.79	222.2	2.6	240	3.8	206.8	5.14	0.883007	92.58333333
Z5	22	13859	1040	1552	28328	87782	0.0739	0.00103	0.17443	0.00203	0.17472	0.02556	0.04468	0.0012	1035.8	28	1036.5	11.14	1036.3	9.35	883.4	23.24	0.883007	100.0192994
Z6	27	9372	538	2124	145532	228313	0.05649	0.00093	0.04533	0.00053	0.35303	0.00588	0.01195	0.00032	470.8	36.34	285.8	3.29	307	4.41	240.2	6.45	0.883007	93.09462524
Z7	24	28267	1669	989	33315	363048	0.05814	0.00076	0.086	0.00098	0.68941	0.00938	0.02442	0.00074	534.5	28.84	531.9	5.82	532.4	5.64	487.6	14.62	0.883007	99.90608565
Z8	17	12478	733	3615	267190	359526	0.05788	0.00088	0.03835	0.00045	0.30603	0.00477	0.01115	0.00032	524.8	33.45	242.6	2.78	271.1	3.71	224.1	6.36	0.883007	89.48727407
Z9	36	12279	710	2558	186410	365893	0.05669	0.00082	0.03804	0.00045	0.29731	0.00446	0.01086	0.00021	478.9	31.9	240.7	2.79	264.3	3.49	218.3	4.21	0.862804	91.07075293
Z10	7	13472	805	3514	133327	187534	0.05821	0.00098	0.0845	0.00109	0.68588	0.01195	0.02037	0.00049	537	36.9	528.6	6.45	530.3	7.2	407.6	9.64	0.862804	99.67942674
Z11	12	9827	633	1640	51500	125019	0.06379	0.00128	0.08298	0.00103	0.7295	0.01533	0.02639	0.00091	734.8	45.09	513.9	6.13	556.3	9	526.6	17.99	0.862804	92.37821319
Z12	28	10186	610	4975	205313	156070	0.05866	0.00092	0.07454	0.0009	0.60276	0.00977	0.01912	0.00039	554.4	33.94	463.5	5.4	479	6.19	382.8	7.79	0.862804	96.76409186
Z13	29	14402	884	4626	373928	452606	0.0603	0.00084	0.03578	0.00042	0.29745	0.00429	0.00984	0.0002	614.2	29.65	226.6	2.6	264.4	3.36	197.9	4.04	0.862804	85.70347958
Z14	27	20957	1121	5770	488207	663142	0.05255	0.0007	0.03517	0.0004	0.25479	0.00355	0.00947	0.0002	309.5	30.12	222.8	2.51	230.5	2.87	190.5	4.07	0.862804	96.65943601
Z15	42	4580	246	1221	98905	134204	0.05295	0.00111	0.03813	0.00047	0.27837	0.00583	0.00989	0.00024	326.5	46.81	241.3	2.92	249.4	4.63	198.8	4.77	0.862804	96.75220529
Z16	16	8468	456	1962	165886	266944	0.053	0.00084	0.03555	0.00042	0.25976	0.00423	0.00946	0.00021	328.6	35.63	225.2	2.61	234.5	3.41	190.3	4.25	0.862804	96.03411514
Z17	9	16328	1024	2714	99500	229734	0.06173	0.00092	0.07695	0.00088	0.65475	0.00985	0.02208	0.00061	664.7	31.61	477.9	5.28	511.4	6.05	441.4	11.98	0.862804	93.44935471
Z18	25	14663	884	5981	459548	446156	0.05967	0.001	0.035	0.0004	0.28789	0.00478	0.01076	0.00033	591.6	35.92	221.8	2.51	256.9	3.77	216.4	6.6	0.862804	86.33709615
Z19	30	11899	704	2603	204445	365497	0.05827	0.00099	0.03556	0.00042	0.28563	0.00487	0.01041	0.00032	539.1	37.53	225.3	2.61	255.1	3.85	209.3	6.31	0.862804	88.31830655
Z20	32	20772	1113	5553	492718	684707	0.05271	0.00082	0.03547	0.00044	0.25775	0.00419	0.00892	0.00027	316.1	34.95	224.7	2.72	232.8	3.38	179.5	5.33	0.862804	96.52061856
Z21	5	6259	345	1962	162202	189065	0.05438	0.00104	0.03608	0.00043	0.27045	0.00515	0.00999	0.00023	386.6	42.24	228.5	2.68	243	4.12	200.9	4.64	0.722136	94.03292181
Z22	25	25734	1492	4348	330120	721751	0.05708	0.00072	0.03948	0.00045	0.31062	0.00411	0.01075	0.00023	493.9	27.96	249.6	2.78	274.7	3.19	216.1	4.59	0.722136	90.86275937
Z23	62	10621	831	2401	129564	295520	0.07698	0.00151	0.04239	0.00058	0.45945	0.00991	0.01484	0.00049	1120.8	38.55	273.2	3.61	383.9	6.33	297.8	9.83	0.722136	71.16436572
Z24	20	13278	756	10365	856644	405582	0.05602	0.00086	0.03676	0.00043	0.28392	0.00445	0.00977	0.00023	453	33.25	232.7	2.7	253.8	3.52	196.5	4.59	0.722136	91.68636722
Z25	0	16430	884	4325	367802	519207	0.05297	0.00078	0.03589	0.00043	0.26204	0.00403	0.00951	0.00024	327.5	33.32	227.3	2.65	236.3	3.24	191.3	4.76	0.722136	96.19128227
Z26	15	13848	789	3704	302050	421501	0.05627	0.00085	0.03618	0.00042	0.28066	0.00431	0.01003	0.00026	462.4	33.29	229.1	2.61	251.2	3.42	201.6	5.22	0.722136</td	

Grain	Pb204 (ppm)	Pb206 (ppm)	Pb207 (ppm)	Pb208 (ppm)	Th232 (ppm)	U238 (ppm)	Pb207/Pb206	Pb206/U238	Pb207/U235	Pb208/Th232	Pb207/Pb206 Age (Ma)	$\pm 2\sigma$	Pb206/U238 Age (Ma)	$\pm 2\sigma$	Pb207/U235 Age (Ma)	$\pm 2\sigma$	Pb208/Th232 Age (Ma)	$\pm 2\sigma$	Rho	Concordancy		
Z1	2	6213	412	1354	106885	214095	0.06393	0.0012	0.03645	0.00049	0.32115	0.00629	0.01042	0.00034	739.5	39.38	230.8	3.08	282.8	4.84	209.6	6.71 0.766703 81.61244696
Z2	11	5709	407	1755	146359	201111	0.06887	0.00127	0.03539	0.00048	0.33592	0.00643	0.00998	0.00031	894.8	37.5	224.2	2.96	294.1	4.89	200.8	6.24 0.766703 76.23257395
Z3	10	16794	896	495	33455	498383	0.05131	0.00077	0.0431	0.00057	0.30477	0.00505	0.01207	0.00049	254.6	34.31	272	3.54	270.1	3.93	242.4	9.7 0.766703 100.7034432
Z4	25	12679	676	3608	421950	0.05156	0.00076	0.0372	0.00048	0.2644	0.00425	0.00901	0.00028	266	33.59	235.5	2.97	238.2	3.41	181.2	5.56 0.766703 98.86649874	
Z5	7	7977	481	1958	140113	215658	0.05827	0.00103	0.04683	0.00063	0.37609	0.00706	0.01177	0.00041	539.2	39.02	295	3.88	324.2	5.21	236.5	8.1 0.766703 90.99321407
Z6	10	8803	511	2098	188627	298596	0.05628	0.00094	0.03643	0.00047	0.28258	0.00499	0.00956	0.00033	462.6	36.77	230.7	2.95	252.7	3.95	192.3	6.62 0.766703 91.29402454
Z7	5	9067	506	1669	153591	311840	0.05417	0.00103	0.03607	0.00048	0.26926	0.00531	0.00932	0.00037	378	42.12	228.4	3	242.1	4.25	187.5	7.47 0.766703 94.34118133
Z8	9	3629	213	758	70600	132745	0.05704	0.00137	0.03443	0.00048	0.27071	0.00664	0.00924	0.00036	492.7	52.84	218.2	3	243.3	5.3	185.9	7.27 0.766703 89.68351829
Z9	13	10007	796	1221	27865	92197	0.07589	0.00138	0.14495	0.0021	1.51617	0.02943	0.03554	0.00161	1092.2	35.94	872.6	11.8	936.9	11.88	705.8	31.34 0.766703 93.13694098
Z10	0	6593	383	1610	153578	251321	0.05626	0.00103	0.03289	0.00044	0.25050	0.0049	0.00905	0.00035	462.5	40.27	208.6	2.74	230.7	3.96	182.1	5.56 0.766703 90.42045947
Z11	8	3033	213	1034	23145	0.08018	0.00178	0.16248	0.0023	1.79587	0.04066	0.04165	0.0017	1201.4	43.13	970.6	12.77	1044	14.77	824.8	33 0.766703 92.96934866	
Z12	19	12345	790	2948	102244	160022	0.06211	0.00094	0.0965	0.00126	0.82625	0.01359	0.02557	0.00104	677.9	31.99	593.9	7.41	611.5	7.56	510.3	20.56 0.766703 97.12183156
Z13	15	5467	367	623	75635	0.05626	0.00128	0.08979	0.00121	0.80778	0.01636	0.02944	0.00139	782.7	40.54	554.3	7.18	601.2	9.19	586.5	27.22 0.766703 92.19893546	
Z14	11	56787	3344	13735	611347	930484	0.05713	0.00074	0.07669	0.00099	0.60399	0.00888	0.02016	0.00086	496.1	28.53	476.3	5.91	479.8	5.62	403.4	17.12 0.766703 99.27052939
Z15	0	22933	1737	4927	111313	185502	0.0733	0.00108	0.15944	0.00214	1.61087	0.02633	0.03977	0.00188	1022.2	29.41	953.7	11.92	974.4	10.24	788.3	36.6 0.766703 97.87561576
Z16	20	8009	445	1674	215380	228424	0.05464	0.0011	0.04107	0.00053	0.30932	0.00632	0.01139	0.0048	397.4	44.31	259.5	3.27	273.7	4.9	228.9	9.66 0.776468 94.81183778
Z17	0	8518	543	1931	79585	128758	0.06226	0.001	0.08162	0.00106	0.70048	0.01204	0.02097	0.00075	683	34.03	505.8	6.32	539.1	7.19	419.5	14.82 0.776468 93.8230384
Z18	54	27957	2292	1975	21262	246462	0.07874	0.0032	0.12625	0.00228	1.3699	0.05302	0.07873	0.01169	1165.7	78.5	766.4	13.02	876	22.72	1531.8	219.12 0.776468 87.48858447
Z19	21	8188	459	1228	116958	305599	0.05444	0.0011	0.03476	0.00049	0.26084	0.0055	0.00918	0.0004	389.4	44.32	220.3	3.04	235.4	4.43	184.6	8.11 0.776468 93.58538658
Z20	0	25257	1281	8835	769467	814757	0.05035	0.0019	0.03431	0.00055	0.23787	0.00867	0.00956	0.00115	211.1	85.12	217.4	3.42	216.7	7.11	192.2	23 0.776468 100.3230272
Z21	21	9380	566	1646	131872	237371	0.05905	0.00111	0.04692	0.00061	0.38191	0.00737	0.01073	0.00049	568.9	40.51	295.6	3.73	328.4	5.41	215.8	9.7 0.776468 90.01218027
Z22	0	7957	402	322	2806	261311	0.04966	0.00103	0.03579	0.00046	0.24503	0.00514	0.00978	0.00055	179.3	47.48	226.7	2.87	222.5	4.19	196.7	10.95 0.776468 101.8876404
Z23	0	20852	1319	3739	17208	253746	0.06186	0.00085	0.10172	0.0013	0.86733	0.01318	0.02549	0.00098	669.3	29.05	624.5	7.6	634.1	7.17	508.8	19.35 0.776468 98.48604321
Z24	16	60926	4730	5157	110714	469474	0.07544	0.00132	0.16468	0.00225	1.71241	0.02139	0.04209	0.00267	1080.3	34.74	982.7	12.45	1013.2	11.94	833.3	51.7 0.776468 96.98973549
Z25	6	10934	839	2867	54963	72987	0.07577	0.00152	0.17098	0.00222	1.78594	0.03578	0.04449	0.00251	1089	39.65	1017.5	12.23	1040.3	13.04	879.8	48.5 0.776468 97.80832452
Z26	12	2977	204	735	61760	101908	0.06711	0.00162	0.16311	0.00005	0.334	0.00815	0.01034	0.00045	841.2	49.43	228.7	3.12	292.6	6.2	208	9.01 0.776468 78.16131237
Z27	0	17722	919	2955	298879	646377	0.05077	0.00078	0.03391	0.00044	0.23699	0.00395	0.00862	0.00037	227.3	35.26	215	2.73	225	3.24	173.5	7.51 0.

Sample Number	176Hf/177Hf	2SE	178Hf/177Hf	2SE	176Lu/177Hf	2SE	176Yb/177Hf	2SE	$\epsilon$ Hf	Corrected	
										176Hf/177Hf	2SE
JA01H15	0.282546189	3.32E-05	1.467309845	0.000251	0.001206186	2.96E-05	0.03581324	0.001197	-2.54	0.282560034	3.37E-05
JA01H14	0.282389852	2.78E-05	1.467371458	0.00035	0.000364039	4.15E-05	0.014234427	0.001527	-0.26	0.28240369	2.85E-05
JA01H13	0.28230566	3.63E-05	1.467407726	0.000343	0.000170959	1.36E-05	0.006599876	0.0004	-5.21	0.282319493	3.68E-05
JA01H12	0.282455808	4.22E-05	1.467298455	0.000329	0.001258187	3.71E-05	0.042839065	0.000999	-5.96	0.282469649	4.27E-05
JA01H11	0.282607449	4.15E-05	1.467118947	0.000367	0.000935506	3.49E-05	0.03292648	0.001385	-1.43	0.282621298	4.19E-05
JA01H10	0.282580342	4.05E-05	1.467170739	0.000277	0.001058597	7.37E-05	0.034214322	0.001517	-1.93	0.282594189	4.1E-05
JA01H9	0.282708363	5.14E-05	1.4676567	0.000361	0.001036413	7.12E-05	0.031003653	0.001287	7.90	0.282722216	5.17E-05
JA01H8	0.282544874	3.67E-05	1.46735766	0.000206	0.00099155	4.31E-05	0.026917503	0.000839	-3.00	0.28255872	3.73E-05
JA01H7	0.282449429	9.27E-05	1.467518183	0.000209	0.00377281	0.000168	0.113818875	0.003779	-5.23	0.282463269	9.29E-05
JA01H6	0.282457716	4.32E-05	1.467350254	0.000189	0.001718376	0.000125	0.053976785	0.004181	-4.02	0.282471557	4.37E-05
JA01H5	0.282278772	6E-05	1.467482196	0.000369	0.001376183	0.000102	0.045403497	0.002259	1.34	0.282292604	6.03E-05
JA01H4	0.282271257	0.000209	1.467443322	0.000662	0.003331255	9.21E-05	0.100656495	0.004153	-1.19	0.282285089	0.000209
JA01H3	0.282456754	4.65E-05	1.467246658	0.000341	0.000714279	2.76E-05	0.023442726	0.000735	3.22	0.282470595	4.69E-05
JA01H2	0.282470363	5.52E-05	1.467485875	0.000369	0.001452156	0.000172	0.054090684	0.005221	-3.02	0.282484205	5.56E-05
JA01H1	0.282178572	5.69E-05	1.467471739	0.000438	0.001097159	8.14E-05	0.037264054	0.000966	0.62	0.282192399	5.72E-05

Supplementary Table 10: Raw Hf data from sample NZ1301 with corrected  $\epsilon$ Hf values

Sample Number	176Hf/177Hf	2SE	178Hf/177Hf	2SE	176Lu/177Hf	2SE	176Yb/177Hf	2SE	$\epsilon$ Hf	Corrected	
										176Hf/177Hf	2SE
JA22H30	0.282559951	3.28E-05	1.467302865	0.00024	0.000961738	9.66E-05	0.030120191	0.001654	1.95	0.282698473	3.34E-05
JA22H29	0.282585361	2.62E-05	1.467395243	0.000167	0.00107865	2.88E-05	0.033001325	0.000544	-2.17	0.282599208	2.69E-05
JA22H28	0.282324961	2.57E-05	1.467164757	0.000212	0.001131399	4.72E-05	0.042644017	0.002023	-5.95	0.282463369	2.64E-05
JA22H27	0.282214967	3.56E-05	1.467295622	0.000182	0.001429767	8.74E-05	0.058943478	0.004533	0.21	0.282228797	3.61E-05
JA22H26	0.282288839	3.61E-05	1.46732937	0.000247	0.000746141	5.45E-05	0.023429102	0.001349	5.81	0.282427229	3.66E-05
JA22H25	0.282274366	2.15E-05	1.467310684	0.000198	0.000617359	1.66E-05	0.023296253	0.000552	-11.87	0.282288199	2.24E-05
JA22H24	0.282572992	2.7E-05	1.467351071	0.000252	0.000521444	1.08E-05	0.018058704	0.000411	21.38	0.282711521	2.77E-05
JA22H23	0.282404735	7E-05	1.467571736	0.000347	0.001535714	0.000108	0.050757107	0.002063	-2.86	0.282418573	7.02E-05
JA22H22	0.282314608	3.47E-05	1.467292707	0.000273	0.000634963	2.03E-05	0.021298895	0.00064	-6.42	0.28245301	3.53E-05
JA22H21	0.282479334	2.7E-05	1.467271746	0.000225	0.00085406	2.02E-05	0.025448565	0.000493	7.39	0.282493176	2.77E-05
JA22H20	0.28226776	3.75E-05	1.467420858	0.000282	0.001041136	0.000121	0.035829529	0.004378	-9.18	0.282406139	3.8E-05
JA22H19	0.282461088	4.25E-05	1.467455834	0.000262	0.000971535	6.27E-05	0.034555764	0.001357	-6.15	0.28247493	4.29E-05
JA22H18	0.282643265	4.1E-05	1.467309943	0.000233	0.001915976	5.02E-05	0.066471268	0.001287	4.56	0.282781828	4.14E-05
JA22H17	0.282432675	3.12E-05	1.467282496	0.000366	0.000359552	2.62E-05	0.013495845	0.000996	1.57	0.282446515	3.18E-05
JA22H16	0.282608783	3.36E-05	1.467310864	0.000309	0.000771262	5.62E-05	0.024380944	0.00183	8.13	0.282747329	3.42E-05
JA22H15	0.282560377	3.96E-05	1.467119501	0.000236	0.001522935	0.000138	0.057715953	0.005233	-1.26	0.282574223	4E-05
JA22H14	0.282635975	4.05E-05	1.467433269	0.000333	0.001027592	5.4E-05	0.035984091	0.002005	4.82	0.282774534	4.1E-05
JA22H13	0.282467397	3.44E-05	1.467402768	0.000342	0.000866162	2.89E-05	0.026928639	0.000561	9.21	0.282481239	3.5E-05
JA22H12	0.282306778	3.36E-05	1.467427676	0.000243	0.000941067	4.36E-05	0.035613903	0.001886	-2.33	0.282445176	3.42E-05
JA22H11	0.282385703	4.9E-05	1.467360082	0.000281	0.001833344	4.57E-05	0.070494216	0.001616	-2.10	0.28239954	4.94E-05
JA22H10	0.282391609	4.22E-05	1.467348585	0.000256	0.00095433	5.11E-05	0.033000962	0.00049	-3.14	0.282530048	4.27E-05
JA22H9	0.282536521	3.69E-05	1.467394647	0.000239	0.000989457	0.000108	0.02983864</				

Sample Number	176Hf/177Hf		2SE	178Hf/177Hf		2SE	176Lu/177Hf		2SE	176Yb/177Hf		2SE	$\epsilon$ Hf	Corrected	
	176Hf/177Hf	2SE		178Hf/177Hf	2SE		176Lu/177Hf	2SE		176Yb/177Hf	2SE			176Hf/177Hf	2SE
JA23H31	0.282457431	2.83E-05	1.467199375	0.000194	0.000510639	1.49E-05	0.018769324	0.000662	3.09	0.282471272	2.9E-05				
JA23H30	0.282256755	4.11E-05	1.467315393	0.000234	0.000850286	2.54E-05	0.028244573	0.001001	3.16	0.282270586	4.16E-05				
JA23H29	0.282458201	5.85E-05	1.467401792	0.000303	0.001450815	6.77E-05	0.044672246	0.001906	0.40	0.282472042	5.89E-05				
JA23H28	0.282627035	3.14E-05	1.467306416	0.000248	0.000691349	6.21E-05	0.022198848	0.001818	0.21	0.282640885	3.2E-05				
JA23H27	0.282263561	3.75E-05	1.467325504	0.000291	0.000808291	5.79E-05	0.028166553	0.001485	2.94	0.282277393	3.8E-05				
JA23H26	0.282611572	7.63E-05	1.467378659	0.000273	0.001312703	9.3E-05	0.038956353	0.00143	-0.65	0.28262542	7.65E-05				
JA23H25	0.282374807	3.32E-05	1.467147432	0.000258	0.000387958	3.13E-05	0.014151918	0.001147	-1.13	0.282388644	3.38E-05				
JA23H24	0.282689951	2.93E-05	1.467343247	0.000212	0.000390623	2.79E-05	0.011887124	0.000898	4.34	0.282703803	2.99E-05				
JA23H23	0.28241875	4.82E-05	1.467281472	0.000287	0.001130388	6.38E-05	0.042849078	0.003768	-1.06	0.282432589	4.86E-05				
JA23H22	0.282565871	3.04E-05	1.467217389	0.000197	0.000585008	1.41E-05	0.019566492	0.000549	-1.65	0.282579717	3.1E-05				
JA23H21	0.282605267	4.48E-05	1.467454258	0.000298	0.001716688	0.000102	0.059180114	0.00428	-1.21	0.282619116	4.52E-05				
JA23H20	0.282495911	3.67E-05	1.467358776	0.000316	0.000724849	2.54E-05	0.021942615	0.000341	0.94	0.282509754	3.72E-05				
JA23H19	0.282412277	4.58E-05	1.467421025	0.000286	0.000627109	4.35E-05	0.013346619	0.000547	22.73	0.282426116	4.62E-05				
JA23H18	0.282263378	2.49E-05	1.46727251	0.00029	0.000400606	5.53E-05	0.014167839	0.001848	-5.42	0.28227721	2.57E-05				
JA23H17	0.282133385	4.83E-05	1.467342446	0.000275	0.000662066	4.68E-05	0.01944235	0.000927	-17.64	0.282147211	4.87E-05				
JA23H16	0.282793768	5.06E-05	1.46729269	0.000219	0.000862171	8.29E-05	0.02700104	0.001673	8.00	0.282807625	5.1E-05				
JA23H15	0.282423028	3.37E-05	1.46731732	0.000244	0.000714583	4.47E-05	0.026363391	0.00168	-0.10	0.282436867	3.43E-05				
JA23H14	0.282601189	3.52E-05	1.467320536	0.00027	0.00113164	8.23E-05	0.034938105	0.001873	-1.33	0.282615038	3.57E-05				
JA23H13	0.282360112	0.000139	1.467772161	0.000376	0.003034603	0.000118	0.08741658	0.005568	-10.24	0.282373948	0.00014				
JA23H12	0.282481078	4.42E-05	1.46735892	0.000245	0.001860082	0.00011	0.061636245	0.002154	-0.42	0.28249492	4.46E-05				
JA23H11	0.282173141	3.89E-05	1.467352998	0.00027	0.000580972	3.89E-05	0.020536428	0.00075	1.03	0.282186969	3.94E-05				
JA23H10	0.282423214	4.45E-05	1.467097657	0.000359	0.001282423	5.52E-05	0.051081541	0.003257	-0.65	0.282437054	4.5E-05				
JA23H9	0.282539351	0.000114	1.467818695	0.000562	0.000791137	6.53E-05	0.020088427	0.001785	14.67	0.282553196	0.000114				
JA23H8	0.282322318	0.0001	1.467375446	0.000437	0.001719567	0.000167	0.05435335	0.003683	1.18	0.282336153	0.0001				
JA23H7	0.282516097	4.29E-05	1.467401523	0.000391	0.000855745	5.9E-05	0.026401769	0.000734	-3.83	0.282529941	4.33E-05				
JA23H6	0.28225153	3.93E-05	1.467438608	0.000431	0.000340813	5.48E-05	0.01268812	0.001967	0.13	0.282265361	3.98E-05				
JA23H5	0.282349069	4.7E-05	1.467443339	0.000305	0.001414991	0.000133	0.04913918	0.005765	-1.46	0.282362905	4.74E-05				
JA23H4	0.282703172	4.89E-05	1.467388834	0.000338	0.001513564	4.91E-05	0.055106721	0.00344	4.52	0.282717026	4.93E-05				
JA23H3	0.281914118	0.000104	1.467656281	0.000546	0.001180171	0.000143	0.041374215	0.002976	2.20	0.281927932	0.000104				
JA23H2	0.282603337	5.47E-05	1.467456844	0.000322	0.001639519	6.39E-05	0.057071749	0.001124	0.20	0.282617186	5.5E-05				
JA23H1	0.281490299	5.31E-05	1.467445202	0.000291	0.00039149	2.7E-05	0.010248835	0.000538	-2.13	0.281504092	5.35E-05				

Supplementary Table 12: Raw Hf data from sample NZ1323 with corrected  $\epsilon$ Hf values

Sample Number	176Hf/177Hf		2SE	178Hf/177Hf		2SE	176Lu/177Hf		2SE	176Yb/177Hf		2SE	$\epsilon$ Hf	Corrected	
	176Hf/177Hf	2SE		178Hf/177Hf	2SE		176Lu/177Hf	2SE		176Yb/177Hf	2SE			176Hf/177Hf	2SE
JA25H30	0.282534869	3.41E-05	1.467104849	0.000291	0.000840312	7									

Analysis	36Ar (V)	%1σ	37Ar (V)	%1σ	38Ar (V)	%1σ	39Ar (V)	%1σ	40Ar (V)	%1σ	40(r)/39(k) ± 2σ	Age (Ma)	± 2σ	40Ar(r) (%)	39Ar(k) (%)	K/Ca	± 2σ
3M30233f0.0000389	20.117	0.0001803	58.413	0.0007140	2.141	0.0542377	0.394	0.7997068	0.055	14.52981 ± 0.14429	210.19 1.97	98.54	41.01	129	151.10		
3M30237f0.0000315	25.991	0.0001023	116.546	0.0002249	3.369	0.0173777	0.697	0.2856152	0.090	15.89322 ± 0.35942	228.71 4.86	96.70	13.14	73	170.25		
3M30232f0.0000714	9.404	0.0000493	228.375	0.0003269	3.496	0.0240509	0.395	0.4197570	0.068	16.56568 ± 0.21323	237.78 2.87	94.92	18.19	210	957.95		
3M30235f0.0000190	45.106	0.0000304	370.589	0.0002322	5.833	0.0164089	0.676	0.2780118	0.066	16.59642 ± 0.38495	238.19 5.18	97.96	12.41	232	1721.93		
3M30234f0.0000225	28.397	0.0000122	875.577	0.0002874	4.102	0.0201742	0.441	0.3435112	0.155	16.69355 ± 0.24549	239.50 3.30	98.04	15.25	714	12499.04		

Results	40(r)/39(k) ± 2σ	Age (Ma)	± 2σ	39Ar(k) (%,n)	K/Ca	± 2σ
Total Fusion Age	15.66569 ± 0.10512 ± 0.67%	225.64 ± 1.64 ± 0.72%	5	391 ± 1337		
Full External Error		± 2.30				
Analytical Error		± 1.42				

**Supplementary Table 14:** Raw  $^{40}\text{Ar}$ - $^{39}\text{Ar}$  data from sample NZ1301 with the calculated total fusion age

Analysis	36Ar (V)	%1σ	37Ar (V)	%1σ	38Ar (V)	%1σ	39Ar (V)	%1σ	40Ar (V)	%1σ	40(r)/39(k) ± 2σ	Age (Ma)	± 2σ	40Ar(r) (%)	39Ar(k) (%)	K/Ca	± 2σ
3M30224f0.0001128	12.540	0.0000165	642.728	0.0004368	2.957	0.0336776	0.451	0.5674568	0.108	15.84871 ± 0.29111	228.11 3.94	94.06	26.63	879	11298.48		
3M30228f0.0000203	36.970	0.0000438	261.419	0.0000820	11.701	0.0061182	0.889	0.1036737	0.300	15.95141 ± 0.79322	229.50 10.72	94.14	4.84	60	314.04		
3M30225f0.0000367	32.781	0.0001904	62.795	0.0004613	2.098	0.0340770	0.417	0.5581467	0.070	16.05754 ± 0.25077	230.93 3.39	98.04	26.94	77	96.67		
3M30226f0.0000248	32.792	0.0000566	188.029	0.0001630	4.811	0.0122201	0.606	0.2065708	0.116	16.29878 ± 0.44509	234.19 6.00	96.42	9.66	93	349.12		
3M30223f0.0000474	15.067	0.0000867	141.544	0.0002125	3.861	0.0156160	0.480	0.2697794	0.095	16.36925 ± 0.31655	235.14 4.26	94.75	12.35	77	219.34		
3M30230f0.0000269	25.862	0.0001639	70.436	0.0001218	5.823	0.0081471	0.854	0.1487557	0.214	17.27337 ± 0.59464	247.27 7.96	94.60	6.44	21	30.11		
3M30229f0.0000140	60.762	0.0000415	260.153	0.0002292	4.882	0.0166197	0.665	0.4068365	0.108	24.22733 ± 0.44701	338.00 5.69	98.97	13.14	172	896.20		

Results	40(r)/39(k) ± 2σ	Age (Ma)	± 2σ	39Ar(k) (%,n)	K/Ca	± 2σ
Total Fusion Age	17.21048 ± 0.14148 ± 0.82%	246.43 ± 2.09 ± 0.85%	7	178 ± 350		
Full External Error		± 2.73				
Analytical Error		± 1.89				

**Supplementary Table 15:** Raw  $^{40}\text{Ar}$ - $^{39}\text{Ar}$  data from sample NZ1303 with the calculated total fusion age

Analysis	36Ar (V)	%1σ	37Ar (V)	%1σ	38Ar (V)	%1σ	39Ar (V)	%1σ	40Ar (V)	%1σ	40(r)/39(k) ± 2σ	Age (Ma)	± 2σ	40Ar(r) (%)	39Ar(k) (%)	K/Ca	± 2σ
3M30215f0.0000144	84.926	0.0000614	195.745	0.0000308	23.998	0.0017106	1.506	0.0289335	0.671	14.39850 ± 4.29482	208.39 58.71	85.13	5.12	12	46.88		
3M30219f0.0000220	52.278	0.0000838	157.484	0.0000721	15.380	0.0056070	0.919	0.0918904	0.349	15.21367 ± 1.26282	219.50 17.16	92.83	16.79	29	90.60		
3M30220f0.0000244	46.539	0.0000934	135.629	0.0000623	12.748	0.0042104	0.787	0.0718681	0.315	15.33805 ± 1.63041	221.19 22.13	89.86	12.61	19	52.57		
3M30221f0.0000397	28.205	0.0000151	852.551	0.0001265	7.641	0.0094527	0.670	0.1578488	0.190	15.44436 ± 0.73970	222.64 10.03	92.49	28.30	268	4577.98		
3M30217f0.0000476	24.781	0.0001327	96.878	0.0001380	7.379	0.0092451	0.623	0.1633554	0.289	16.13253 ± 0.79476	231.95 10.72	91.30	27.68	30	58.06		
3M30216f0.0000078	148.488	0.0000172	833.420	0.0000418	19.268	0.0031714	1.478	0.0549233	0.406	16.57994 ± 2.24798	237.97 30.23	95.74	9.50	79	1323.53		

Results	40(r)/39(k) ± 2σ	Age (Ma)	± 2σ	39Ar(k) (%,n)	K/Ca	± 2σ
Total Fusion Age	15.63699 ± 0.52279 ± 3.34%	225.25 ± 7.13 ± 3.16%	6	133 ± 784		
Full External Error		± 7.31				
Analytical Error		± 7.08				

**Supplementary Table 16:** Raw  $^{40}\text{Ar}$ - $^{39}\text{Ar}$  data from sample NZ1323 with the calculated total fusion

Analysis	Zircon Number	Ox%(O )	Ox%(Si)	Ox%(Zr)	Ox%(Hf)	Sum
T1	21	0	0.3322	0.4326	0.0948	0.8596
T2	28	0	31.9031	64.5661	1.3619	97.8311
T3	10	0	0.3547	0.3133	0.0002	0.6682
T4	9	0	32.7465	66.0082	1.7295	100.4842
T5	117	0	34.6855	61.6517	1.455	97.7922
T6	7	0	32.5668	65.8554	1.6791	100.1013
T7	112	0	36.2037	61.8624	1.2353	99.3014
T8	110	0	33.5839	64.6248	1.8227	100.0314
T9	109	0	32.607	62.5446	1.4716	96.6232
T10	5	0	33.0798	65.0249	2.4848	100.5895
T11	104	0	33.3316	64.1601	1.5687	99.0604
T12	103	0	34.0808	63.4565	1.8283	99.3656
T13	4	0	32.5387	65.8271	1.7158	100.0816
T14	100	0	33.1581	63.7067	1.8493	98.7141
T15	3	0	33.1629	65.7359	1.9226	100.8214
T16	1	0	32.9543	65.1864	1.8177	99.9584
T17	95	0	34.1555	62.222	1.7374	98.1149
T18	16	0	32.838	66.1522	1.8603	100.8505
T19	74	0	27.7142	56.4377	1.2238	85.3757
T20	72	0	32.4612	57.0679	1.2154	90.7445
T21	66	0	33.5043	63.7372	1.5323	98.7738
T22	11	0	33.1324	65.413	1.8208	100.3662
T23	65	0	32.8976	65.8607	1.5734	100.3317
T24	64	0	32.8917	64.3626	1.9861	99.2404
T25	62	0	32.5638	65.4951	1.993	100.0519
T26	56	0	33.0701	64.1638	1.786	99.0199
T27	55	0	32.7355	63.6985	1.8718	98.3058
T28	53	0	37.9383	59.8044	1.4315	99.1742
T29	48	0	32.7288	64.88	2.1282	99.737
T30	49	0	33.459	61.8161	1.4877	96.7628

**Supplementary Table 19: Raw microprobe data from sample NZ1301**

Analysis	Zircon Number	Ox%(O )	Ox%(Si)	Ox%(Zr)	Ox%(Hf)	Sum
T1	1	0	31.3844	62.8207	5.7435	99.9486
T2	5	0	33.1132	66.3036	1.582	100.9988
T3	10	0	32.828	65.2066	1.9543	99.9889
T4	56	0	33.2686	64.3886	2.0157	99.6729
T5	11	0	32.5416	65.4782	1.9576	99.9774
T6	15	0	32.1244	63.0393	2.3909	97.5546
T7	19	0	33.1116	65.5516	1.9015	100.5647
T8	68	0	34.5915	62.4792	1.575	98.6457
T9	25	0	32.5445	65.9384	1.4836	99.9665
T10	26	0	32.9956	65.0639	1.6821	99.7416
T11	28	0	32.7641	65.4574	1.5145	99.736
T12	29	0	32.507	65.4771	1.7948	99.7789
T13	32	0	32.6702	64.8687	1.7578	99.2967
T14	75	0	36.161	58.9947	1.9588	97.1145
T15	36	0	32.9992	65.3503	1.3746	99.7241
T16	80	0	32.5698	65.2142	2.1428	99.9268
T17	82	0	35.8448	53.4273	1.3987	90.6708
T18	38	0	32.9302	65.8988	1.8608	100.6898
T19	40	0	32.5156	64.7921	2.154	99.4617
T20	41	0	31.5996	64.4798	2.7707	98.8501
T21	92	0	31.668	64.0765	1.4794	97.2239
T22	96	0	35.3211	60.9023	1.5368	97.7602
T23	100	0	32.384	63.8914	1.9648	98.2402
T24	103	0	33.1244	62.4353	1.6691	97.2288
T25	105	0	34.7776	60.937	1.5601	97.2747
T26	108	0	32.5428	65.1094	1.7578	99.41
T27	111	0	33.7569	64.1862	1.6622	99.6053
T28	114	0	33.9948	61.2863	1.7578	97.0389
T29	118	0	33.6394	62.068	1.346	97.0534
T30	120	0	33.8963	62.5344	2.1536	98.5843

**Supplementary Table 20:** Raw microprobe data from sample NZ1304

Analysis	Zircon Number	Ox%(O )	Ox%(Si)	Ox%(Zr)	Ox%(Hf)	Sum
T1	46	0	32.7796	61.854	1.3025	95.9361
T2	48	0	32.5423	64.6584	1.4153	98.616
T3	49	0	32.7833	63.9293	2.4492	99.1618
T4	33	0	32.9856	65.4781	1.5706	100.0343
T5	54	0	35.8027	58.6202	1.511	95.9339
T6	55	0	32.3211	64.6244	1.6886	98.6341
T7	61	0	33.6162	62.8292	1.4077	97.8531
T8	37	0	32.6238	64.4381	1.9521	99.014
T9	44	0	33.0486	65.4985	1.9988	100.5459
T10	69	0	34.4143	63.1183	1.9241	99.4567
T11	45	0	32.9555	65.2747	1.3338	99.564
T12	70	0	34.6514	62.026	1.44	98.1174
T13	73	0	31.7314	65.5629	2.1222	99.4165
T14	74	0	33.0488	65.397	1.5846	100.0304
T15	82	0	18.5018	49.8427	0.785	69.1295
T16	88	0	32.5424	65.1066	2.3612	100.0102
T17	90	0	28.8873	61.8707	1.988	92.746
T18	108	0	36.8446	58.313	1.5752	96.7328
T19	110	0	34.2679	63.1833	1.5136	98.9648
T20	26	0	27.9266	65.0228	2.4111	95.3605
T21	21	0	32.8567	65.7014	1.7917	100.3498
T22	20	0	31.5557	63.3229	1.4655	96.3441
T23	19	0	32.9905	66.0082	1.8634	100.8621
T24	18	0	32.3241	64.1187	1.5011	97.9439
T25	12	0	32.8102	65.9075	2.3203	101.038
T26	11	0	32.8809	65.6177	1.8961	100.3947
T27	10	0	33.4254	65.7802	1.4812	100.6868
T28	5	0	32.8612	65.3041	2.0013	100.1666
T29	3	0	32.8326	64.3137	1.9509	99.0972
T30	2	0	32.6153	64.746	2.5026	99.8639

**Supplementary Table 21:** Raw microprobe data from sample NZ1323

Analysis	Zircon Number	Ox%(O )	Ox%(Si)	Ox%(Zr)	Ox%(Hf)	Sum
T1	31	0	32.8449	65.0931	1.6802	99.6182
T2	34	0	32.8184	63.9901	1.9972	98.8057
T3	33	0	33.1075	64.0807	1.5877	98.7759
T4	35	0	33.8869	62.2955	2.2059	98.3883
T5	36	0	34.4399	62.4839	1.7064	98.6302
T6	40	0	33.2111	65.0201	1.8616	100.0928
T7	41	0	31.3273	57.3078	1.9267	90.5618
T8	49	0	33.2028	66.0386	1.8839	101.1253
T9	52	0	25.9157	51.7838	0.5513	78.2508
T10	55	0	33.1857	64.0077	1.5595	98.7529
T11	56	0	33.6096	59.1034	1.1044	93.8174
T12	57	0	35.09	60.3087	1.592	96.9907
T13	61	0	33.7691	62.265	1.6689	97.703
T14	70	0	33.5773	63.3042	1.6565	98.538
T15	82	0	33.8413	61.8496	2.3999	98.0908
T16	19	0	33.1558	65.5426	1.7728	100.4712
T17	83	0	35.3843	62.106	1.1225	98.6128
T18	96	0	34.96	63.0538	1.908	99.9218
T19	12	0	34.4451	63.9589	1.8517	100.2557
T20	11	0	32.751	65.2094	1.5038	99.4642
T21	10	0	33.5749	64.7256	1.8871	100.1876
T22	101	0	33.304	65.2516	2.1925	100.7481
T23	7	0	32.9175	64.7038	2.0894	99.7107
T24	5	0	34.4213	62.959	1.7609	99.1412
T25	110	0	35.3097	62.0317	2.0255	99.3669
T26	109	0	12.1639	25.1377	0.1172	37.4188
T27	113	0	32.6846	61.9088	1.6314	96.2248
T28	30	0	32.4739	64.385	2.2486	99.1075
T29	27	0	33.1691	65.5404	2.0554	100.7649
T30	25	0	33.8279	64.451	1.5971	99.876

**Supplementary Table 22:** Raw microprobe data from sample NZ1324

Element	T1	T2	T3	T4	T5	T6	T7	T8	T9	T10	T11	T12	T13	T14	T15	T16	T17	T18	T19	T20	T21	T22	T23	T24	T25	T26	T27	T28	T29	T30
Si	<8120054.	<8200577.	<2290752.	261966.5	239890.3	240155.5	202253.9	308524.4	245073.3	284024.3	252010.9	295652.9	257144.1	242414.2	299076.8	238654.5	226772	260369.6	243472.2	234978.8	207755.5	232451.3	200081.1	264455.3	276431.9	243903	210353.2	181928.3	259413.3	238185.3
Ti	<70626.60	414410.7	<19136.42	29.68	<20.41	<20.96	<18.42	<23.96	<20.80	<22.02	<19.75	<21.81	<21.03	<19.86	<19.51	<18.93	53.13	<20.44	30.86	<18.48	15.89	<19.42	<22.35	<25.16	<22.53	<17.25	34.49	18.18	<20.83	<28.56
Y	5072.69	2014.43	2996.35	1463.94	1200.09	1143.8	1078.02	1947.38	1151.13	2491.24	2316.48	1875.5	1255.21	3136.05	245.91	1867.85	1462.51	1342.67	1156.9	1349.28	1107.36	886.88	1438.31	2084.12	1320.74	1435.79	3748.44	952.51	1613.58	1057.57
Zr	1216363	291564.7	302588.2	395252.9	356532.1	410146.9	356999.3	468088.1	400926.5	417378.7	385206.9	464699.9	423712.8	404983.5	480795.2	409922.1	368981.6	452407.7	432371.3	434952.2	341514.9	438226.2	363828.7	426945.1	473038.4	420128.4	377116.2	315312.1	465980.8	398705.4
Nb	186.96	339.5	40.99	6.35	4.48	4.26	3.39	5.88	4.59	36.91	10.14	6.83	4.18	9.07	4.89	10.96	9.16	6.46	4.47	3.99	5.34	3.19	3.55	9.53	5.04	3.38	7.95	3.43	9.36	12.46
La	<74.04	210.95	<15.81	0.512	29.59	0.026	<0.023	<0.019	<0.022	<0.030	<0.028	2.57	0.064	0.026	0.018	0.044	0.06	<0.022	0.04	0.303	0.076	<0.029	6.46	<0.037	1.7	1.34	<0.025	0.104	0.033	<0.040
Ce	79.91	369.15	43.59	62.08	100.26	18.58	5.47	18.38	29.5	32.97	90.51	64.77	31.09	37.88	18.79	82.18	45.95	32.46	54.57	49.66	53.32	33.72	50.16	24.5	33.48	16.72	10.74	20.43	63.14	15.04
Pr	<33.57	<48.79	<12.61	0.422	7.46	0.07	0.037	0.064	0.078	0.174	0.189	0.949	0.096	0.099	0.029	0.095	0.065	0.077	0.308	0.231	0.059	0.075	1.53	0.156	0.825	1.036	0.042	0.23	0.041	0.066
Nd	<325.98	<204.79	183.51	6.17	29.36	1.19	0.63	0.87	1.75	3.94	3.14	8.17	1.27	2.68	0.55	2.01	1.07	1.39	5.03	3.18	1.3	1.66	7.76	3.51	6.44	9.46	1.01	3.01	1.32	0.9
Sm	233.28	239.57	115.69	9.77	9.85	3.38	2.34	3.69	3.56	10.13	7.48	12.38	3.43	9.21	1.47	5.48	3.79	3.87	9.57	5.72	3.32	3.7	5.09	8.84	9.05	13.21	4.23	6.26	2.48	2.69
Eu	<70.00	<62.30	<30.11	3.59	1.83	0.914	1.057	1.2	1.05	0.168	2.73	3.37	0.95	3.21	1.22	1.32	1.55	1.58	2.06	2	0.749	1.01	1.75	0.265	0.82	0.525	0.426	1.33	0.71	0.188
Gd	<282.33	<318.22	<71.26	37.81	24.74	17.47	18.08	24.81	51.7	44.45	50.76	18.73	56.21	6.65	33.19	25.31	22.91	38.96	25.79	17.83	15.21	25.69	41.81	36.13	41.16	37.12	24.98	16.65	17.76	
Tb	<66.90	<62.77	16.08	11.61	8.42	7.14	7.48	10.09	6.82	19.42	15.75	7.33	21.73	2.04	12.68	9.62	9.15	12.57	9.04	7.08	6.09	9.07	16.24	12.77	13.73	19.28	8	6.76	7.29	
Dy	417.23	<191.77	164.01	127.63	103.49	92.28	95.96	147.75	86.34	235.91	190.26	171.81	94.33	277.64	22.62	158.21	120.61	121.61	130.47	115.04	96.04	75.4	114.1	199.48	141.83	160.74	279.48	87.45	93.55	95.29
Ho	76.44	62.35	79.91	44.43	37.53	36.31	62.43	33.98	88.74	74.41	60.62	37.22	100.84	7.24	61.31	49.05	46.57	42.24	44.06	37.22	28.41	46.07	72.31	48.07	52.38	122.31	31.85	43.12	38.09	
Er	424.83	336.27	480	205.56	165.28	165.81	150.85	300.43	164.57	388.11	331.83	253.49	170.43	441.27	30.59	269.26	210.21	207.8	160.95	198.88	177.56	129.79	225	324.26	191.37	201.86	624.48	141.38	239.88	173.32
Tm	47.88	104.83	107.47	50.08	41.21	41.12	36.07	81.31	43.76	92.65	76.51	57.67	45.74	104.15	7.76	68.27	54.22	52.18	35.19	51.18	45.57	35.52	55	71.01	41.5	47.85	166.98	32.51	71.58	39.48
Yb	1155.53	281	2017.91	555.5	478.51	479.79	400.4	981.17	539.01	945.17	837.85	654.58	532.93	1134.37	98.49	758.77	631.28	583.47	334.15	631.37	510.77	423.86	582.57	692.74	435.42	500.5	1814.91	317.26	947.56	426.66
Lu	350.61	103.12	215.53	89.47	77.78	82.18	67.29	168.56	92.96	137.45	133.64	103.42	82.24	179.82	16.06	122.16	94.81	92.15	51.12	104	74.89	71.7	115.28	98.91	65.51	70.07	273.5	49.26	167.07	61.66
Hf	15235.63	11548.62	15132.18	14665.79	12338.09	14238.41	10475.08	15456.11	14613.21	21070.57	13302.24	15503.59	14549.62	15681.67	16303.23	15413.71	14732.78	15774.95	15132.18	14613.22	12993.58	15440	13342.1	16841.71	16900.21	15144.9	15872.47	12138.81	18046.68	15235.63
Hf (wt%)	<b>4.520356</b>	<b>1.154862</b>	<b>1.513218</b>	<b>1.466579</b>	<b>1.233809</b>	<b>1.423841</b>	<b>1.047508</b>	<b>1.545611</b>	<b>1.461321</b>	<b>2.107057</b>	<b>1.330224</b>	<b>1.550359</b>	<b>1.454962</b>	<b>1.568167</b>	<b>1.630323</b>	<b>1.541371</b>	<b>1.473278</b>	<b>1.577495</b>	<b>1.513218</b>	<b>1.461322</b>	<b>1.299358</b>	<b>1.544</b>	<b>1.33421</b>	<b>1.684171</b>	<b>1.690021</b>	<b>1.51449</b>	<b>1.587247</b>	<b>1.213881</b>	<b>1.804668</b>	<b>1.523563</b>
Ta</																														

Element	T1	T2	T3	T4	T5	T6	T7	T8	T9	T10	T11	T12	T13	T14	T15	T16	T17	T18	T19	T20	T21	T22	T23	T24	T25	T26	T27	T28	T29	T30
Si	274107.8	163867.3	362169.7	197796.6	243035	227385.6	146295.2	194526.9	245996.6	193430.9	236259.8	224654.3	291454	271285.6	279658.7	270649.1	260586.9	211176.4	222907.8	229436	211565.6	197092.5	243614.5	271401.9	202056.3	254541.3	199180.1	482107.1		
Ti	<36.64	<14.27	29.04	30.41	127.46	<18.06	<17.53	28.45	<21.09	19.41	<29.06	<27.36	<39.35	<33.80	<48.06	<33.35	<37.28	<25.62	<30.25	<19.17	<18.59	<26.97	23.85	18.09	<31.49	<39.06	<22.27	<22.07	53.93	<64.49
Y	262.01	1815.42	1789.33	858.43	2690.07	786.54	977.03	1767.49	1939.49	2717.42	3205.81	5023.53	2586.51	2331.15	2056.1	789.04	1233.54	1153.08	1735.82	1804.82	935.73	1222.89	790.77	1284.82	512.89	1960.29	2278.72	2414.76	3639.17	5775.05
Zr	507601.2	304347.3	540183.4	377840.3	455135.4	365786.1	277636.7	371563.5	384288.1	344230.7	377398.9	380958	482014.3	493466.3	492160.3	469286.5	428317.3	382245.8	421693.2	383054.5	397671.1	378386.1	395697.7	356574	455550.8	535496.4	371991.9	428716.1	344043.3	763778.9
Nb	1.45	4.16	9.55	2.33	3.24	3.55	3.94	5.87	11.23	7.3	10.57	10.93	3.03	9.87	1.87	1.42	5.91	4.14	4.53	8.05	3.07	5.34	2.91	4.99	0.73	2.63	3.79	3.96	10.92	20.49
La	<0.034	0.017	13.78	<0.0151	0.19	19.09	0.021	0.068	<0.031	0.518	0.03	0.458	0.025	0.23	0.03	<0.035	0.113	0.316	3.05	0.574	0.042	2.04	5.03	0.407	0.047	0.012	0.568	1.26	43.14	0.129
Ce	20.09	6.4	43.62	21.34	5.35	83.16	12.24	19.37	28.25	4.25	34.84	136.3	52.89	21.2	8.27	1.18	26.15	40.83	38.34	33.15	29.7	74.09	43.41	27.26	1.57	17.37	28.69	58.6	170.62	47.89
Pr	0.059	0.169	6.62	0.033	0.189	5.04	0.054	0.13	0.077	0.242	0.222	1.02	0.488	0.358	0.078	0.138	0.117	0.141	1.98	0.32	0.071	1.25	1.39	0.364	0.142	0.102	0.464	0.608	25.02	0.339
Nd	0.83	3.04	49.17	0.91	2.18	22	0.94	1.9	2.13	1.7	3.95	19.29	8.86	4.75	2.32	2.26	1.25	1.82	15.72	3.92	1.62	9.48	7.73	3.22	3.53	1.74	6	7.04	125.8	6.22
Sm	0.75	6.92	23.45	3.03	6.58	6.39	2.83	6.56	4.66	4.35	9.48	33.12	19.54	9.44	6.22	8.44	2.84	3.85	16.35	8.57	2.92	7.76	4.93	5.02	11.33	5.16	11.75	13.96	51.11	20.97
Eu	0.67	0.227	3.8	0.683	0.406	1.72	0.31	0.294	0.93	0.241	2.46	10.11	2.19	2.02	1.96	0.355	0.344	1.18	0.92	1.55	0.75	2.36	0.8	0.477	0.75	1.86	2.27	2.01	1.66	0.73
Gd	5.3	32.75	68.17	16.04	42.7	15.74	17.36	29.89	32.15	35.18	64.26	158	84.48	50.9	39.16	50.9	19.06	21.4	59.77	41.72	15.86	29.82	17.55	23.68	43.6	33.85	53.48	53.54	107.4	129.82
Tb	1.62	13.54	19.99	5.94	19.62	4.59	6.98	12.19	12.65	16.02	23.04	48.46	26.48	17.34	14.23	14.24	8.04	7.79	18.14	14.19	5.83	9.45	6.07	9.06	10.97	13.1	18.68	19.17	33.85	49.94
Dy	20.45	163.63	202.76	73.23	244.87	56.91	90.87	152.44	163.3	230.72	286.51	510.38	259.95	217.94	174.87	110.6	103.18	93.79	206.5	181.6	69.53	98.45	73.4	115.14	78.33	170.54	221.71	233.98	401.44	638.18
Ho	8.32	58.67	71.24	28.01	82.54	24.7	36.43	55.54	67.32	102.31	119.72	183.4	86.97	85.06	66.95	27.29	41.64	37.97	69.27	70.1	28.03	39.73	27.25	47.06	17.53	69.38	82.69	85.83	142.93	220.81
Er	39.75	258.05	303.31	130.04	337.52	115.33	171.24	253.08	336.86	472.97	556.79	817.02	371.39	364.14	306.24	102.3	199.44	180.08	267.29	318.61	141.42	189.19	123.96	206.73	48.91	295.69	345.15	364.81	603.29	911.83
Tm	11.33	66.12	64.59	32.93	73.23	27.61	39.45	62.71	81.97	107.45	119.83	179.71	77.51	78.15	67.81	23.4	49.42	42.85	54.24	68.67	38.27	48.58	28.66	44.46	7.62	65.93	75.78	83.88	132.15	199.2
Yb	129.96	693.11	577.6	380.03	678.39	295.31	377.81	629.23	850.52	1057.21	1134	1681.88	674.8	771.6	669.56	253.57	512.28	472.09	516.23	673.28	427.55	510.07	295.4	451.12	56.35	691.67	793.23	890.77	1305.79	1957.24
Lu	25.88	97.38	84.71	58.46	94.15	63.67	61.51	101.76	135.08	172.01	167.7	252.41	93.04	135.33	115.02	40.93	83.32	81.11	72.24	111.84	68.06	87.65	48.86	69.24	6.95	111.2	123.28	130.54	176.09	245.85
Hf	17696.46	12001.44	20768.69	13318.35	15785.12	14318.96	11936.99	16553.39	16949.39	16315.95	11310.34	12210.89	17995.8	13437.07	17696.46	20022.47	16857.81	13357.36	12835	14509.76	15193.23	14509.76	15801.23	12729.01	19675.65	16078.52	12560.26	16970.6	16543.21	21221.51
Hf (wt%)	<b>1.769646</b>	<b>1.200144</b>	<b>2.076869</b>	<b>1.331835</b>	<b>1.578512</b>	<b>1.431896</b>	<b>1.193699</b>	<b>1.655339</b>	<b>1.694939</b>	<b>1.631595</b>	<b>1.131034</b>	<b>1.221089</b>	<b>1.79958</b>	<b>1.343707</b>	<b>1.769646</b>	<b>2.002247</b>	<b>1.685781</b>	<b>1.335736</b>	<b>1.2835</b>	<b>1.450976</b>	<b>1.519323</b>	<b>1.450976</b>	<b>1.580123</b>	<b>1.272901</b>	<b>1.967565</b>	<b>1.607852</b>	<b>1.256026</b>	<b>1.69706</b>	<b>1.654321</b>	<b>2.122151</b>
Ta	0.418	2.24	3.87	1.074	1.404	0.778	2.09	2.07</																						